



TALLINN UNIVERSITY OF TECHNOLOGY
SCHOOL OF ENGINEERING
DEPARTMENT OF ELECTRICAL POWER ENGINEERING AND MECHATRONICS

DESIGNING AND OPTIMIZATION OF FORKLIFT COMBINED WITH SCISSOR LIFT

KAHVELTÕSTUKI PROJEKTEERIMINE JA OPTIMEERIMINE KOOS KÄÄRKAHVELTÕSTUKIGA

MASTER THESIS

Student: Adithyavishnu Vaikkath

Student code: 195987MAHM

Supervisor: Leo Teder, Asst Professor

Tallinn 2022

(On the reverse side of title page)

AUTHOR'S DECLARATION

Hereby I declare, that I have written this thesis independently.

No academic degree has been applied for based on this material. All works, major viewpoints and data of the other authors used in this thesis have been referenced.

"18" May 2022.

Author: Adithyavishnu Vaikkath

/signature /

Thesis is in accordance with terms and requirements

"18" May 2022.

Supervisor: Leo Teder

/signature/

Accepted for defence

"....."20... .

Chairman of theses defence commission:

/name and signature/

Non-exclusive licence for reproduction and publication of a graduation thesis¹

I Adithyavishnu Vaikkath (date of birth: 08/02/1994) (author's name)

1. grant Tallinn University of Technology (TalTech) a non-exclusive license for my thesis
Designing and optimization of forklift combined with scissor lift.,

supervised by

Leo Teder, Assistant Professor

1.1 to be reproduced for the purposes of preservation and electronic publication of the graduation thesis, incl. to be entered in the digital collection of the library of Tallinn University of Technology until expiry of the term of copyright;

1.2 to be published via the web of Tallinn University of Technology, incl. to be entered in the digital collection of the library of Tallinn University of Technology until expiry of the term of copyright.

1. I am aware that the author also retains the rights specified in clause 1 of the non-exclusive licence.

2. I confirm that granting the non-exclusive licence does not infringe other persons' intellectual property rights, the rights arising from the Personal Data Protection Act or rights arising from other legislation.

_____ (date)

¹ *The non-exclusive licence is not valid during the validity of access restriction indicated in the student's application for restriction on access to the graduation thesis that has been signed by the school's dean, except in case of the university's right to reproduce the thesis for preservation purposes only. If a graduation thesis is based on the joint creative activity of two or more persons and the co-author(s) has/have not granted, by the set deadline, the student defending his/her graduation thesis consent to reproduce and publish the graduation thesis in compliance with clauses 1.1 and 1.2 of the non-exclusive licence, the non-exclusive license shall not be valid for the period.*

Department of Electrical Power Engineering and Mechatronics

THESIS TASK

Student: Adithyavishnu Vaikkath, 195987 MAHM

Study programme, MAHM02/19 - Mechatronics

main specialty: Mechatronics

Supervisor(s): Leo Teder, Assistant Professor.

Consultants:(name, position)

..... (company, phone, e-mail)

Thesis topic:

(in English) *Designing and Optimization of forklift combined with scissor lift*

(in Estonian) Kahveltõstuki projekteerimine ja optimeerimine koos käärikahveltõstukiga

Thesis main objectives:

1. Suitable design and the FEA on the structure
2. Optimization and simulation of design

Thesis tasks and time schedule:

| No. | Task | Month |
|-----|--|----------|
| 1 | Literature review and Assembly Mechanism | December |
| 2 | Developing the practical design | March |
| 3 | Designing SolidWorks Model | April |
| 4 | Stability of the design developed | July |
| 5 | Stress and Strain analysis, Displacement analysis, and optimization of components before and after assembly. | October |
| 6 | Simulation of entire assembly | December |
| 7 | Thesis defense | june |

Language: English **Deadline for submission of thesis:** "18" May 2022

Student: Adithyavishnu Vaikkath "18" may 2022

/signature/

Supervisor: Leo Teder "18" May 2022

/signature/

Head of study programme: Anton Rassõlkin "18" May 2022

/signature/

Terms of thesis closed defense and/or restricted access conditions to be formulated on the reverse side

CONTENTS

| | |
|--|----|
| PREFACE | 9 |
| LIST OF FIGURES | 10 |
| LIST OF TABLE | 12 |
| List of abbreviations..... | 13 |
| 1 INTRODUCTION..... | 14 |
| 2 LITERATURE REVIEW | 16 |
| 2.1 Forklift designs and FEM analysis | 16 |
| 2.2 Survey on scissor lift | 18 |
| 2.3 Controlling system prototypes | 20 |
| 2.4 Conclusion of literature review..... | 22 |
| 3 DESIGNING CRITERIA | 23 |
| 3.1 Different assemblies' ideas proposed - design 1: 180°rotate forks with hydraulic pump..... | 24 |
| 3.2 Design 2: fork pulling with lead screw | 25 |
| 3.3 Comparison of design ideas proposed..... | 26 |
| 3.4 Stability of the design | 27 |
| 3.4.1 Centre of gravity without the load | 29 |
| 3.4.2 Center of gravity with the load of 1002 Kg | 30 |
| 3.4.3 Stability triangle..... | 32 |
| 4 DRIVING SYSTEM | 33 |
| 4.1 Hydraulic circuit..... | 33 |
| 4.2 Electrical circuit | 36 |
| 5 STATIC ANALYSIS OF THE COMPONENT..... | 38 |
| 5.1 Fork | 38 |
| 5.2 Fork guide | 41 |
| 5.3 Fork mount | 44 |
| 5.4 Forklift level2 guide..... | 47 |
| 5.5 Forklift drive guide | 50 |
| 5.6 Forklift mount | 53 |
| 5.7 Forklift linear guide | 56 |
| 5.8 Scissor lift top plate | 59 |
| 5.9 Scissor link | 62 |
| 5.10 Truck Frame..... | 65 |
| 5.11 Lead screw..... | 68 |
| 5.12 Optimization and simulation | 71 |
| 6 ESTIMATION GRAPHS..... | 73 |

| | |
|--|-----|
| 6.1 Force estimation of the scissor lift actuator (use sf_unit_actuate3 model) | 73 |
| 6.2 Motor torque estimation of the linear guide (use sf_unit_actuate4) | 74 |
| 7 DYNAMIC ANALYSIS | 76 |
| 7.1 Analysis of the lead screw with load | 76 |
| 7.2 Stress analysis of scissor lift components..... | 77 |
| 8 Summary..... | 79 |
| 1.1 Limitations..... | 79 |
| 1.2 Future work | 80 |
| KOKKUVÕTE | 81 |
| Piirangud..... | 81 |
| Tulevased tööd | 82 |
| 9 REFERENCES..... | 83 |
| APPENDIX 1 | 85 |
| APPENDIX 2 | 86 |
| APPENDIX 3 | 87 |
| APPENDIX 4 | 88 |
| APPENDIX 5 | 89 |
| APPENDIX 6 | 90 |
| APPENDIX 7 | 91 |
| APPENDIX 8 | 92 |
| APPENDIX 9 | 93 |
| APPENDIX 10 | 94 |
| APPENDIX 11 | 95 |
| APPENDIX 12 | 96 |
| APPENDIX 13 | 97 |
| APPENDIX 14 | 98 |
| APPENDIX 15 | 99 |
| APPENDIX 16 | 100 |
| APPENDIX 17 | 101 |
| APPENDIX 18 | 102 |
| APPENDIX 19 | 103 |
| APPENDIX 20 | 104 |
| APPENDIX 21 | 105 |
| APPENDIX 22 | 106 |
| APPENDIX 23 | 107 |
| APPENDIX 24 | 108 |
| APPENDIX 25 | 109 |
| APPENDIX 26 | 110 |

| | |
|-------------------|-----|
| APPENDIX 27 | 111 |
| APPENDIX 28 | 112 |
| APPENDIX 29 | 113 |
| APPENDIX 30 | 114 |
| APPENDIX 31 | 115 |
| APPENDIX 32 | 116 |
| APPENDIX 33 | 117 |
| APPENDIX 34 | 118 |
| APPENDIX 35 | 119 |
| APPENDIX 36 | 120 |
| APPENDIX 37 | 121 |
| APPENDIX 38 | 122 |
| APPENDIX 39 | 123 |
| APPENDIX 40 | 124 |
| APPENDIX 41 | 125 |
| APPENDIX 42 | 126 |
| APPENDIX 43 | 127 |
| APPENDIX 44 | 128 |
| APPENDIX 45 | 129 |
| APPENDIX 46 | 130 |
| APPENDIX 47 | 131 |
| APPENDIX 48 | 132 |

PREFACE

The idea of this thesis is to develop a design where the system can provide both the functions of scissor lift and forklift. The design is developed by combining the basic design of a scissor lift and forklift. The platform used for developing the design is SolidWorks. SolidWorks gives the platform to build the design in several different proposed designs. The possibility of each different design was checked to get fixed on the most feasible and practically possible design. The new design provides a new mechanism that allows the possibility to conduct both crucial functions of the scissor lift and forklift. The stability of the design is checked as the center of gravity during the lifting process is checked with the load and without load. The next main aim was to optimize the design to lift at least one ton and reach the height of 7 meters. The driving system for the design to lift the load is developed by compiling hydraulic and electrical circuits into the system. Static analysis of each component of the design is conducted with the application of load according to its position. The simulation of the design was developed through the Simscape. The force for each actuator to reach the maximum extension is calculated. Then the dynamic analysis of the most crucial components is conducted, and changes are made to get the optimized model.

LIST OF FIGURES

| | |
|---|----|
| Figure 3.2.1 Top view of the design | 26 |
| Figure 3.2.2 Normal 3D view | 26 |
| Figure 3.4.1 Midpoint of the truck (red mark)..... | 28 |
| Figure 3.4.2 Design forklift position | 29 |
| Figure 3.4.3 Design loading position (with load) | 30 |
| Figure 4.1.1 Forklift subsystem part 1 hydraulic circuit..... | 34 |
| Figure 4.1.2 Forklift level 1 hydraulic circuit | 34 |
| Figure 4.1.3 Scissor lifts hydraulic circuit | 35 |
| Figure 4.1.4 Forklift level hydraulic circuit..... | 35 |
| Figure 4.1.5 Combined assembly of the hydraulic circuit. Skydrol_LD4 shows the hydraulic fluid tank. | 36 |
| Figure 4.2.1 Electrical circuit for lead screws | 37 |
| Figure 5.1.1 Stress of fork | 39 |
| Figure 5.1.2 Displacement of fork | 39 |
| Figure 5.1.3 Strain of fork | 40 |
| Figure 5.1.4 Factor of safety of the fork..... | 41 |
| Figure 5.2.1 Stress of fork guide..... | 42 |
| Figure 5.2.2 Displacement of fork guide | 42 |
| Figure 5.2.3 Strain of fork guide | 43 |
| Figure 5.2.4 Factor of safety of fork guide | 44 |
| Figure 5.3.1 Stress of fork mount | 45 |
| Figure 5.3.2 Displacement of fork mount | 45 |
| Figure 5.3.3 Strain of fork mount..... | 46 |
| Figure 5.3.4 Factor of safety fork mount..... | 47 |
| Figure 5.4.1 Stress of fork lift..... | 48 |
| Figure 5.4.2 Displacement of fork lift | 48 |
| Figure 5.4.3 Strain of fork lift | 49 |
| Figure 5.4.4 Factor of safety of fork lift | 50 |
| Figure 5.5.1 Material properties of forklift drive guide | 50 |
| Figure 5.5.2 Stress of forklift drive guide | 51 |
| Figure 5.5.3 Displacement of forklift drive guide..... | 52 |
| Figure 5.5.4 Strain of forklift drive guide | 52 |
| Figure 5.5.5 Factor of safety of the forklift drive guide | 53 |
| Figure 5.6.1 Stress of forklift mount..... | 54 |
| Figure 5.6.2 Displacement of forklift mount | 55 |
| Figure 5.6.3 Strain of forklift mount | 55 |

| | |
|--|----|
| Figure 5.6.4 Factor of safety of the forklift mount | 56 |
| Figure 5.7.1 Stress of forklift linear guide | 57 |
| Figure 5.7.2 Displacement of forklift linear guide | 58 |
| Figure 5.7.3 Strain of forklift linear guide..... | 58 |
| Figure 5.7.4 Factor of safety of the forklift linear guide..... | 59 |
| Figure 5.8.1 Stress of scissor lift top plate | 60 |
| Figure 5.8.2 Displacement of scissor lift top plate | 61 |
| Figure 5.8.3 Strain of scissor lift top plate..... | 61 |
| Figure 5.8.4 Factor of safety of the of scissor lift top plate | 62 |
| Figure 5.9.1 Stress of scissor link | 63 |
| Figure 5.9.2 Displacement of scissor link | 64 |
| Figure 5.9.3 Strain of scissor link..... | 64 |
| Figure 5.9.4 Factor of safety for scissor link | 65 |
| Figure 5.10.1 Stress of truck frame..... | 66 |
| Figure 5.10.2 Displacement of truck frame | 67 |
| Figure 5.10.3 Strain of truck frame | 67 |
| Figure 5.10.4 Factor of safety of the truck frame | 68 |
| Figure 5.11.1 Stress of lead screw | 69 |
| Figure 5.11.2 Displacement of lead screw | 70 |
| Figure 5.11.3 Strain of lead screw | 70 |
| Figure 5.11.4 Factor of safety of lead screw | 71 |
| Figure 6.1.1 Y-axis actuator shows displacement, and X-axis shows time. | 73 |
| Figure 6.1.2 Y-axis shows actuator force, and X-axis shows time. | 73 |
| Figure 6.1.3 X-axis shows time, and Y-axis shows hydraulic pressure..... | 74 |
| Figure 6.2.1 Y-axis shows angular velocity, and X-axis shows time | 74 |
| Figure 6.2.2 Y-axis shows actuator torque, and X-axis shows time..... | 75 |

LIST OF TABLE

| | |
|--|----|
| Tabel 3.3.1 The advantages of the second design over the 1st one | 27 |
|--|----|

List of abbreviations

CAD – Computer Assisted Drawing

FEM – Finite Element Method

FEA – Finite Element Analysis

ADC – Analog to Digital Convertor

GCM – General Circulation Model

VGCM – Variable General Circulation Model

CPU – Central Processing Unit

AC – Alternating Current

DC – Direct Current

N – Newton

m – Meter

Pa – Pascal

1 INTRODUCTION

Here my thesis deals with the design of a machine that combines the forklift with a scissor lift. Forklift and scissor lift has been an integral part of certain industries for almost a century. In the current situation, we can say that almost every warehouse has either one of them for loading and stacking purposes. Different types of forklifts can be used in different conditions of the warehouse, applications, fuel options, and features of the forklift. Forklifts are an important piece of equipment that, when necessary, can perform different tasks. A few basic components are used to build almost all forklifts: the frame, power source, mast, counterweight, forks, and load backrest. The frame of the forklift, usually powered by propane tanks or rechargeable batteries, contains a counterweight that keeps the truck's body in place as the load pushes down on the forks. Along the mast, the forks lift, which stabilizes the load while the backrest stops it from dropping on top of the cabin. Most people have them for moving materials from the yard to the house or workshop. A big downside of forklifts is that they are difficult to drive. You need to be vigilant about them and learn the best way to use them.

The scissor lift is used mostly as a table lift to lift individuals. It has a criss-cross base under the support platform. It moves upright in the vertical direction as the frame gathers itself together and drives the platform in line with height and weight. This can also be powered by hydraulic, pneumatic, or mechanical power for height extension. It is available on the market in various sizes and shapes. Some designs can reach 18.8 meters. They are very easy to run, reducing the operators' tardiness and fatigue.

So we aim to combine the functions of both machines into one. As we know, the forklift which can be used inside a warehouse are relatively small; they can only lift the loads to a maximum height of 1 or 2 meters. But there are scissor lifts which can lift more than 8 or 9 meters are easily used inside the warehouses. So by combining these features, we can produce a machine that can load the weight by itself and take it to the vertical height, which is far beyond the forklift limits. The forklift, which can lift the load to a height of 8 m, is very large and need a very big space for working. There is no way that it can use in internal infrastructure. Our design gives the advantage of loading and lifting the weight to a height of 8 meters with a machine that perfectly fits inside a warehouse.

Also, we are planning to make the design which works on a remote control system. This allows our design to work even in very remote areas, which will be a real tough spot for humans to be as we know that most forklift accidents are due to tipping of the forklift.

But in our design, even in any situation, if anything goes wrong, this will not affect the operator, so that this helps to increase the safety of the operator who doesn't have to be in there. It will also have no steering mechanism, as a single 'H' bridge DC motor drive kit will drive all the motors operating the system. To reduce speed and to increase torque, these engines would have a gear reduction feature.

Currently, in most industries where they have a warehouse, they have both scissor lifts and forklifts. The people have to use both of these hand to hand to complete their tasks. In a situation like this where the people are afraid to come out and work these operators and loading jobs, we need a machine which increases the efficiency and amount of work it does with the help of a very less number of operators. Covid situations had indeed made a serious scarcity of manpower in every industry. Our design helps to reduce the number of people needed for the job of loading and to stack the loads in a Warehouse. As we know that this combines the features of both, we also needed less number of machines.

Also, the author of this report is so passionate about designing a new machine where one has to come up with a new design to successfully do a specific task. As here, the author has to come up with a design that is safe and efficient at the same time. To do so, the author chooses SolidWorks, where the machine can be simulated, and also stress analysis, strain analysis, and design optimization can be done. That gives another motivation for the author.

This study aims to find an acceptable and secure design for a system that can perform both the functions of a scissor lift and forklift. A machine can be controlled by a remote control system. So Solidworks was found by the author to perform this role as it can perform finite element analysis of the structure in that same software. This mission is therefore specifically aimed at:

- Develop a possible design
- Check the stability of the design
- Build the system of lifting
- Static analysis of design
- Simulation of design
- Dynamic analysis of design

2 LITERATURE REVIEW

This chapter discusses the latest studies and researches carried out on the forklift and scissor lift, about new designs on it. The latest literature that describes the previous approaches that are closely related to the purpose of this study will be further discussed in this section, and the ideas will be used to describe a possible solution for our system design.

2.1 Forklift designs and FEM analysis

Since our design of the model is a new one, there are very few works that are similar to the one we are doing. But when we are considering the forklift and scissor lift separately, there is a lot of work which deals with different designing aspects and defects of it. Since scissor lift is a much simpler machine compared to a forklift; most of the work is more focused on the Forklift, which is also what the author is looking forward to finding.

Lifting and loading Equipment like forklift and scissor lift has been used in industries for at least a century. Now, let's take the case of a forklift, which is a major part of our design. While designing a machine like a forklift, there are several factors to be considered. One of the main factors is the strength of the machine to lift the load to a required height. For that, we need to do a FEM analysis for our model. The method of calculating structural strength and predicting component fatigue life based on computer-aided design (CAD) and finite element method (FEM) has been widely used in the engineering field, with the advancement of finite element numerical simulation technology and the broad application of large-scale commercial finite element software. We can do FEM analysis in different software like Ansys [1], SolidWorks [2], MSC SimXpert Nastran Finite Element software [3]. Gu et al. analyzed the simplified fork structure and the rated payload, then accomplished the static analysis based on ANSYS, and simulation results provided a theoretical reference for the structural design of the forklift fork. He and Wang performed finite element analysis software of ANSYS to analyze the mechanical properties of two kinds of structures commonly used in forks at present, and a basic conclusion was gotten that the hanger-type fork fitted for the environment with a light load and high work efficiency. [1] From the above statement, it is clear that Ansys is one of the commonly used software by scholars for FEM analysis.

Ansys Mechanical and Ansys Structural are the primary Ansys solutions in the structural field. We can import geometries, optimize meshing, and set boundary conditions using such solutions. We can perform analyses of the system's power, vibration, motion, and thermal properties after these preprocessing measures and obtain graphic representations showing how these properties differ under the chosen conditions across the geometry. Then change your design to fix any problem areas based on these outcomes and run the simulation again till showing an optimal design of the component or system under construction after a couple of iterations. Another option is with SolidWorks, where we can't provide the unequaled depths in any simulation domain. But in SolidWorks, we can use finite element analysis to calculate stresses and displacements of parts and assemblies under internal and external loads. [2]. While doing it in SolidWorks, we don't have to import or export the files.

One of the prominent works [2] which the author found in SolidWorks is a work that has been carried out force analysis on a three-section working device. Through calculation proved that the telescopic boom of forklifts working in the lower position is the most dangerous situation. Then used the FEA components of SolidWorks Simulation to carry out finite element analysis, obtaining FEA results, and proved it is reasonable via stress testing on a test sample machine. So this helped the author to fix the software to be used for designing and conducting fea analysis. Also, there is an option for optimization, which can be done on different iterations of the result of forces applied to the machines. [2] The article by Ömer Yavuz Bozkurt [3] then suggests the Finite Element Approach and potential modifications based on the original geometry of components. Such geometry was used to improve the reliability of the forklift design concerning stress distributions in the critical area. Analyses were performed in compliance with standard regulations relating to the sections investigated. The maximum lateral, vertical, and longitudinal force values applicable to the head guard and its application types have been calculated under the standard EN ISO 3471. Under compulsion loading conditions, structural parts of the forklift such as the frame and head guard were studied. [3]

In the 5th IEEE Region 10 Humanitarian Technology Conference 2017 [4], some researchers come with an idea of a prototype to prevent the topple over the problem of forklifts with multidimensional features like overload detection system and center of gravity correction mechanism. From the proceedings of this conference, problems such as overturning prevention during the motion of the machine can be achieved using means of height detection, means of detection of cargo weight, and the means of detection of lateral acceleration to detect lateral acceleration in a lateral direction. This has been achieved by using Controller; here it is Raspberry Pi. Analog input transducers

first feed into the ADC and then convert the digital signal from the ADC feed to the Raspberry Pi. The driver's input from the keyboard is fed to the Raspberry Pi at the same time. In Raspberry Pi, these data are then processed and determined to determine the center of gravity of the loaded truck. The corresponding output is created by the motor driver for driving wheel motors and fork actuators at a safe speed. [4] Also, another similar work on the stability of the forklift design was introduced by Jesus Felez and Alvaro Bermejo [5]. Here researchers used MPC controllers to control the pitch angle so that it can prevent the vehicle from tipping over. In conclusion, the vehicle with the controller can then execute acceleration and braking maneuvers in a faster and safer manner. [5]

2.2 Survey on scissor lift

The scissor lift part of our design comprises the function of taking the load to a vertical height that is beyond the reach of a forklift. There are several types of scissor-lift. In this section, the author came across some recent works on this criss-cross mechanism of lifting. In order to integrate this mechanism into the author's mechanism, the basic structure and design of the scissor are found from a patent by Tom Beamish [6]. This patent is a drawing that gives an idea about the different sectional views of the scissor lift. But Louis BAFILE and a group of researchers [7] went more deeply into the detailing of the drawings. This patent deals with all the different parts like a base, a retractable lift mechanism, a work platform, a linear actuator, and a battery that comprises a scissor lift. It also explains the working for each part as the retractable lift mechanism has a first end attached to the base and can be switched between a position extended and a position retracted. In order to support a load, the work platform is designed. The work platform is coupled to the second end of the retractable lift mechanism and protected by it. The linear actuator is configured between the extended position and the retracted position to selectively shift the retractable lift mechanism. There is an electric lift motor in the linear actuator. The battery is designed to apply power to the motor of the electric lift. The fully electric scissor elevator is entirely devoid of moving fluids. Also, Murphy in [8] has come up with a design of a scissor lift which comprises a frame, a base, a scissor lift system, an actuator, a pair of pivot mechanisms, a pair of sliding guide members, a probe connector, and the cross. The positioning of the scissor lift mechanism The actuator is provided between the frame and the platform. The pair of pivot mechanisms lift and lower the horizontal position of the platform. The frame pair between ground

level and recipient hitch level stretches alongside the frame and connects the frame to the pivot mechanisms when sliding guide members. The connector of the probe is a receiver hitch for the cargo lift to be transported by a truck. The cross-bar is to connect the pair of pivot mechanisms to the connector of the probe. These designs give the author an idea about the structure of the scissor lift and the type of mechanism to be used in work.

The next step was to look for quantitative analysis of the scissor lift, which will be able to give an idea about the specifications of parts. Like here author found a research paper by Omar [9] where the research is based on a quantitative analysis scope of design, lifting to a height of 8 m and carrying capacity of 150 kg. The work defines the specifications that the author has to follow while designing the scissor-lift part like the scissor lift arm structure, scissor lift capacity by force analysis, ball-screw selection, actuator selection, material selection for the arms, and ball-screw mounting. This also gives an idea of specifications that has to be followed on the vehicle and its movements like force analysis, differential efficiency, which is required to change the axis of rotation, actuator selection, gearbox design, power requirement, and motor control. There is also a Finite element analysis on scissor-lift, which was conducted by Cengiz Görkem Dengiz and his group of researchers [10]. With a load-carrying capacity of 500kg and a working height of 2m, the design and analysis of a scissor lift system were carried out. The SolidWorks software has developed the solid model and assembly of the device, which was more useful for the author. The scissors and pins were made from materials from St37 and St52. The solid model and device simulation in the SolidWorks software was also carried out. The motion analysis was performed to choose the type of piston and to determine the piston force by the finite element method before the analysis of the device. The system's hydraulic circuit was developed using the Fluid-Sim software. The hydraulic accumulator in the system began to ensure the safe operation of the system in the event of any pressure loss (power failure, engine failure, etc.). By the Von-Mises hypothesis, the maximal stress of the device was calculated at the attachment points of the upper pair of scissors. The maximum deformation occurred at the upper shear link point, and this value was estimated to be 0.6941 millimeters. When there was no loading on the platform, the degree of deformation at the same stage was measured as 0.1173 millimeter. In order to open and close the system securely, a scissor lifting system has a double-acting hydraulic cylinder with a stroke of 400 millimeters and a diameter of 70 millimeters. The pump's maximum working pressure was also calculated as ~116 bar. According to the measurement of motor power at 1.5 kiloWatt, the electric motor was selected for this system. The minimum safety coefficient on the scissors was

detected as 4.3 when the machine was loaded with 500kilogram. Also, 6.2 was calculated as the minimum safety coefficient on the pins [10].

The optimal design for the scissor lift and its mathematical model has been established for the research in [11] by Sun and Liu. Here they have conducted a kinematic and kinetic simulation analysis with MATLAB/Simulink. The relative kinetic relationship, as well as the rules of change between the hydraulic cylinder and other components, have been developed. With Pro/E, a 3-D model of the scissor lifting mechanism was developed. Based on the results of simulation analysis, the design of the mechanism was optimized in Pro/Mechanical, which can direct and enhance the further design. The concept is scientific and rational and could serve as a theoretical guide and guideline for the design of other uses of the scissor lifting mechanism. [11] This research was a basic reference for the author to start with mathematical calculations to be conducted in the whole thesis.

Scissor lift with real-time self-adjustment capability based on the mechanism of variable gravity compensation appears to be one of the groundbreaking research[12] that also provides Naoyuki Takesue and his group of researchers with more knowledge on various mechanisms of gravity compensation. The author has built a mechanism in this study to enhance the inherent protection of vertical lifting machines against large actuators and to reduce their energy consumption. A variable GCM that uses two types of springs and can vary the compensation force was proposed in the studies. A VGCM-based scissor lift (pantograph lift) is proposed in this paper that uses three springs and a smaller actuator. A prototype is built and assembled, and the prototype's performance is experimentally tested. The findings show that the designed scissor lift meets the requirements of the design. Also, a load estimator is set up based on the scissor lift's dynamic model. A method of real-time self-adjustment that adjusts the compensation force automatically is proposed, and its effectiveness is checked. [12]

2.3 Controlling system prototypes

This section discusses the different types of remote-controlled systems and prototypes which will be useful for the author's work. In carrying out any operational task, all industries must be capable of using digital technologies. In order to improve a company's efficiency and output, the use of intelligent machines and automation

continues to be carried out. With the intention that the industry will thrive in the digital age as it is today, the use of conventional machines is gradually reduced and replaced with automatic machines. There are already some similar machines that work under the command of a remote in the industry. Here we found a prototype developed by Dani Setiawan and Abdul Tahir in the 2nd International Conference on Natural & Social Sciences [13]. There were three phases: first, designing machine construction and defining material requirements; second, constructing machine parts, installing and programming the control system; and third, running tests. The prototype, which is powered by the sun via solar panels and uses batteries to store energy, works with a maximum lifting capacity of 50 kilograms. There are several ways to do this, like using the Arduino Mega 2560, which employs the Atmega 2560 microcontroller chip. There is also a work where the Arduino Mega 2560 is equipped with a 16 MHz crystal and has been used in prototype forklift robots with an Android smartphone as its control device. In another study entitled Arduino Nano-Based Automatic Forklift Robot, the Arduino microcontroller of the nano type has also been used to control a forklift robot.

KAMIYA et al [14] used a system where a vehicle communication unit and a remote control device that has a remote communication unit and is used to remotely control the forklift. The received radio wave amplitude of a remote control signal is acquired by the wireless vehicle CPU of the commercial vehicle remote control system. The two communication units communicate wirelessly and decide whether the forklift is located in a permitted range based on the results of the communication.

In another research, Pappas et al [15] has come up with a device is given that can be placed on or inside a forklift, according to one or more embodiments. The machine can include a lifting system that raises or lowers the forklift vertically, a power supply, a memory that stores readable and executable components of the computer, and a processor that executes readable and executable components of the computer stored in the memory. The processor can be coupled operatively with: the plurality of sensors that sense conditions associated with the forklift, a context component that describes the forklift context, an analysis component that analyzes information from the plurality of sensors and the context component, and a control component that controls the forklift based on an analysis component performance, where the control involves the forklift being automatically raised or lowered. This has been the most recent work on automating the work of forklift, which helped the author to know more about the sensors used in the system and their working.

2.4 Conclusion of literature review

- Here most of the analysis was found to be done on the same design which is already in the industry. There is no research where the author could find a new prototype where the whole new design was developed.
- There are where few works that deal with the remote controlling system of the forklift or scissor lift. The only work done was a prototype that was only able to lift 50 kilograms.
- The author gets the idea of using SolidWorks as the designing and analyzing software as the file has to be converted and exported to other formats if FEA has been done in Ansys or any other software.
- There has only been a single work that gives the information in Automating the whole process of lifting. So that using that it is the current situation seems unrealistic as the author sticks on to the idea of a remote control system.
- The Current Situation of Covid-19 has been a major scarcity of human resources in the industries, which defines the importance of the work as it increases the efficiency of manpower.

3 DESIGNING CRITERIA

When it comes to forklift construction, there are a few aspects to consider first, such as the essential components of forklifts, the power supply being used, how the loading mechanism operates, the truck's size, and so on. These are the fundamentals of a forklift design, and they must be determined first before moving on to other details such as part dimensions and wheel selection. Also, there are fundamentals of scissor lift which is combined with this design. We'll go through the simple design guidelines in this chapter and get a sense of the truck's overall design. The basic components of the design start with a frame of the truck. The loading device, counterweight, power source, and wheels are all mounted to the forklift's foundation. The fuel and hydraulic tanks can already be built into the frame as part of the frame assembly.

Then comes the loading section of the design, where the machine lifts the weight and place it over the scissor lift. The mast, carriage, lifting chain, and forks are all included in this section. The mast is the vertical component that raises and lowers the load. It's hydraulically driven, and one or more hydraulic cylinders control it. In our build, it will be mounted in front of the forklift's frame. The carriage is where the forks or other connectors are attached. It moves up and down and is connected to the mast rails by chains or directly to the hydraulic cylinder. The mast and carriage are connected by a lifting line. When operating, forks are the bits that come into close contact with the cargo. Here the mast is connected to the sliding mechanism where a hydraulic cylinder helps to pull the load back to the center of the scissor lift.

The mass added to the rear of a lift truck frame is known as the counterweight. The counterweight's job is to stabilize the load that's being lifted. Usually, when a lift is powered by electricity, the huge lead-acid battery will serve as a counterweight. But in this work, the weight of the base part of the frame is increased to obtain stability while lifting the load to the required height.

An internal combustion engine, which can run on LP gas, CNG gas, oil, or diesel fuel, is one of the key alternatives. The electric forklift or scissor lift, on the other hand, is powered by either a battery or fuel cells to power the electric motors. A lift's electric

motors can be either DC or AC in nature. For our design, we chose an electric battery, which would serve as part of the counterweight.

The type of tire to use is determined by the working conditions. If the lift is used mainly indoors, solid tires should be used; if it is used outdoors, pneumatic tires should be used. Since we use our truck indoors, sturdy tires are the best option.

3.1 Different assemblies ideas proposed - design 1: 180° rotate forks with hydraulic pump

As we are combining two mechanisms of forklift and scissor lift, we have tried a different method of assemblies. That means we have a design of forklift which lifts the load from the ground, and then we have a design of forklift which can lift the weight to a height of 8 meters. In order to combine these two mechanisms, we have come up with a design that can rotate the load to a 180-degree angle after the lifting action of the forklift. This mechanism has its own disadvantages. The primary issue is the equipment's size. We need to make the piston long for the design to exceed a certain height. The piston must be slightly longer than the cylinder. A longer cylinder means a greater loading radius. Since the whole cylinder system must be hidden under the bottom of the design, we must raise the scissor lift. Also, in this type of assembly, other factors like torque and momentum while rotating must be considered. The structure shown in the figure 3.1.1 shows a similar example.

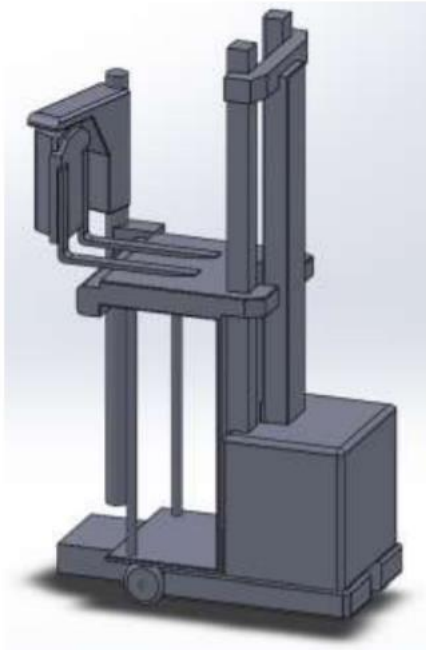


Figure 3.1.1 Test design

3.2 Design 2: fork pulling with lead screw

Secondly, the author looks forward to the idea of using a lead screw system to pull back the load from the forklift system to the center of the scissor lift. At first, the forklift assembly, which includes the cylinder, chain, and fork, is placed on the chassis of the design to decrease the forces needed to lift up the design, as shown in the figure. But the main problem with this design is the working of both mechanisms. Also, found it impossible to fix the conveyor system, so in order to pull the weight back, the author used a screw mechanism. In order to support this mechanism, this is mounted and fixed upon the scissor lift, as shown in Figures 3.2.1 and 3.2.3.

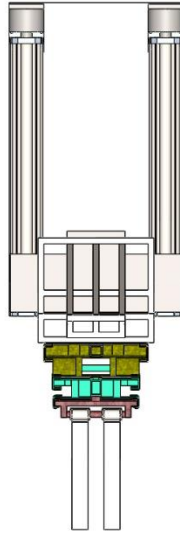


Figure 3.2.1 Top view of the design

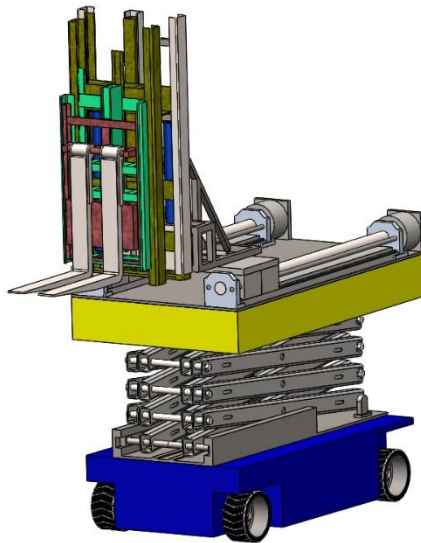


Figure 3.2.2 Normal 3D view

3.3 Comparison of design ideas proposed

Tabel 3.3.1 The advantages of the second design over the 1st one

| | Design 1 | Design 2 |
|---|----------|----------|
| Torque | Yes | NA |
| Loading and transportation efficiency | Low | High |
| Rotation angle | 180 | 0 |
| Flexibility in terms of cargo and attachments | Low | High |
| Vehicle stability | medium | High |

3.4 Stability of the design

Since we are dealing with lifting load, considering safety is one of the important factors. For a 4-wheel forklift, the stabilization mechanism consists of three points of contact: two front wheels and the middle of the rear axle. When a forklift raises cargo, the center of gravity seems to change to the front wheel line due to the added weight, which contributes to our first issue, loading mechanism stability. We need to make sure the truck doesn't fall over while sitting idle. We need to examine whether the forklift is stable under static conditions, as we already have data on the mass properties of all the components. As a result, the forklift's center of gravity must remain within the safety triangle. If we want to increase the size of the safety triangle from one to two, we need to widen the gap between the two front wheels while also shortening the length of the auto body. As long as the truck's center of mass remains within triangle 2, such a move is legal.

The author used the same idea for the stabilization of the forklift part of the design. Here the author has found the center of mass of each part of the mechanism while lifting the load at different positions. Then a common reference place is taken, and the perpendicular distance to this place is calculated. After getting the mass and

perpendicular distance from a particular axis, i.e., x-axis and z-axis, calculate the center of mass on that particular plane. Since there is no lateral movement y-axis is ignored.

In this design, the center of gravity changes mainly at four positions. Here the author has considered the different center of gravity while lifting a 1-ton load. The center of gravity must remain inside the triangle in order to consider the change in the center of gravity while the lifting process by the forklift part of the assembly, the stability pyramid, is considered. This assembly doesn't use the lifting process of the forklift assembly beyond a limit. So, Z-axis factor in the stability pyramid doesn't play many roles here.

In order to find the center of mass in Solidworks, the author starts with a part where a command is added. So under features, it's gonna be in reference geometry. This will provide a visual indicator at the spot of the center of mass of the part. In the mass properties, we can see the X, Y, Z properties which give the distance of this point from each reference plane. The position of this point can be changed by adding mass to different sides of the part. Similarly, in assembly, the author inserts the center of mass at the assembly level and can be changed according to the changes in the size and mass of different parts. The center of gravity is measured with respect to the origin of the machine, which is located at the bottom center of the truck, as shown in figure 3.4.1.

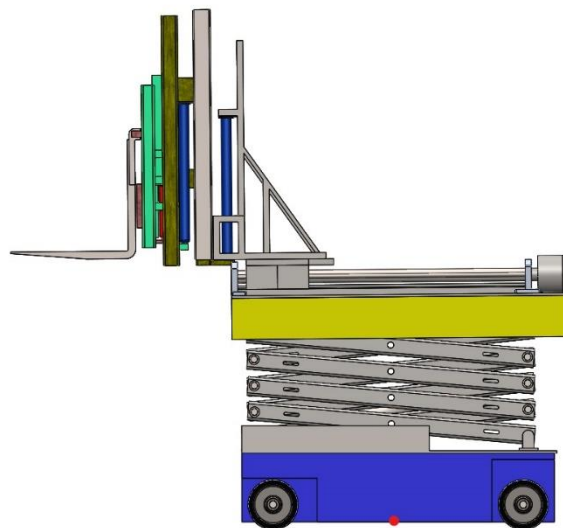


Figure 3.4.1 Midpoint of the truck (red mark)

3.4.1 Centre of gravity without the load

The total mass of the machine = 13413.346 Kg

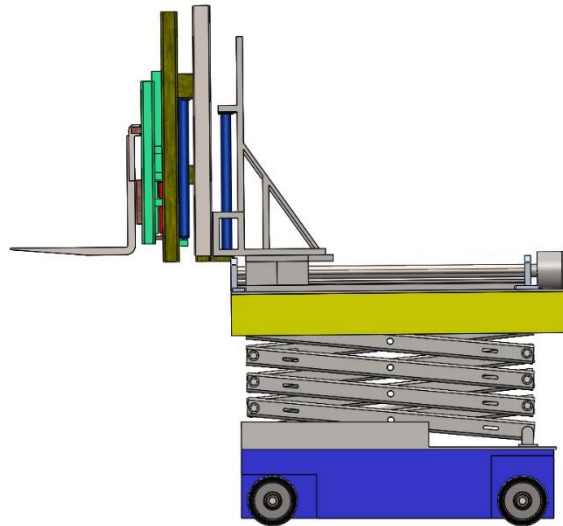


Figure 3.4.2 Design forklift position

1. Design neutral position

The location of the centre of gravity in relation to the machine's central frame may be found in appendix 22. The moment of inertia on each axis is also calculated for each location.

$$X = -13.07\text{mm}$$

$$Y = 773.62\text{mm}$$

$$Z = -1.57\text{mm}$$

2. Design forklift position

Refer to the appendix 23 for the position of the centre of gravity with respect to the centre frame of the machine. Also the moment of inertia on each axis for each position is also determined.

$$X = 156.74\text{mm}$$

$$Y = 773.62\text{mm}$$

$$Z = -1.57\text{mm}$$

3. Design loading position

More information on the position of the centre of gravity in relation to the machine's centre frame, as well as the moments of inertia at each position, may be found in appendix 24.

$$X = 157.74\text{mm}$$

$$Y = 710.31\text{mm}$$

$$Z = -1.57\text{mm}$$

From the appendix 22 to 24 , the x-axis in all of the figures depicting the center of gravity (without load) ranges from -13,07mm to 157.74mm, the y axis from 772.62 to 710.07, while the z-axis does not vary. Also the moment of inertia at each axis is also considered which can be The x-axis represents the forward and back movement of the center of mass, while the y axis represents the up and down movement of the center, which is dependent on the machine's height. The z-axis remains unchanged since there is no horizontal movement. According to the behaviour of the center of mass under no load condition, it is clear that the design system is stable under the no load condition. Also the stability triangle of the design has an area of 1575000mm² and the horizontal deviation of the centre of gravity stays within this area. As the centre of gravity stays within the stability triangle.

3.4.2 Center of gravity with the load of 1002 Kg

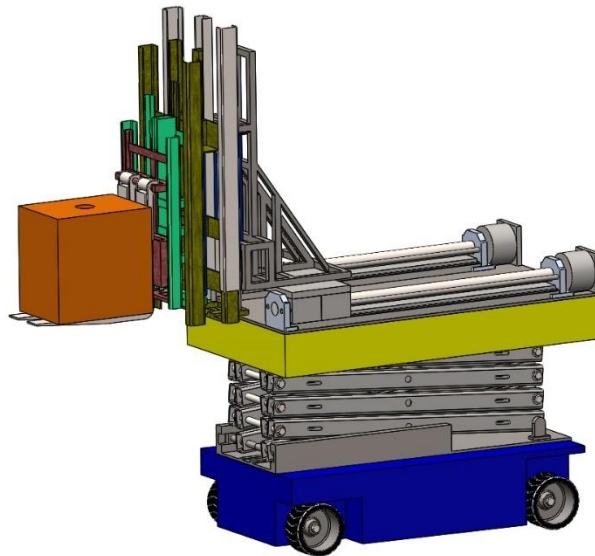


Figure 3.4.3 Design loading position (with load)

1. Design forklift loading position

Appendix 25 has more information on the centre of gravity's position in respect to the machine's centre frame, as well as the moments of inertia at each position. Position of the centre of gravity with respect to the centre frame of the machine is given below.

$$X = 277.73\text{mm}$$

$$Y = 699.22\text{mm}$$

$$Z = -1.73\text{mm}$$

2. Design loading position (with load)

More information on the position of the centre of gravity in relation to the machine's centre frame, as well as the moments of inertia at each position, may be found in appendix 26. Position of the centre of gravity with respect to the centre frame of the machine is given below.

$$X= 277.15\text{mm}$$

$$Y=846.16\text{mm}$$

$$Z=-1.73\text{mm}$$

3. Neutral position (with load)

The location of the centre of gravity in relation to the machine's central frame may be found in appendix 27. The moment of inertia on each axis is also calculated for each location. Position of the centre of gravity with respect to the centre frame of the machine is given below.

$$X= 26.86\text{mm}$$

$$Y=857.13\text{mm}$$

$$Z=-1.73\text{mm}$$

4. Design lifting position at 4 meters from the ground

For the location of the machine's centre of gravity in relation to the central frame, see appendix 28. The moment of inertia on each axis is also computed for each location. Position of the centre of gravity with respect to the centre frame of the machine.

$$X= -16.86\text{mm}$$

$$Y=1382.13\text{mm}$$

$$Z=-1.73\text{mm}$$

5. Design lifting position at maximum (7 meters from ground level)

Appendix 26 has more details on the position of the centre of gravity in respect to the machine's centre frame, as well as the moments of inertia for each axis. Position of the centre of gravity with respect to the centre frame of the machine.

$$X= -44.84\text{mm}$$

$$Y=1970.58\text{mm}$$

$$Z=-1.73\text{mm}$$

With the increase of load, the researcher tested the machine's center of mass. The variance was high at first, as predicted, but after adding a counterweight to the machine, the author achieved a much better result, as demonstrated in the above figures. These results are predicted to fall within the stability triangle, making the design safer. At the greatest height of the lifting action, the x-axis in all of the images displaying the center of gravity (with load) ranges from 277.73 to -44.84 millimeters, the y axis from 699.22 to 1970.58 millimeters, and the z-axis does not fluctuate. Well, the researcher

discovered a little difference in the z-axis with and without load, which is easily overlooked. It is also observed that the center of gravity of the system is always located near to the center axis of the system. Therefore, it can be concluded that the system is stable under the load condition (1002 Kg load).

3.4.3 Stability triangle

The stability triangle of the design can be found by connecting the front two wheels and the pivot point on the back axle. Here the tilting of the machine due to the variation in the center of mass in the horizontal plane is considered. But in this design, the center of mass varies vertically. Therefore here, the author considers the stability pyramid. The stability of the forklift system is considered as calculating the stability pyramid of the system. Here author calculated the stability pyramid during the neutral position and high lifting position with the dimensions of the design and considered the centre of gravity during the neutral position as its centre point. While considering the stability triangle of the design in the horizontal plane, the area of the triangle is calculated to be 1575000mm^2 . Also, the researcher considered the stability pyramid of the design exactly at the neutral and maximum height of the design. At the neutral positioning of the design, the stability pyramid has a length of 1500mm and base height of 2100mm and a pyramid height of 3962.18mm. Therefore the whole volume of the stability pyramid is 2080144500mm^3 at neutral and 5755144500mm^3 at maximum height. The author considers the centre of gravity at neutral as the midpoint of the triangle. As the deviation in the above coordinates proves to be minimal, hence it is easily proved the centre of gravity stays within the volume of the pyramid in each scenario.

4 DRIVING SYSTEM

4.1 Hydraulic circuit

Here the author comes up with the system for the actuation of the lifting cylinders and steering cylinders with hydraulics. The author has used the system where it uses one hydraulic tank, a hydraulic pump, filter, solenoid-operated direction control valve, and six single-acting double cylinders.

The spool within the direction control valve regulates the pressure from a pump to either side of a hydraulic cylinder in this hydraulic actuation system. The cylinder expands and contracts in response to the pressure applied from both sides. The pump's shaft will be driven by a motor, which will regulate the speed, and a control system will modify the valve's position. This is the fundamental system that the author will use for the design; the number of cylinders will vary depending on the amount of lifting operations performed by design.

To use this system in a SolidWorks design, the author must first create it in Simulink using Simscape fluids, then connect it to the model. This is done by typing `ssc new` into the Matlab command window, which will open a Simulink model using Simscape model parameters. The author chose a fixed displacement pump with an ideal hydraulic reference as an input, which symbolizes the hydraulic tank, as the starting point for the system design. The fluid must then pass via a directional control valve before reaching the actuator. As a result, the design required at least a one-way directional valve to function. The specifications of the selected valve in Simulink are adjusted in accordance with the datasheet, and the valve's size must also be increased to match the pump. The valve's P port is then linked to the pump's output. However, the author installs a pressure relief valve in between to lessen the pressure of the fluid pushed by the pump. The relief valve's characteristics were also altered to meet design requirements. The hydraulic reference is on the low side of the relief valve and directional valve. After that, a hydraulic actuator is installed and linked to the directional control valve. The author now defines cylinder specifications such as piston stroke, width, and hard stop parameters. The mechanical connection of the cylinders is to be connected to the 3D design and the output to the scope. The author repeats the same process to the total number of cylinders needed for the procedure.

The system's inputs must now be given as a single input to the pump. The pump is an ideal mechanical connection with a perfect angular velocity source as the input. This source is also fixed in space, and the stable block determines the pump's rotational speed. The spool placement is the following input, and the author utilizes a Simulink signal to do this. The indications for the movement of the spool in the meter are generated using a sine wave. After that, a hydraulic fluid block is added to define the hydraulic fluid and the specifications. But here, in this design, the author focuses more on the lifting action than the steering aspects. Therefore, researcher made the combined circuit for the different sets of hydraulic cylinders used in the design.

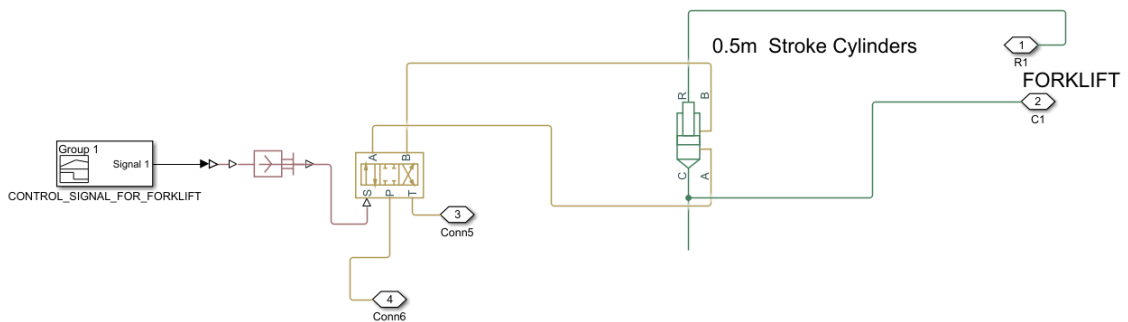


Figure 4.1.1 Forklift subsystem part 1 hydraulic circuit

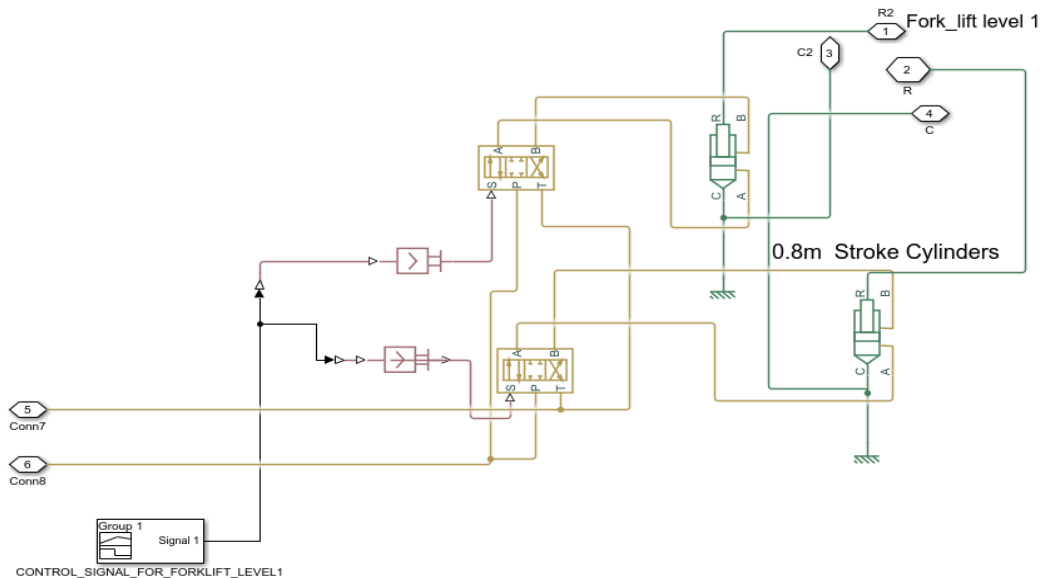


Figure 4.1.2 Forklift level 1 hydraulic circuit

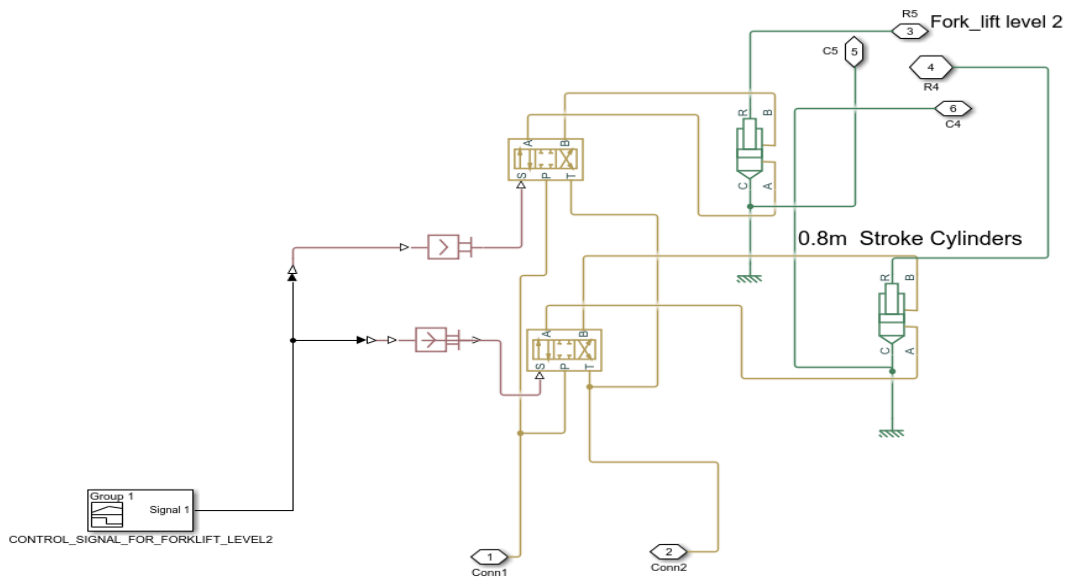


Figure 4.1.4 Forklift level hydraulic circuit

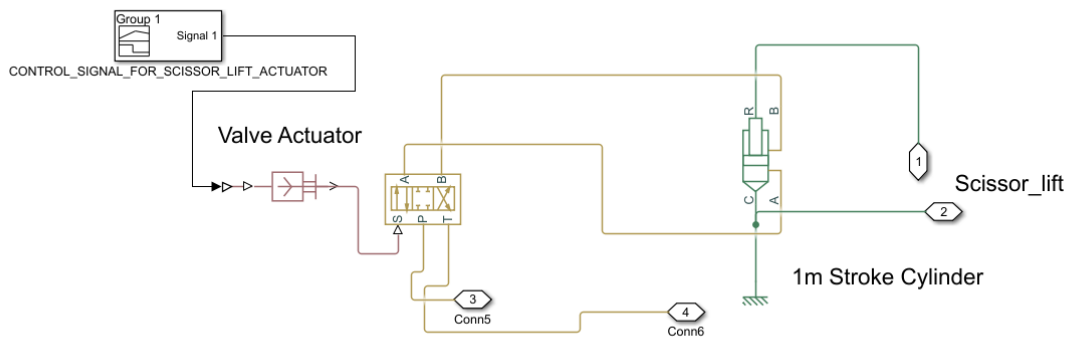


Figure 4.1.3 Scissor lifts hydraulic circuit

When the author completed the circuit for the entire assembly, another issue arose. The problem was that the circuit needed to be compiled with the design, which took a long time and left several functions inoperable. As a result, the researcher had to divide the circuits into separate units for each system's functions. There are three levels of forklifts in this system; the author first designs a different hydraulic circuit for the first level forklift, represented in figure4.1.1 as the forklift subsystem, and has a stroke length of 0.5m. The courses for the second and third cylinders are labeled forklift level 1 and forklift level 2, respectively, as illustrated in figure4.1.2 and figure4.1.3. These systems likewise include two 0.8m stroke length cylinders. As indicated in the diagram, distinct

control signals are sent to each valve actuator, causing the directional control valve to function correctly. The author then turned his attention to the scissor lift's hydraulic circuit. This circuit comprises a single hydraulic cylinder with a 1m stroke length, as shown in figure 4.1.4. The fluid from the valve and the input to the directional control valve both exit the figure, as shown in each image. Figure 4.1.5 shows a single hydraulic tank connected to each figure, and the author utilized the Skydrol LD-4. Low density, good thermal stability, valve erosion prevention, and deposit management are all hydraulic fluid properties. It has earned a reputation as the gold standard among Type IV fluids due to its high thermal stability under real-world settings.

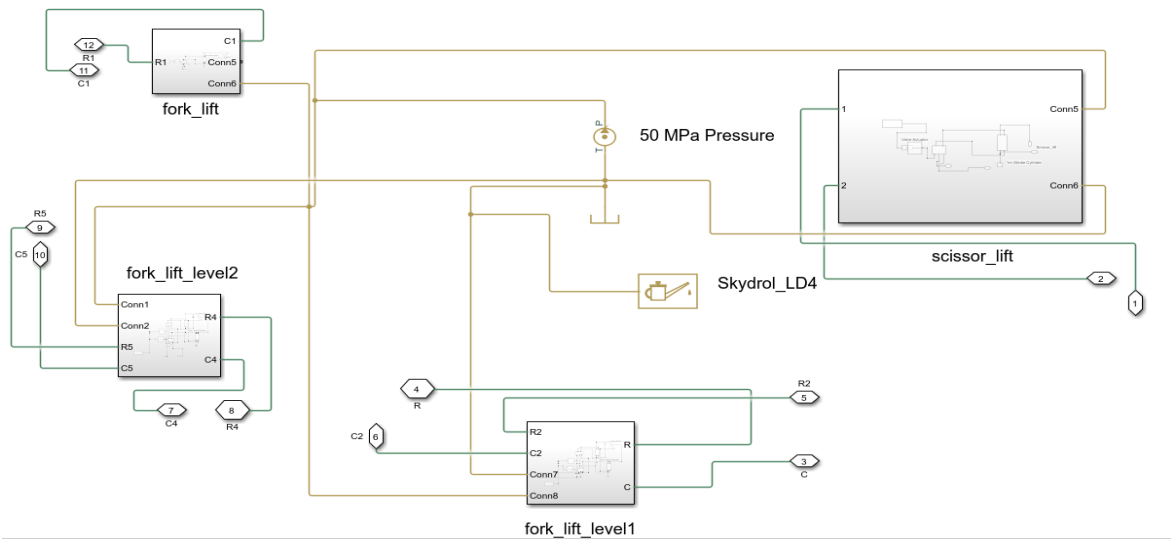


Figure 4.1.5 Combined assembly of the hydraulic circuit. Skydrol_LD4 shows the hydraulic fluid tank.

4.2 Electrical circuit

The electrical circuit is depicted in figure 4.2.1. This circuit is responsible for dragging the design's forklift assembly back and forth on the scissor lift assembly. The author employs two pulse width modulation generators, two h bridge circuits, and two 1.5 kW dc motors linked to two separate lead screws in this circuit. Because the dc motor rotates clockwise and anticlockwise, the author employed h bridge circuits to shift the polarity of the voltage applied to it. PWM generators were used to implement H-bridge, and the

same unit provides the signal to these circuits since both lead screws must revolve simultaneously.

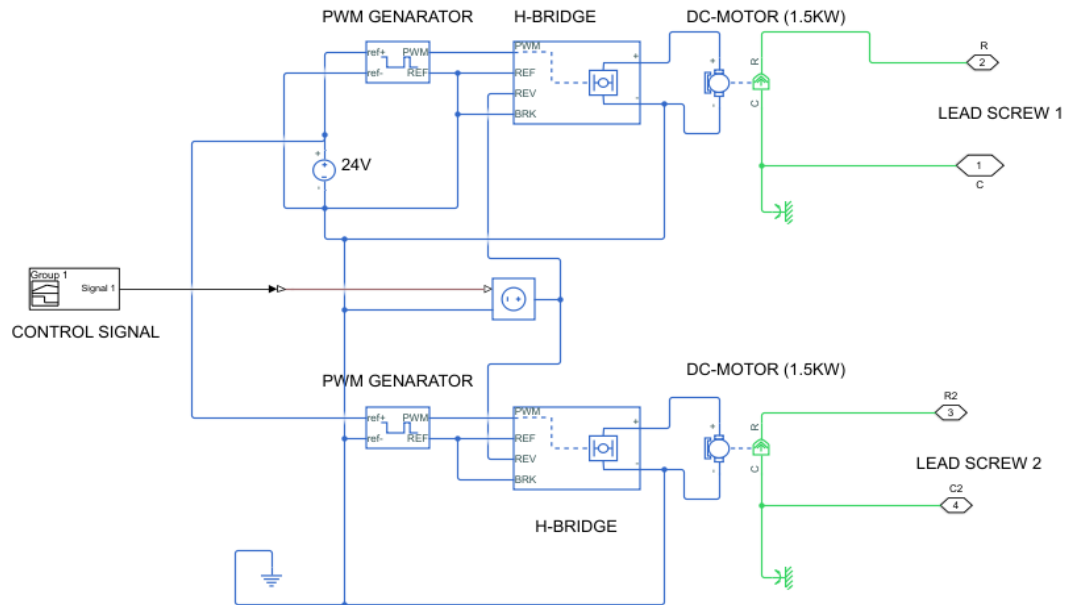


Figure 4.2.1 Electrical circuit for lead screws

5 STATIC ANALYSIS OF THE COMPONENT

In the static analysis, the author considers the components' stress, strain, and displacement while having the load. This helps to give an understanding of the strength of the design and also about the deformations happening, if any.

5.1 Fork

According to the static analysis performed for the fork, it is observed that when applying a 10000N load to the fork, the von mises stress is not exceeding the yield stress of the fork material. Therefore, it can be concluded that under the static condition, the forks are strong enough to handle a 10000N load. Since the design is lifting 1000Kg, in actual operation, the applied force for 1 Fork is 5000N. Therefore, the fork design will not be failed during the actual operation.

Alloy steel is steel composed of materials like molybdenum, manganese, nickel, chromium, vanadium, silicon, and boron. Combining these elements increases the overall strength, hardness, wear resistance, and toughness. Alloy steels offer economy, durability, high strength, high strength to weight ratio, and highly efficient performance under harsh and unfavorable conditions. Maximum Elastic modulus (resistance offered by a material against deformation when a stress is applied to it) and tensile strength (maximum load a material can support without breaking or stretching) for alloy steel is 210000N/mm² and 723.8256 N/mm². Material has a Poisson's ratio of 0.28 N/A (deformation of the material in directions perpendicular to the specific direction of loading). Yield strength – 620.422N/mm²(maximum stress that can be imposed on a material without causing plastic deformation. Mass Density – 7700kg/m³ (Material density per unit volume). Material properties of fork is available in the appendix 48.

Stress

Here author applied the maximum load of 5000N for each fork. The figure shows that the stress doesn't go above 0.00145N/mm², and from the property of the material, the

tensile strength and yield strength are both above that. Therefore it is proved that stress for the fork stays within the limit.

Model name: Fork
Study name: Static 1(-Default-)
Plot type: Static nodal stress Stress1

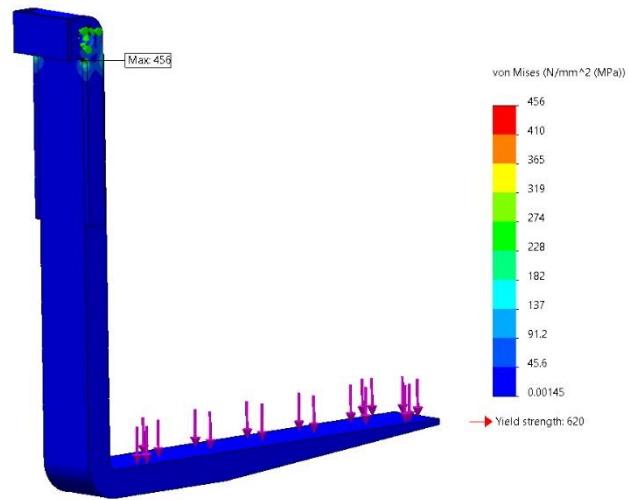


Figure 5.1.1 Stress of fork

Displacement

The deformation of the fork after applying 5000 N is shown in the figure, and it is obvious that the deformation is maximum at the tip of the fork. At the tip of the fork, the maximum deformation goes to 7.82mm, which is affordable as the remaining section of the fork stabilizes the load.

Model name: Fork
Study name: Static 1(-Default-)
Plot type: Static displacement Displacement1

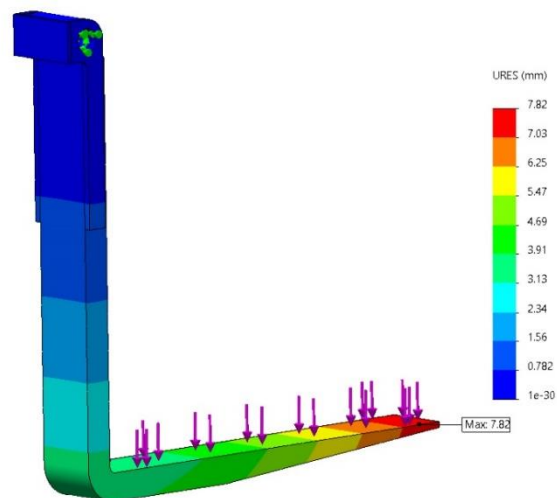


Figure 5.1.2 Displacement of fork

Strain

Here the strain on the component is calculated during the application of load. And from the figure, it is during the analysis; that the equivalent strain stays stable at most of the sections of the component below 0.000000033. This is acceptable as the ratio of stress to the elastic modulus for the material stays above for the given material than the produced strain.

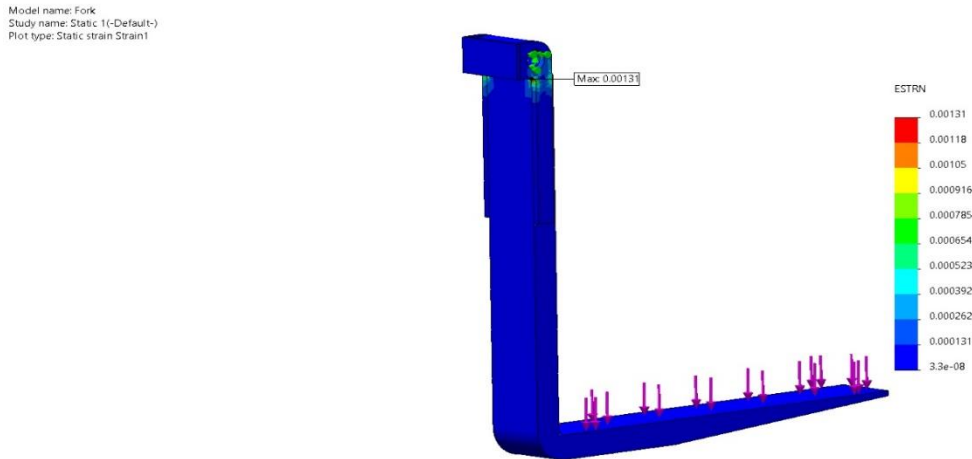


Figure 5.1.3 Strain of fork

Factory of safety

When a 10000N load is applied to the fork, the von mises stress does not exceed the yield stress of the fork material, according to the static analysis done on the fork. This can also be plainly identified by analyzing the FOS contour figure. The lowest FOS value, according to it, is 1.36. As a result, it may be determined that the forks are capable of handling a 10000N load in a static situation. During the real operation, the fork design will not fail.

Model name: Fork
Study name: Static: 1(-Default-)
Plot type: Factor of Safety Factor of Safety/1
Criterion: Automatic
Factor of safety distribution: Min FOS = 1.4

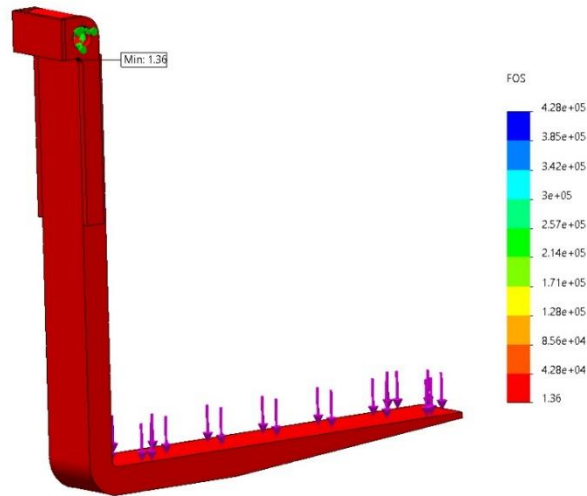


Figure 5.1.4 Factor of safety of the fork

5.2 Fork guide

According to the static analysis performed for the fork guide, it is observed that when applying a 12000N load to the fork, the von mises stress is not exceeding the yield stress of the fork material. Therefore, it can be concluded that under the static condition, the fork guides are strong enough to handle a 12000N load which is less than the actual operation load.

Galvanized steel is corrosion-resistant steel widely used to make corrosion-resistant nuts, nails, and bolts. It has good tensile strength and is widely used for outdoor purposes. They are manufactured by the hot-dip galvanizing method, which provides long-term corrosion protection t, making it a suitable option. We are using the Linear Elastic isotropic model, which has a mass density of 7870 kg/m^3 and a tensile strength of 3569.5 N/m^2 . Material properties of fork guide is available in the appendix 47.

Stress

The fork guide designed by the author has a yield strength of 203900000 N/m^2 . But here, the maximum stress produced by applying load on the design stays very low. As the maximum point on the component for the stress remains below $0.0000000000521 \text{ N/m}^2$. Hence it is proved the component can easily manage the stress produced by the load.

Model name: fork_guide
Study name: Static 1(-Default-)
Plot type: Static nodal stress Stress1

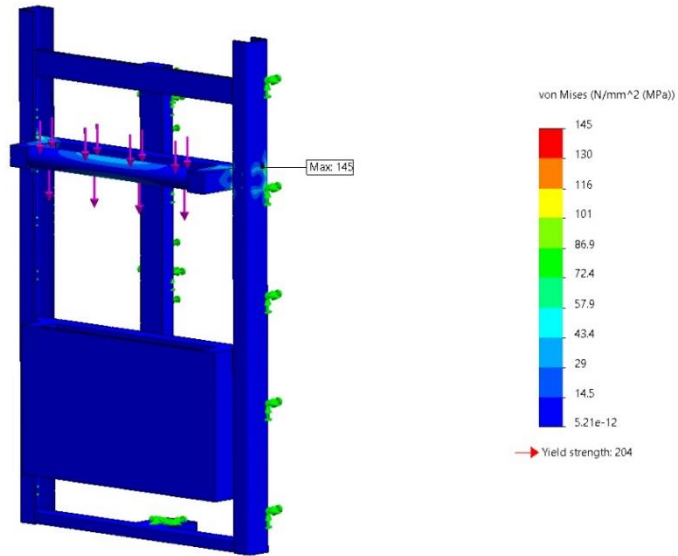


Figure 5.2.1 Stress of fork guide

Displacement

This figure refers to deformation produced during the application of load. It is shown in the figure that the maximum deformation is happening at the base of the guide. This deviation is not exceeding more than 0.347 mm, which is a negligible quantity.

Model name: fork_guide
Study name: Static 1(-Default-)
Plot type: Static displacement Displacement
Deformation scale: 1

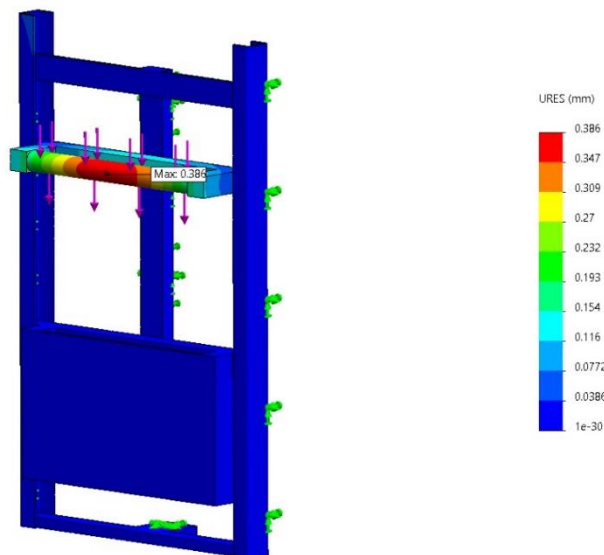


Figure 5.2.2 Displacement of fork guide

Strain

During the application of load, the strain on the component is determined. And as seen in the picture, the corresponding strain remains steady through the component's section

below .000000000000000036. This is acceptable since the stress to elastic modulus ratio for the specified material remains higher than the resultant strain.

Model name: fork_guide
Study name: Static 1(-Default-)
Plot type: Static strain Strain1
Deformation scale: 1

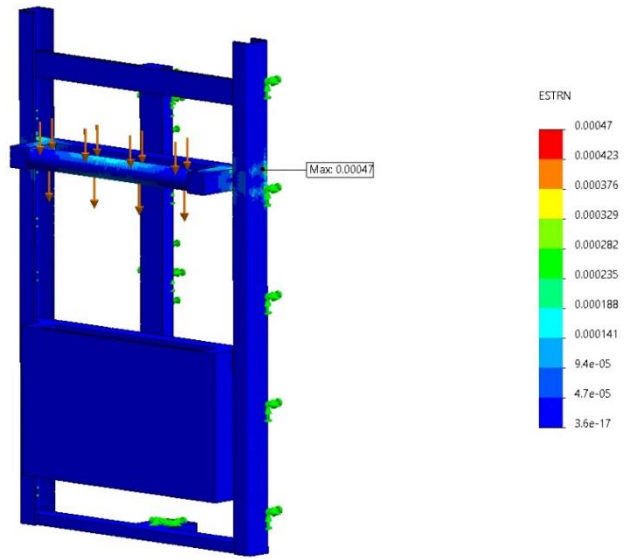


Figure 5.2.3 Strain of fork guide

Factor of safety

When a 12000N load is applied to the fork guide, the von mises stress does not exceed the yield stress of the fork material, according to the static analysis done on the fork guide. This can also be plainly identified by analyzing the FOS contour figure. The lowest FOS value, according to it, is 1.41. As a result, it may be determined that the fork guide is capable of handling a 12000N load in a static situation. During the real operation, the fork design will not fail.

Model name: fork_guide
Study name: Static 1(-Default-)
Plot type: Factor of Safety Factor of Safety1
Criterion: Automatic
Factor of safety distribution: Min FOS = 1.4

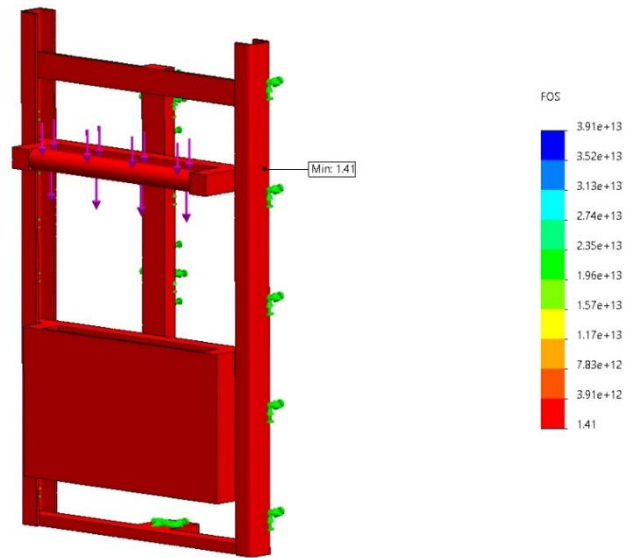


Figure 5.2.4 Factor of safety of fork guide

5.3 Fork mount

Based on the static analysis performed on the Fork mount, it is observed that the fork mount can stand for 16000N force. In actual operation, the fork mount should be able to handle a load of around 10000N. Therefore, based on the results of the static analysis, it can be concluded that the Fork Mount is strong enough to work with the actual operation of the system.

Compared to other steels, plain carbon steel has a low carbon content and is cold worked low carbon steel that cannot be easily tempered. It has a good tensile strength(350-370Mp), percentage elongation of 28-40%(strain at fracture in tension), and high ductility so that it can be highly used in cold-rolled steels. Plain carbon steels are strong, tough, and relatively cost-effective compared to other steels, which makes them a suitable option for our application. It has a Poisson's ratio of 0.28 N/A and a yield strength of 220594000 N/M². All the material properties of fork mount is available in the appendix 46.

Stress

The yield strength of the author's fork mount is 220600000 N/m². Again, the maximum stress produced by applying load to the design remains quite low. As the highest stress on the component remains below 51700000 N/m², it may be concluded that the component can readily manage the load's stress.

Model name: fork_mount
Study name: Static 1(-Default-)
Plot type: Static nodal stress Stress1

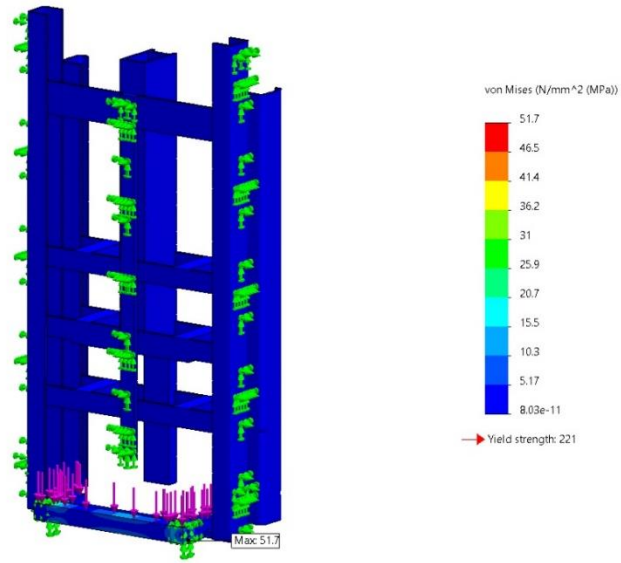


Figure 5.3.1 Stress of fork mount

Displacement

Here the author looks into the deformation produced by the load on the fork mount. As the stress stays within the limit, deformation also remains within the limit. Here from the figure, it is shown that the maximum deformation is 0.0393 mm, which is again very inconsiderable.

Model name: fork_mount
Study name: Static 1(-Default-)
Plot type: Static displacement Displacement1

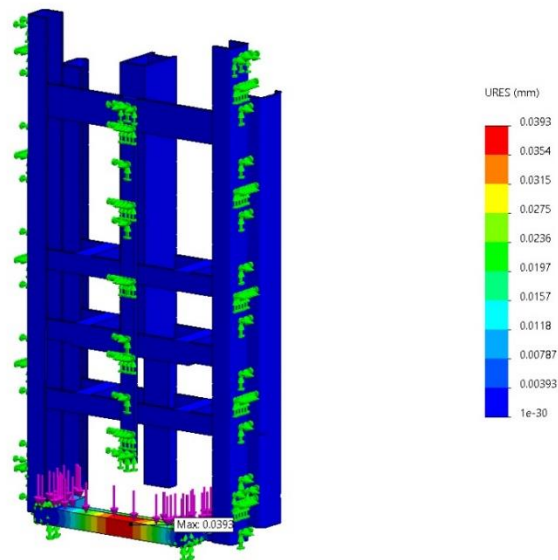


Figure 5.3.2 Displacement of fork mount

Strain

The strain on the component is determined during the application of load. And as shown in the above analysis, the equivalent strain remains constant throughout the component's section below 0.0000294. This is again allowed because the stipulated material's stress to elastic modulus ratio remains higher than the resultant strain, which is 0.001050462.

Model name: fork_mount
Study name: Static 1(-Default-)
Plot type: Static strain Strain1

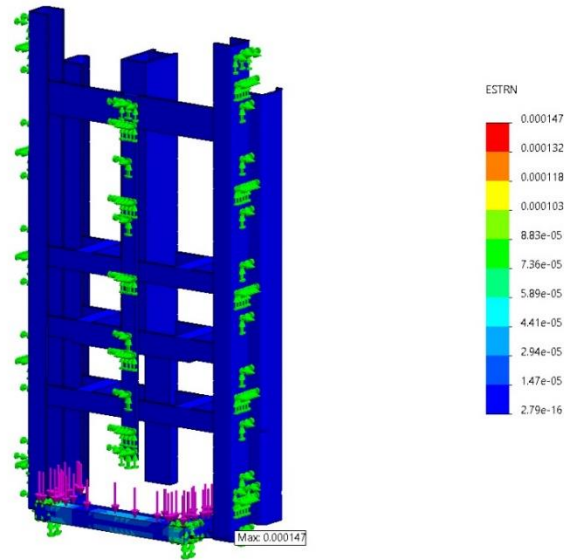


Figure 5.3.3 Strain of fork mount

Factory of safety

When a 16000N load is applied to the fork guidemount, the von mises stress does not exceed the yield stress of the fork material, according to the static analysis done on the fork mount. This can also be plainly identified by analyzing the FOS contour figure. The lowest FOS value, according to it, is 4.27. As a result, it may be determined that the fork mount is capable of handling a 16000N load in a static situation. During the real operation, the fork design will not fail.

Model name: fork_mount
Study name: Static 1(-Default-)
Plot type: Factor of Safety Factor of Safety1
Criterion: Automatic
Factor of safety distribution: Min FOS = 4.3

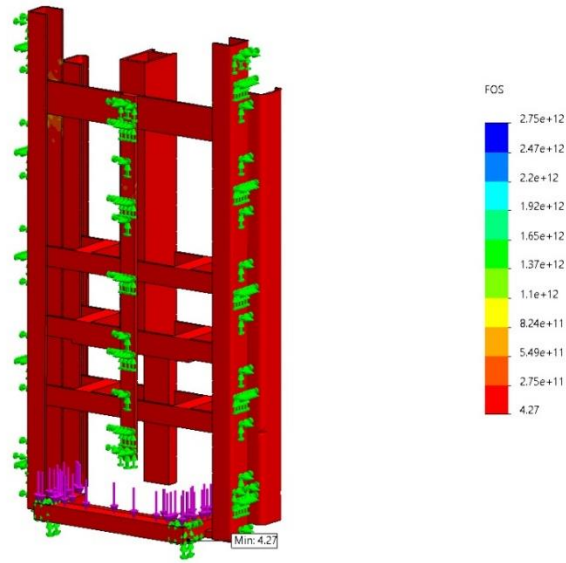


Figure 5.3.4 Factor of safety fork mount

5.4 Forklift level2 guide

According to the static analysis that is performed for the forklift level2 guide, it is observed that when applying a 16000N load to the forklift level2 guide, the von mises stress is not exceeding the yield stress of the manufactured material. Therefore, it can be concluded that under the static condition, the forklift level2 guide is strong enough to handle a 16000N load which is less than the actual operation load.

As described in the previous section 5.2, we are using the same galvanized steel with similar characteristics and properties in this scenario. Material properties of forklift level2 guide is available in the appendix 45.

Stress

On the forklift guide, the applied load is 16000 N, and the yield strength of the material is approximately 203900000 N/m². The figure shows the maximum stress produced by the load is 40400000N/m² which stays lower than our value. Therefore the stress factor for this component doesn't affect the working of the design.

Model name: fork_lift_second_guide
Study name: Static 1(-Default-)
Plot type: Static nodal stress Stress1

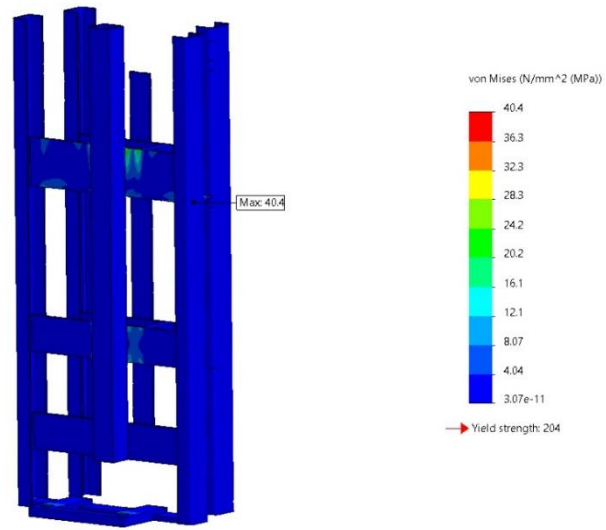


Figure 5.4.1 Stress of fork lift

Displacement

Deformation for the forklift mount was the only issue we have been concerned about and came to design support which produces very less deviation. From the above analysis, we have found the maximum deviation produced by design is 0.133 mm. Again author manages to diminish the deviation to a negligible level.

Model name: fork_lift_second_guide
Study name: Static 1(-Default-)
Plot type: Static displacement Displacement1

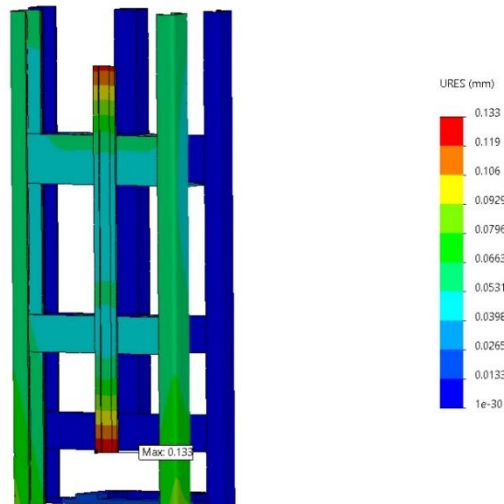


Figure 5.4.2 Displacement of fork lift

Strain

Here the strain component doesn't seem to be varying much. The equivalent strain stays constant throughout the component's part below 0.00000769 , as indicated in the preceding study. This is permitted once more since the specified material's stress to elastic modulus ratio is greater than the consequent strain of 0.001019162 .

Model name: forklift_second_guide
Study name: Static 1(-Default-)
Plot type: Static strain Strain1

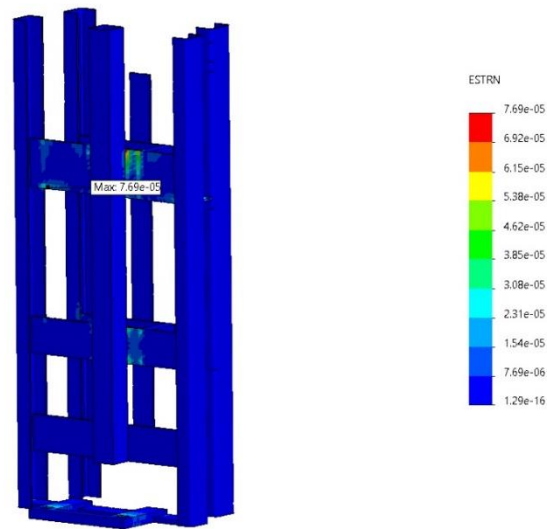


Figure 5.4.3 Strain of fork lift

Factor of safety

When a 16000N load is applied to the forklift second guide, the von mises stress does not exceed the yield stress of the selected material for the static analysis done on the forklift second guide. This can also be plainly identified by analyzing the FOS contour figure. The lowest FOS value, according to it, is 5.05 . As a result, it may be determined that the forklift second guide is capable of handling a 16000N load in a static situation. During the real operation, the fork design will not fail.

Model name: forklift_second_guide
 Study name: Static 1(-Default-)
 Plot type: Factor of Safety Factor of Safety1
 Criterion: Automatic
 Factor of safety distribution: Min FOS = 5.1

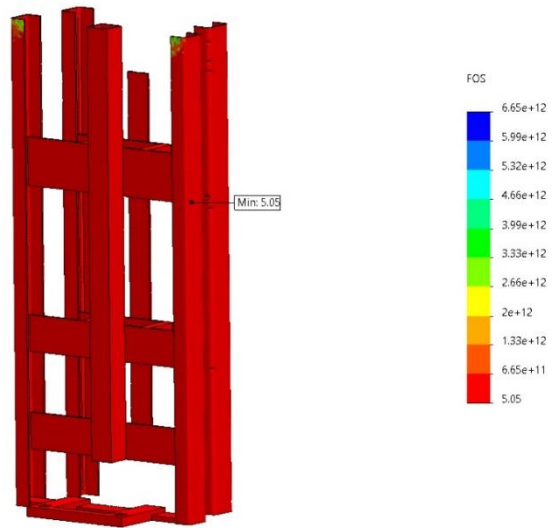


Figure 5.4.4 Factor of safety of forklift

5.5 Forklift drive guide

According to the static analysis that is performed for the forklift drive guide, it is observed that when applying a 22000N load to the forklift drive guide, the von mises stress is not exceeding the yield stress of the manufactured material. Therefore, it can be concluded that under the static condition, the forklift drive guide is strong enough to handle a 22000N load which is less than the actual operation load.

Alloy steel is steel composed of materials like molybdenum, manganese, nickel, chromium, vanadium, silicon, and boron. Combining these elements increases the overall strength, hardness, wear resistance, and toughness. Alloy steels offer economy, durability, high strength, high strength to weight ratio, and highly efficient performance under harsh and unfavorable conditions. Here we have a tensile strength of 723825600 N/M² and a mass density of 7700 kg/m³. Material properties of forklift drive guide is available in appendix 44

Stress

The maximum yield strength of the author's forklift drive guide is 62040000 N/m². Again, the maximum stress produced by applying load on the side in the vertical direction of the design remains quite low compared to the whole available stress. As the

Figure 5.5.1 Material properties of forklift drive guide

highest stress on the component remains below 23300000 N/m², it may be concluded that the component can readily manage the load's stress.

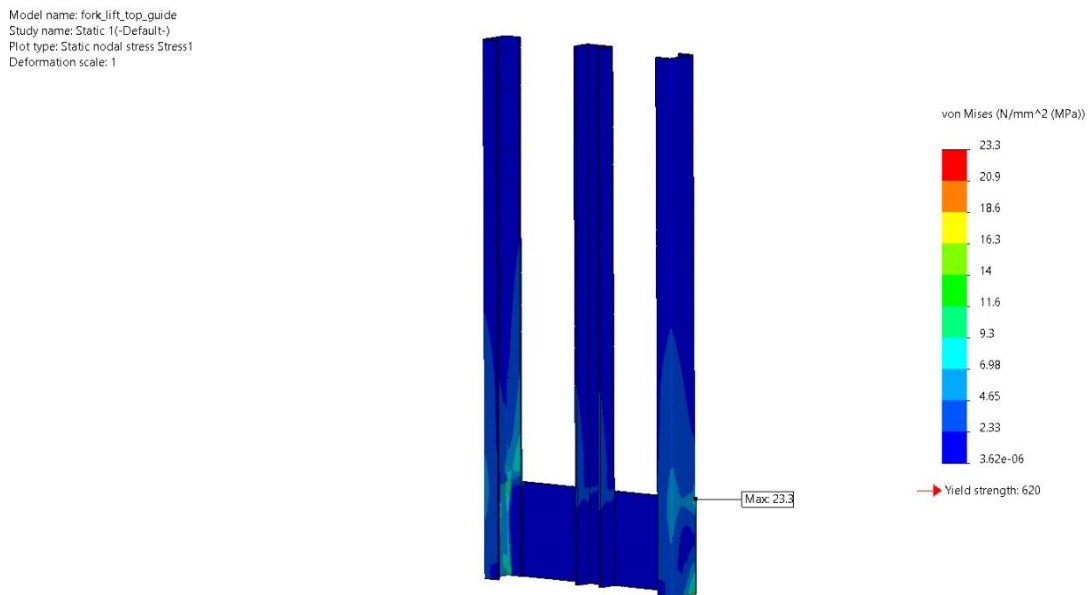


Figure 5.5.2 Stress of forklift drive guide

Displacement

This figure refers to the rate of deformation produced during load application. It is shown in the figure that the maximum deformation is happening not on the base but on both sides of the guide in the vertical direction. This deviation is not exceeding more than 0.535 mm, which is a negligible quantity.

Model name: forklift_top_guide
Study name: Static 1(-Default-)
Plot type: Static displacement Displacement1
Deformation scale: 1

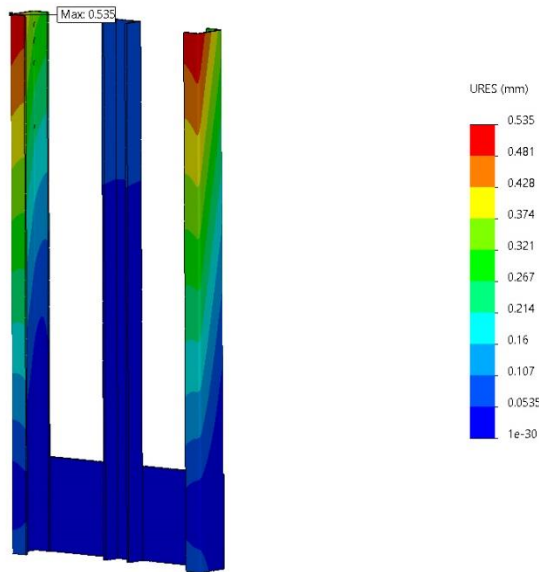


Figure 5.5.3 Displacement of forklift drive guide

Strain

Just as in the previous scenarios, the strain on the component is calculated during the load application. During the analysis, the equivalent strain stays stable at most of the component sections but is greater than the previous case of 0.00000514 . This is acceptable as this slightest change still ensures that the ratio of stress to the elastic modulus for the material stays above the given material than the produced strain.

Model name: forklift_top_guide
Study name: Static 1(-Default-)
Plot type: Static strain Strain1
Deformation scale: 1

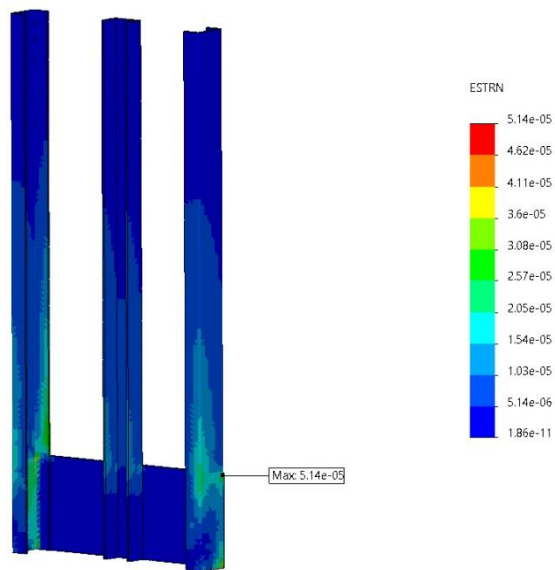


Figure 5.5.4 Strain of forklift drive guide

Factor of safety

When a 22000N load is applied to the forklift drive guide, the von mises stress does not exceed the yield stress of the selected materia for the static analysis done on the forklift drive guide. This can also be plainly identified by analyzing the FOS contour figure. The lowest FOS value, according to it, is 26.7. As a result, it may be determined that the forklift drive guide is capable of handling a 22000N load in a static situation. During the real operation, the fork design will not fail.



Figure 5.5.5 Factor of safety of the forklift drive guide

5.6 Forklift mount

According to the static analysis that is performed for the forklift mount, it is observed that when applying a 25000N load to the forklift mount, the von mises stress is not exceeding the yield stress of the manufactured material. Therefore, it can be concluded that under the static condition, the forklift mount is strong enough to handle a 25000N load which is less than the actual operation load.

AISI 1020 is a commonly used plain carbon steel with low hardenability properties and low tensile strength. It has good weldability, high strength, ductility, and machinability. In addition to a high yield strength of 420Mpa, it has a tensile strength of 350 Mpa as it is easy to harden or carburize, which makes it a suitable option for this application. AISI 1020 offers a shear module (deformation of a material when a force is acting parallel

to the surface while an opposing force is acting on the opposite face simultaneously). The information regarding this properties of the component is provided in appendix 43.

Stress

The maximum yield strength of the author's forklift mount is 3500000000 N/m². Again, the maximum stress produced by applying load on the side in the vertical direction of the design remains quite low compared to the whole available stress. As the highest stress on the component remains below 20300000 N/m², it may be concluded that the component can readily manage the load's stress if it is in a manageable and well-balanced state.

Model name: forklift_mount
Study name: Static 1(-Default)
Plot type: Static nodal stress Stress1
Deformation scale: 1

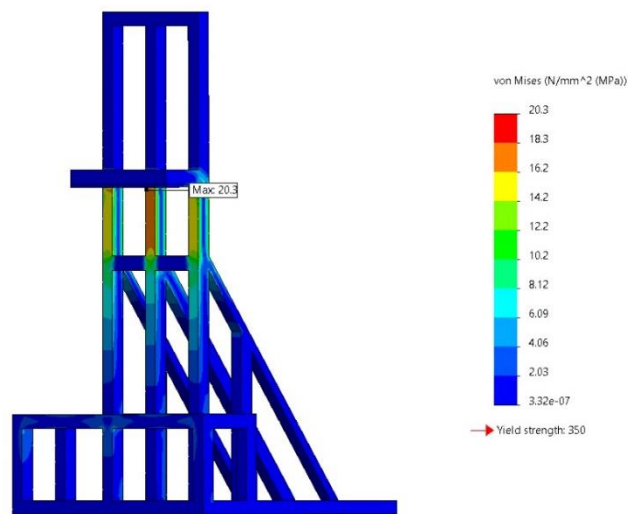


Figure 5.6.1 Stress of forklift mount

Displacement

This figure refers to deformation produced during the application of load. It is shown in the figure that the maximum deformation is happening not at exact base of the mount but in slightly higher section in horizontal direction. This deviation is not exceeding more than 0.77 mm which is a not too large as considering the maximum upper limit capacity of the design.

Model name: forklift_mount
Study name: Static 1(-Default-)
Plot type: Static displacement Displacement1
Deformation scale: 1

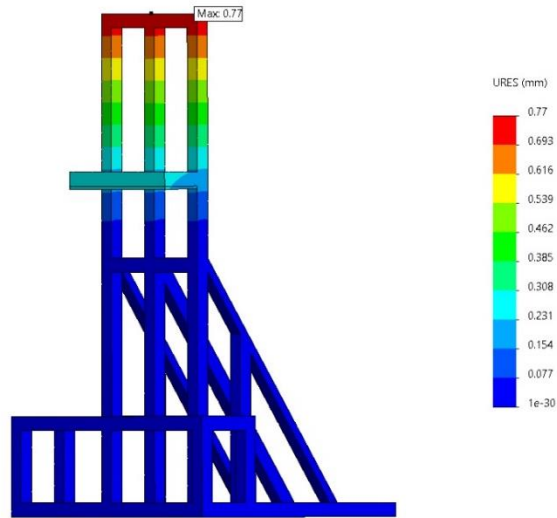


Figure 5.6.2 Displacement of forklift mount

Strain

Here, the strain on the component is calculated during load(force) application. In the figure analysis, the equivalent strain stays stable at most of the component sections below 0.000006509 . This is acceptable as the stress ratio to the elastic modulus for the material stays above for the given material than the produced strain.

Model name: forklift_mount
Study name: Static 1(-Default-)
Plot type: Static strain Strain1
Deformation scale: 1

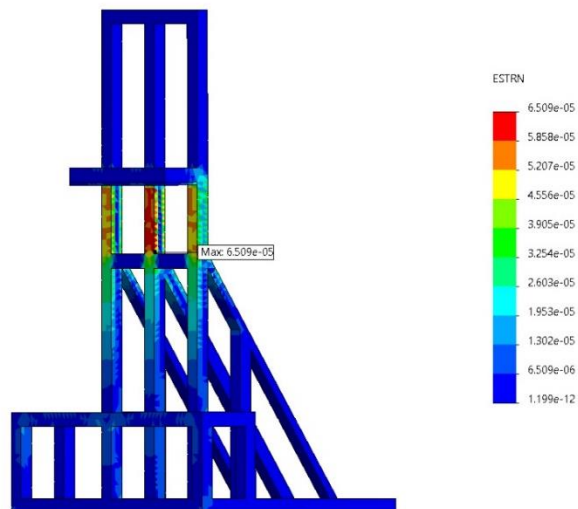


Figure 5.6.3 Strain of forklift mount

Factor of safety

When a 25000N load is applied to the forklift mount, the von mises stress does not exceed the yield stress of the selected materia for the static analysis done on the forklift mount. This can also be plainly identified by analyzing the FOS contour figure. The lowest FOS value, according to it, is 17.2. As a result, it may be determined that the forklift mount is capable of handling a 25000N load in a static situation. During the real operation, the fork design will not fail.

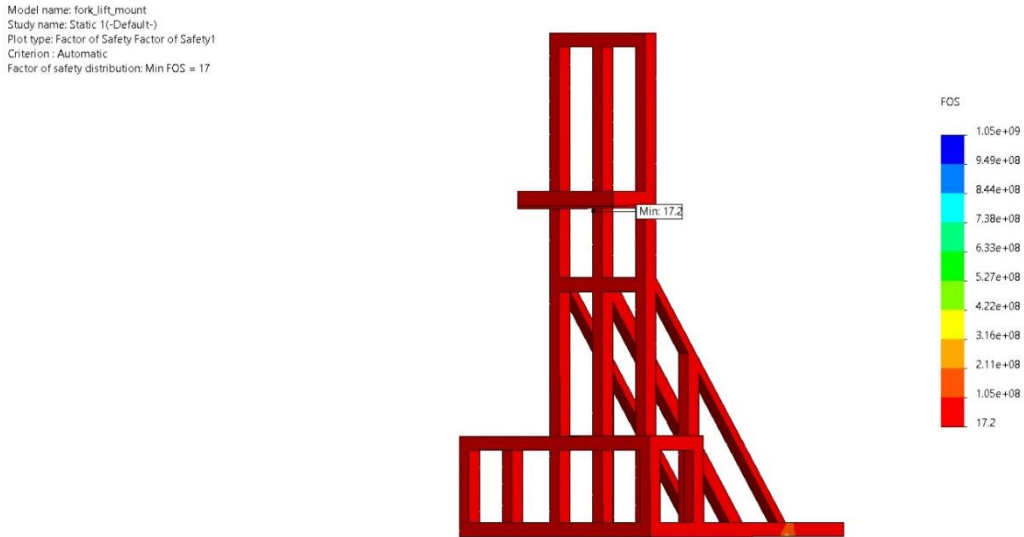


Figure 5.6.4 Factor of safety of the forklift mount

5.7 Forklift linear guide

According to the static analysis that is performed for the forklift-Linear guide, it is observed that when applying a 30000N load to the forklift-Linear guide, the von mises stress is not exceeding the yield stress of the manufactured material. Therefore, it can be concluded that under the static condition, the forklift-Linear guide is strong enough to handle a 30000N load which is less than the actual operation load.

We are using the same AISI 1020 in this scenario with similar properties and characteristics as we explained in the previous section 5.6. For more information regarding the properties refer to appendix 42.

Stress

The yield strength of the forklift-linear guide is 3500000000 N/m². Again, the maximum stress produced by applying load to the design remains quite low, 12800000N/m², compared with the maximum stress capacity of the guide. As the highest stress on the component remains extremely below the highest capacity. It can be concluded that the component can readily manage the load's stress. So, we can say that the design will be well-balanced.

Model name: linear guide
 Study name: Static 1(-Default-)
 Plot type: Static nodal stress Stress1

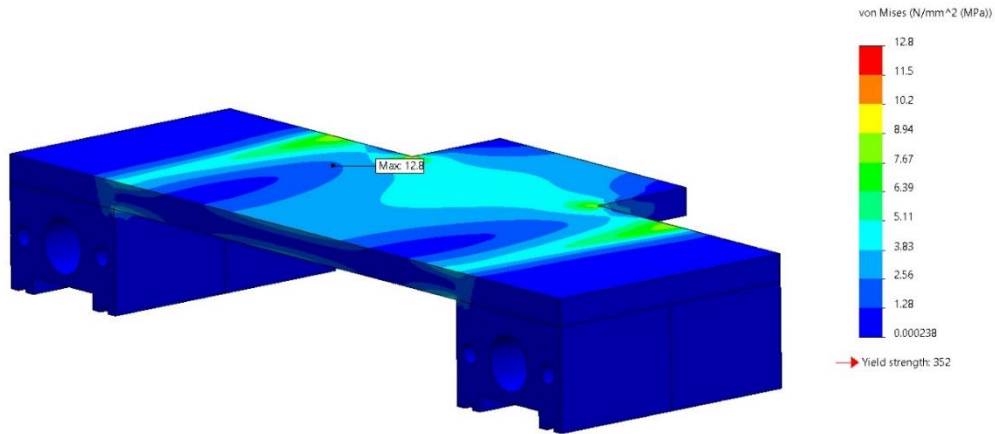


Figure 5.7.1 Stress of forklift linear guide

Displacement

The figure describes the amount of deformation produced during the application of load on the linear forklift guide. Maximum deformation is happening at the center of the forklift. This deviation is not exceeding more than 0.0989mm, which is very less and within our expected limit, and it can be neglected.

Model name: linear guide
Study name: Static 1(-Default-)
Plot type: Static displacement Displacement1

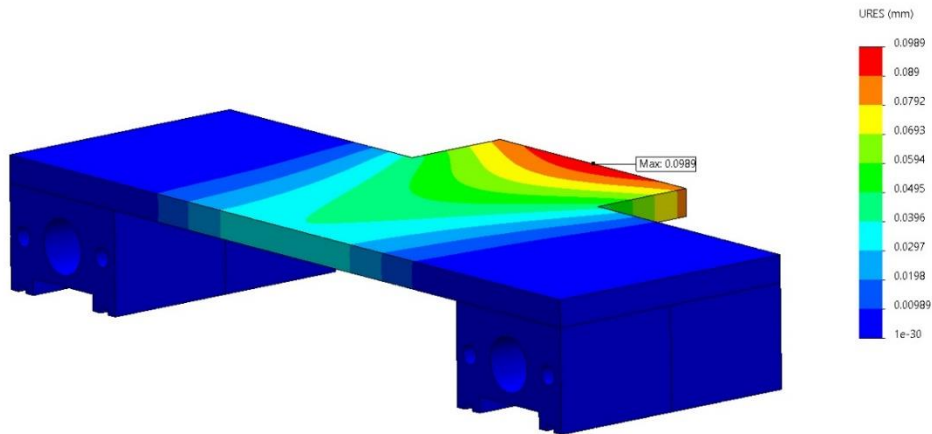


Figure 5.7.2 Displacement of forklift linear guide

Strain

As in previous scenarios, we are measuring strain by applying a load. And from the figure, it can be clearly known that the equivalent strain stays mostly on the center of the forklift, which is below 0.0000433. This is acceptable as the ratio of stress to the elastic modulus for the material stays above the produced strain on the component. From the figure, we can see that the strain is acting uniformly through the entire component in the vertical direction.

Model name: linear guide
Study name: Static 1(-Default-)
Plot type: Static strain Strain1

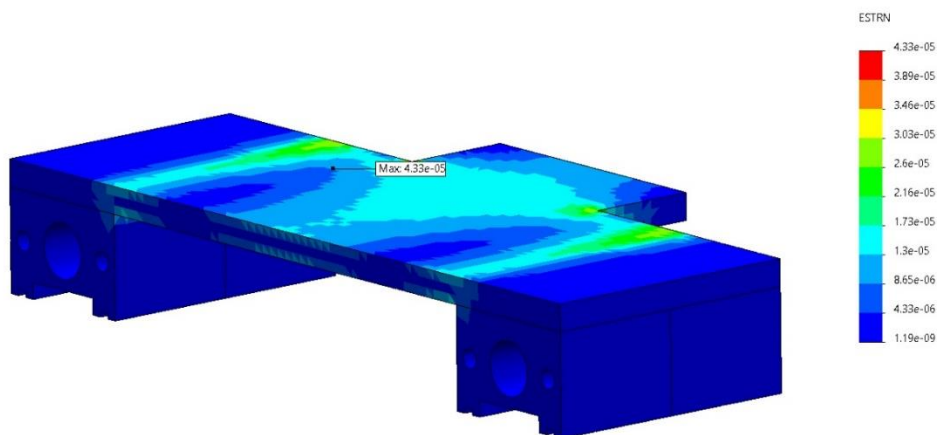


Figure 5.7.3 Strain of forklift linear guide

Factor of safety

When a 30000N load is applied to the forklift linear guide, the von mises stress does not exceed the yield stress of the selected materia for the static analysis done on the forklift linear guide. This can also be plainly identified by analyzing the FOS contour figure. The lowest FOS value, according to it, is 27.5. As a result, it may be determined that the forklift linear guide is capable of handling a 30000N load in a static situation. During the real operation, the fork design will not fail.

Model name: linear guide
Study name: Static 1(-Default-)
Plot type: Factor of Safety Factor of Safety1
Criterion : Automatic
Factor of safety distribution: Min FOS = 28

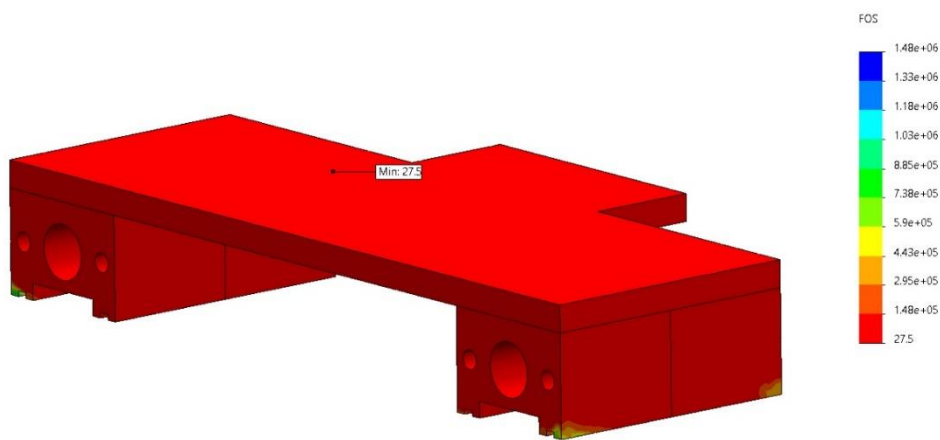


Figure 5.7.4 Factor of safety of the forklift linear guide

5.8 Scissor lift top plate

The Scissor lift top plate holds the forklift mechanism and the external load. According to the static analysis that is performed for the top plate, it is observed that when applying a 30000N load to the forklift top plate, the von mises stress is not exceeding the yield stress of the manufactured material. Therefore, it can be concluded that under the static condition, the scissor lift top plate is strong enough to handle a 30000N load which is less than the actual operation load.

Aluminum Alloys are alloys with aluminum has a major content along with typical alloy elements such as copper, magnesium, manganese, silicon, tin, and zinc. They are differentiated into various types based on the combination of elements such as

Dularamin(copper & aluminum) and Alnico (Aluminium, nickel, and copper). They have an elastic module of 70 Gpa along with a specific heat capacity of about 816 to 1050/kg K. They have a thermal expansion coefficient (rate of expansion of material upon exposure to temperature. The properties window of the material is shown in appendix 41.

Stress

Scissor lift top plate has a maximum yield strength of 27574200 N/m². As we discussed in the previous scenarios the maximum stress produced by applying load to the design remains quite low in this case too. As the highest stress on the component remains below 5160000N/m², and the stress is acting uniformly through the component from the vertical direction. it may be concluded that the component can readily manage the load's stress and it will be well balanced.

Model name: scissor_lift_top_plate_frame_mod
 Study name: Static 1(-Default-)
 Plot type: Static nodal stress Stress1

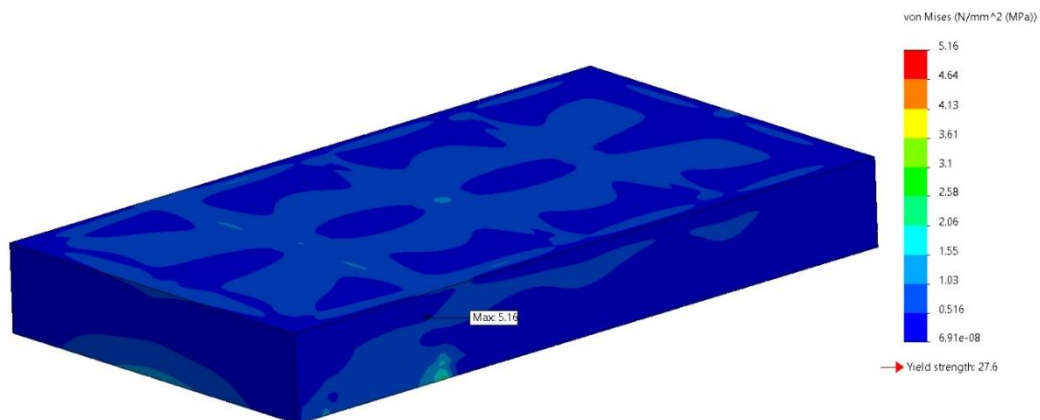


Figure 5.8.1 Stress of scissor lift top plate

Displacement

This figure shows the amount of deformation and region in which it is acting on the scissor top lift during the application of load. it is shown in the figure that the maximum deformation is happening in certain portion of the component which is not uniform. This deviation is not exceeding more than 0.0513 mm which is more or less negligible as compared to our expected limits.

Model name: scissor_lift_top_plate_frame_mod
Study name: Static 1(-Default-)
Plot type: Static displacement Displacement1

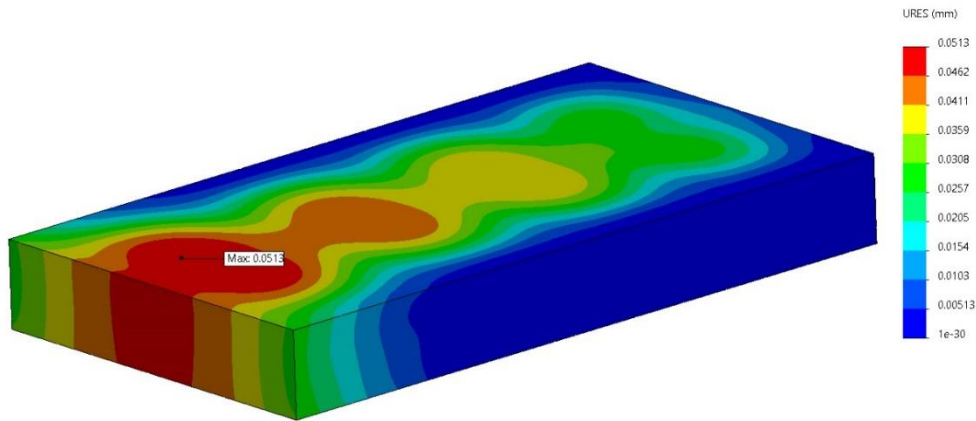


Figure 5.8.2 Displacement of scissor lift top plate

Strain

By applying a load on the component, the strain is calculated in the best possible way. And from the figure and our analysis shows that the equivalent strain stays stable in most of the section of the component below 00000507 as long as the ratio of stress to the elastic modulus is greater than the produced strain. This value is considered as a value within our maximum expected limit.

Model name: scissor_lift_top_plate_frame_mod
Study name: Static 1(-Default-)
Plot type: Static strain Strain1

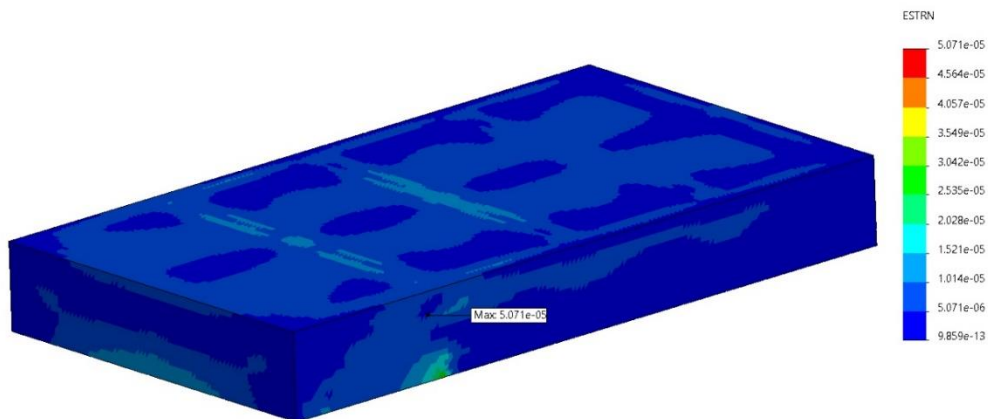


Figure 5.8.3 Strain of scissor lift top plate

Factor of safety

When a 30000N load is applied to the forklift top plate, the von mises stress does not exceed the yield stress of the selected materia for the static analysis done on the forklift top plate. This can also be plainly identified by analyzing the FOS contour figure. The lowest FOS value according to that it is 5.35. As a result, it may be determined that the forklift top plate is capable of handling a 30000N load in a static situation. During the real operation, the fork design will not fail.

Model name: scissor_lift_top_plate_frame_mod
Study name: Static 1(-Default-)
Plot type: Factor of Safety Factor of Safety1
Criterion : Automatic
Factor of safety distribution: Min FOS = 5.3

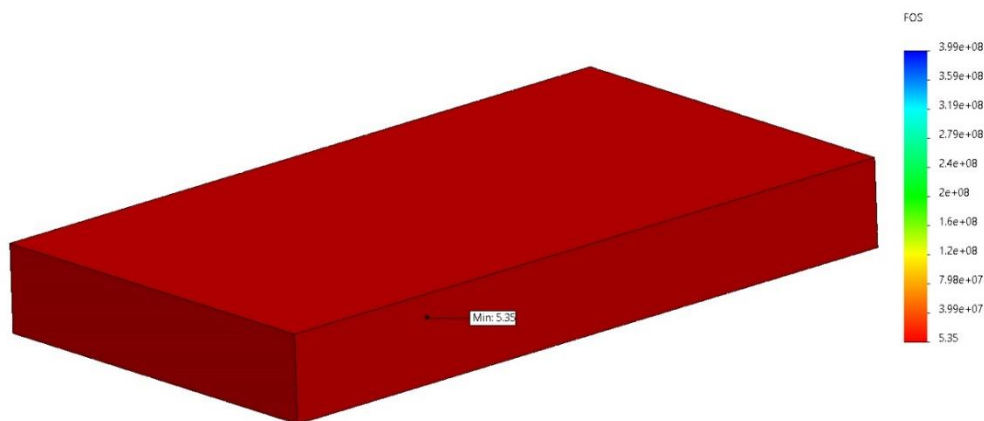


Figure 5.8.4 Factor of safety of the of scissor lift top plate

5.9 Scissor link

The Scissor link is a critical component of the scissor lift mechanism. According to the static analysis that is performed for the scissor link, it is observed that when applying a 15000N load to the scissor link, the von mises stress is not exceeding the yield stress of the manufactured material. Therefore, it can be concluded that under the static condition, the scissor link is strong enough to handle a 30000N load which is less than the actual operation load.

AISI 304 is the most commonly used stainless that contains chromium and nickel as the main component. They are less electrical and thermally conductive than carbon steel. It has excellent drawing and good formability properties. As they contain only 0.7 % of carbon, they are less tougher than other steel. They can be easily deformed by applying stress and excellent corrosion resistance. They are easy to sanitize, which makes them even more suitable for this purpose. It has a Poisson ratio of 0.29 N/A and mass density

of 8000 kg/m³ with elastic modulus of 190000000000 N/m². Refer to appendix 40 for the material properties of scissor link.

Stress

The Scissor link has a maximum yield strength capacity of 206800000 N/m². As we analyzed the design, the maximum stress produced by applying load to the design remains less compared to its maximum capacity. As the stress on the component remains below 209000000N/m², it may be concluded that the component can readily manage the load's stress, and it will work in a balanced state.

Model name: scissor_leg
Study name: Static 1(-Default-)
Plot type: Static nodal stress Stress1



Figure 5.9.1 Stress of scissor link

Displacement

This figure represents the deformation caused in a scissor link upon application of load. It is shown in the figure that the maximum deformation is happening on the sides of the link uniformly. This deviation is not exceeding more than 0.168 mm, which is within our expected limits.

Model name: scissor_leg
Study name: Static 1(-Default-)
Plot type: Static displacement Displacement1

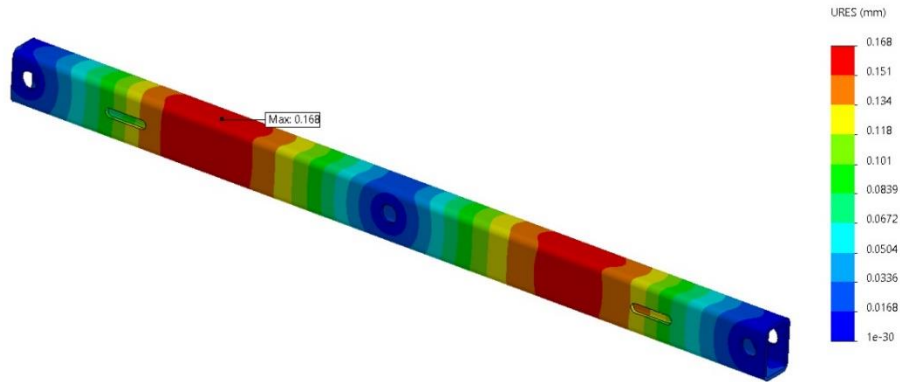


Figure 5.9.2 Displacement of scissor link

Strain

As like in the previous scenario, strain is again calculated by the application of load. By analyzing the figure, the equivalent strain stays stable at most of the sections of the component below 0.0000456. As the obtained strain in the element is less than the ratio of stress to elastic modules, we can ensure our element will work in a well-balanced state.

Model name: scissor_leg
Study name: Static 1(-Default-)
Plot type: Static strain Strain1

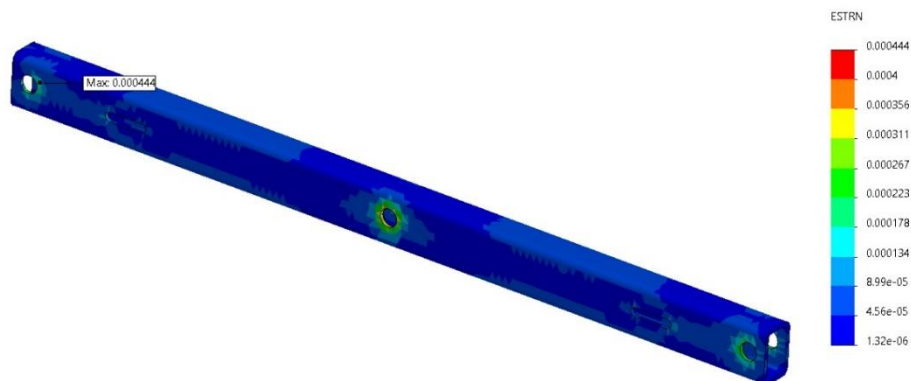


Figure 5.9.3 Strain of scissor link

Factor of safety

When a 15000N load and 25000Nm torque is applied to the forklift scissor link, the von mises stress does not exceed the yield stress of the selected materia for the static analysis done on the scissor link. This can also be plainly identified by analyzing the FOS contour figure. The lowest FOS value, according to it, is 1.7. As a result, it may be determined that the forklift scissor link is capable of handling a applied load and torque in a static situation. During the real operation, the fork design will not fail.



Figure 5.9.4 Factor of safety for scissor link

5.10 Truck Frame

According to the static analysis that is performed for the truck frame, it is observed that when applying a 50000N load to the truck, the von mises stress is not exceeding the yield stress of the manufactured material. Therefore, it can be concluded that under the static condition, the truck frame is strong enough to handle a 50000N load which is less than the actual operation load.

AISI 4340 steel is a medium carbon low alloy steel. It has very high toughness and strength and is composed of nickel-chromium-molybdenum steels. It is very much flexible to be pre-hardening and tempering. It has a good shock and impact resistance along with excellent abrasion and wears resistance. It has good ductility. Here we use AISI 4340 mainly because we need a better hardenability in order to obtain the required strength requirements. Appendix 39 refers to these properties from solidworks window.

Stress

The maximum yield strength of the truck frame is 4700000000 N/m². It is tougher and has good tensile strength. From our analysis, minimum stress acting on the component are 1010000N/m², respectively. So the maximum value of stress in our component is extremely small compared to its maximum capacity, and it is acting from the vertical direction on the top of the truck frame. So here component should satisfy the requirement that the author's system needs.

Model name: truck_simscape
Study name: Static 1(-Default-)
Plot type: Static nodal stress Stress1

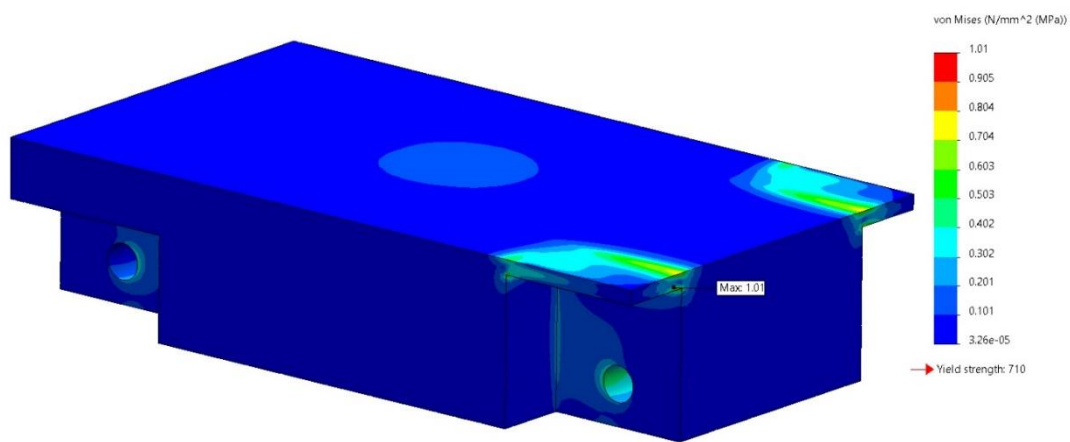


Figure 5.10.1 Stress of truck frame

Displacement

The figure represents the deformation caused in a truck frame upon application of load. It is shown in the figure that the maximum deformation is happening on the side frames of the truck frame. This deformation or elongation is not exceeding more than 0.00415mm, which is within our expected limits and can be managed by our system.

Model name: truck_simscape
Study name: Static 1(-Default-)
Plot type: Static displacement Displacement1

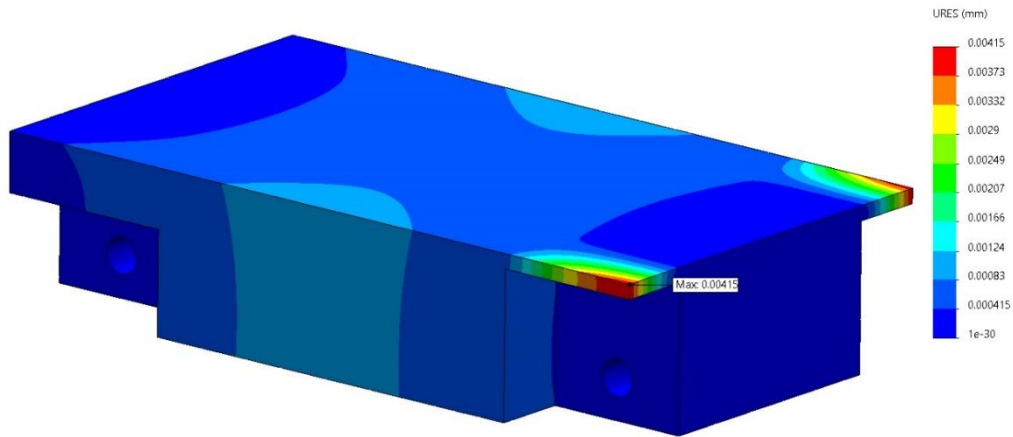


Figure 5.10.2 Displacement of truck frame

Strain

Strain is measured by the application of load. By analyzing the figure, the resultant maximum strain stays not stable at most of the sections of the component as it is almost acting on the side frames of the truck frame, which is below 0.000000357 . As the obtained strain in the element is less than the ratio of stress to elastic modulus, it is ensured that our element will work in an expected manner satisfying all the requirements.

Model name: truck_simscape
Study name: Static 1(-Default-)
Plot type: Static strain Strain1

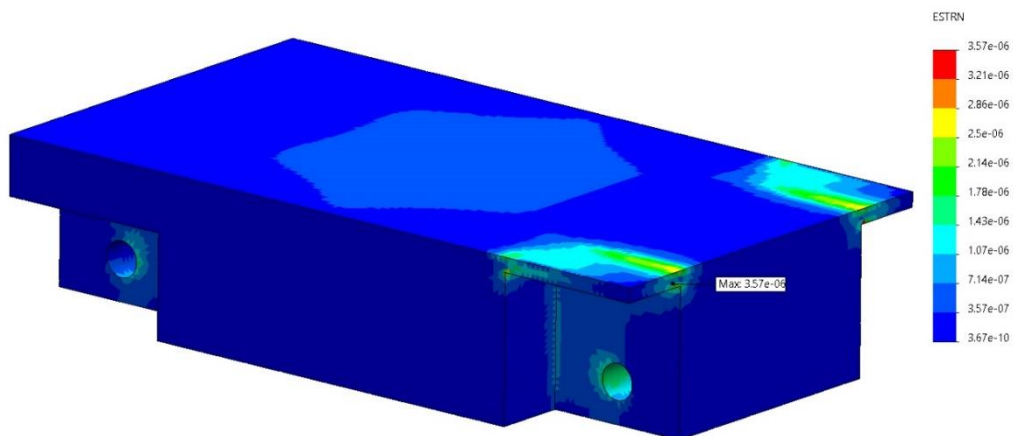


Figure 5.10.3 Strain of truck frame

Factor of safety

When a 50000N load is applied to the forklift truck frame, the von mises stress does not exceed the yield stress of the selected materia for the static analysis done on the scissor link. This can also be plainly identified by analyzing the FOS contour figure. The lowest FOS value, according to it, is 706. As a result, it may be determined that the forklift truck frame is capable of handling a applied load and torque in a static situation. During the real operation, the fork design will not fail.

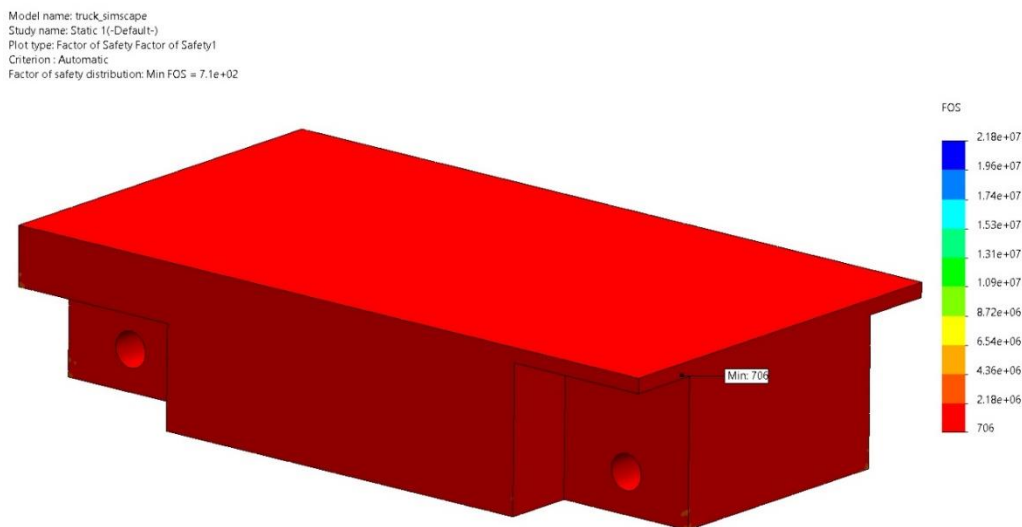


Figure 5.10.4 Factor of safety of the truck frame

5.11 Lead screw

The lead screw is the critical component of the forklift mechanism. In this machine, the lead screw is used to move the forklift during the loading, holding, and unloading processes. Therefore, the strength of the lead screw has to be maximum to maintain the durability and the accurate performance of this machine. To analyze the strength of the design lead screw, a static analysis is performed to observe the behavior of the lead screw for a 30000N load. From the simulation results, it is observed that the lead screw can stand against a 30000N load which is less than the actual operating load of 20000N. Therefore, it can be concluded that the design lead screw is strong enough to handle the forklift mechanism and the external load of 1000Kg. The following figures show the results obtain during the static analysis. The material properties regarding the lead screw is given in appendix 38.

Stress

As in here, the loads are divided according to the actual function of the component. The yield strength of the material that we used for the component is 292000000 N/m². From the analysis, the stress variant does not even reach a point 6090000N/m². Therefore the component can easily withstand the stress applied during the process.

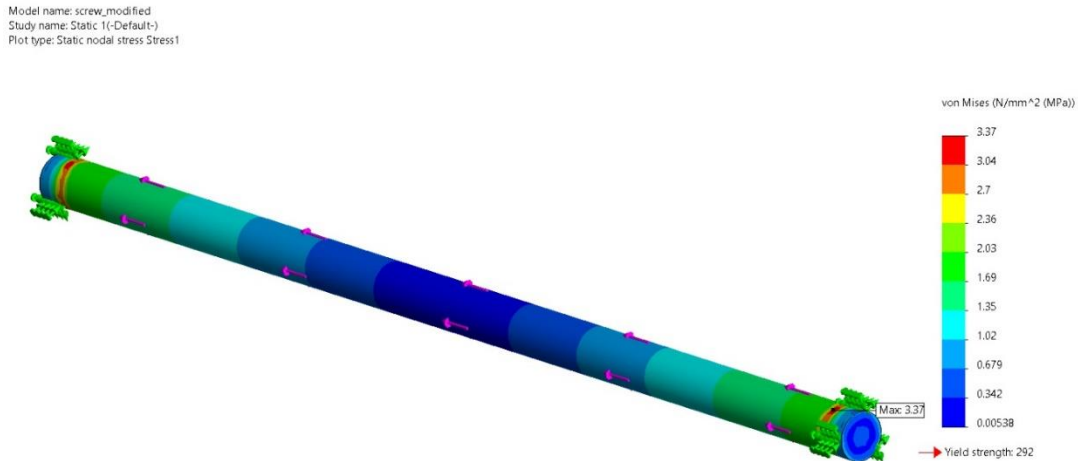


Figure 5.11.1 Stress of lead screw

Displacement

This analysis deals with the deformation of the Lead screw through the application of load at each point through the different axis. And here, the author has the maximum deviation only up to 0.00544 mm that too at the center of the screw. As the considered load is much higher than the actual load, the deviation seems unimportant.

Model name: screw_modified
Study name: Static 1(-Default-)
Plot type: Static displacement Displacement1

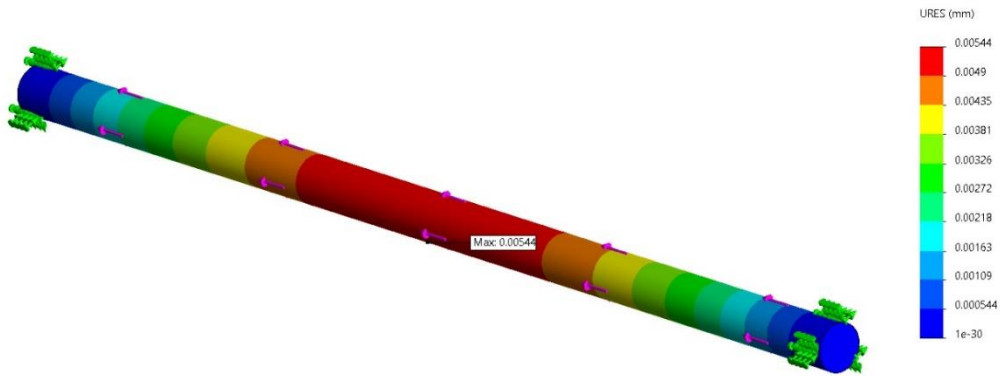


Figure 5.11.2 Displacement of lead screw

Strain

The strain component does not appear to vary significantly in this case. As shown in the previous analysis, the equivalent strain remains constant throughout the component's section below 0.0000128 . This is allowed once more since the stress to elastic modulus ratio of the specified material is larger than the resulting strain.

Model name: screw_modified
Study name: Static 1(-Default-)
Plot type: Static strain Strain1

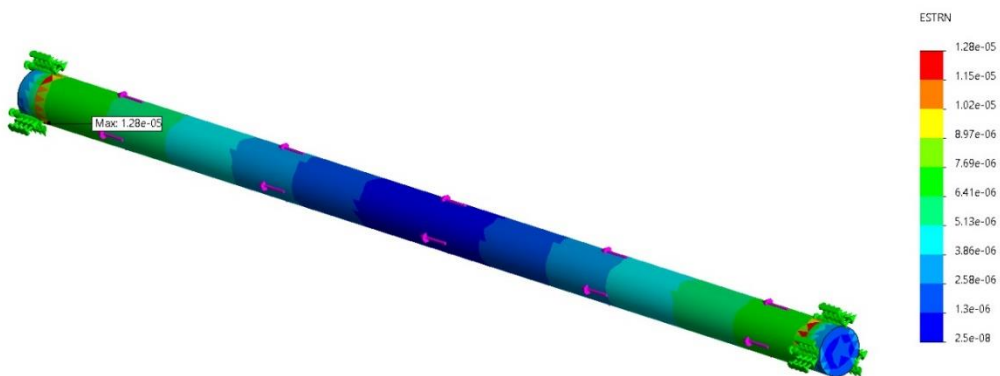


Figure 5.11.3 Strain of lead screw

Factor of safety

When a 30000N axial load is applied to the lead screw, the von mises stress does not exceed the yield stress of the selected materia for the static analysis done on the lead

screw. This can also be plainly identified by analyzing the FOS contour figure. The lowest FOS value, according to it, is 86.5. As a result, it may be determined that the lead screw is capable of handling a applied load and torque in a static situation. During the real operation, the fork design will not fail.

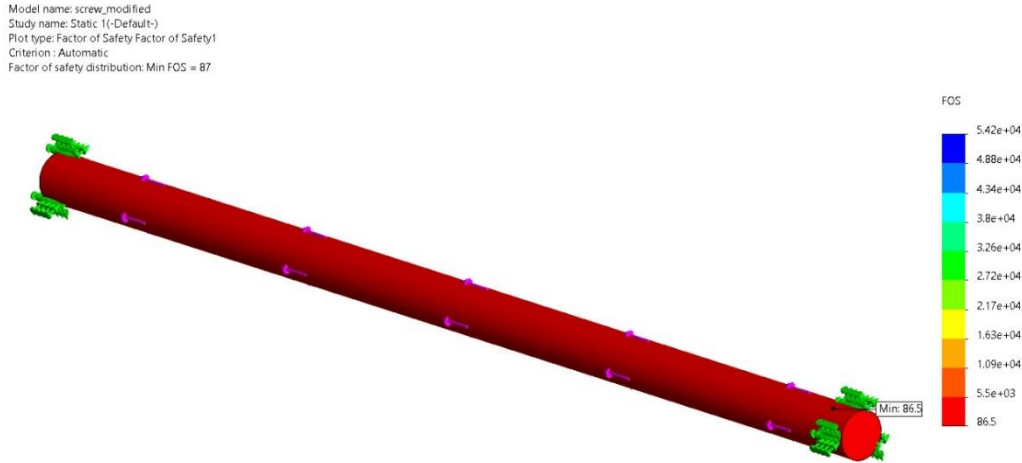


Figure 5.11.4 Factor of safety of lead screw

5.12 Optimization and simulation

Design optimization can raise a product's value by enhancing its performance in its operational environment and lowering its manufacturing costs by reducing the amount of material necessary to create it. If the author intends to find the best of numerous different design configurations, he will have to change the design parameters. The design variables are those parameters. Dimensions, or the number of instances in a pattern, material qualities, loads, spring stiffness—or any other component of a design with a discernible "optimal" value or concern the researcher had to deal with joint faults in this case. The optimization program would choose the minor material condition permitted by the dimensional variables right away. During the design optimization, the author encountered numerous defects due to the vast number of joints in the design. The author reduced the number of joints and used a single component instead.

To do the simulation author had to go through specific steps. First and foremost, the author had to establish the design's static analysis. In this case, the author must define the stress analysis of each section with each load quantity. The load variation is determined by the placement of each component in the design. The strain and displacement study with these loads is also something the author is looking forward to. To do the analysis, the author assigned materials to each section of the design based on the degree of stress it will be exposed to. Because the material database is identical to the SOLIDWORKS material library, the materials used in the design are reused. The mechanical qualities are needed to solve a particular sort of analysis. The meshing of the model and execution of the analysis are the following steps in the simulation. Simulation knows how the model acts in the actual world thanks to the Free Body Diagram stage. The assignment of loads, fixtures, contacts, and connectors is the most significant phase in the process. Author has finished the assembly and the static analysis of the assembly is done as shown in the appendix 19 to 21 . Hence from the stress strain and deformation analysis , it is proved that the system is stable.

6 ESTIMATION GRAPHS

6.1 Force estimation of the scissor lift actuator (use sf_unit_actuate3 model)

Cylinder displacement for maximum expansion of the scissor lift

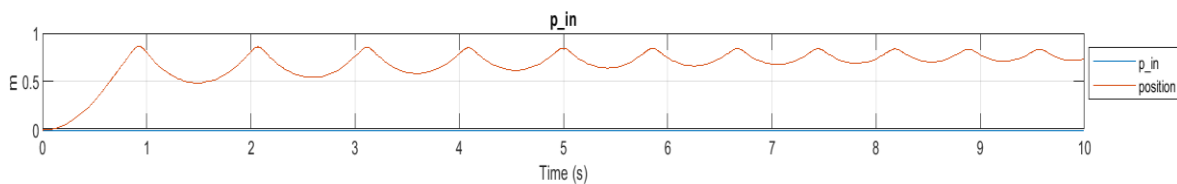


Figure 6.1.1 Y-axis actuator shows displacement, and X-axis shows time.

The graph shows the displacement of the actuator when lifting the load. In this system, a 1m stroke hydraulic actuator is used for the scissor lift to get the maximum lifting height. For simulation purposes, the lifting speed is increased, but in the real application, the operation speed is far slower than the given graph. However, even with the higher speed operation, the design model is performed well during the simulation. Therefore, for slower speeds, the system will work perfectly.

Corresponding actuator force

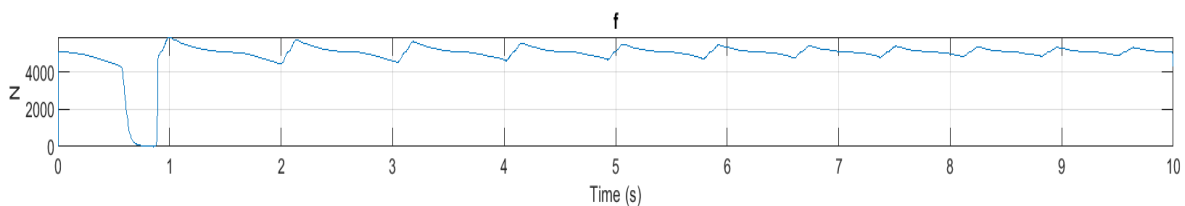


Figure 6.1.2 Y-axis shows actuator force, and X-axis shows time.

The graph shows the variations in actuator force based on time. As shown in the graph, the scissor lift actuator generates around 5000N load to lift the load of 10000N. Here the sudden drop in the graph indicates the time for the fork to get to its position and start the process of lifting; as the actuator starts the process of lifting, then the force remains stable.

Corresponding hydraulic pressure

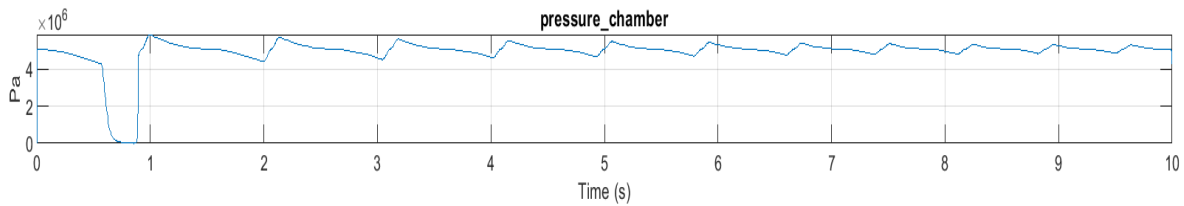


Figure 6.1.3 X-axis shows time, and Y-axis shows hydraulic pressure

The graph shows the hydraulic pressure variation based on time. As shown in the graph, the scissor lift actuator is required 5Mpa hydraulic fluid pressure to lift the 10000N load.

6.2 Motor torque estimation of the linear guide (use sf_unit_actuate4)

Angular velocity of the linear actuator

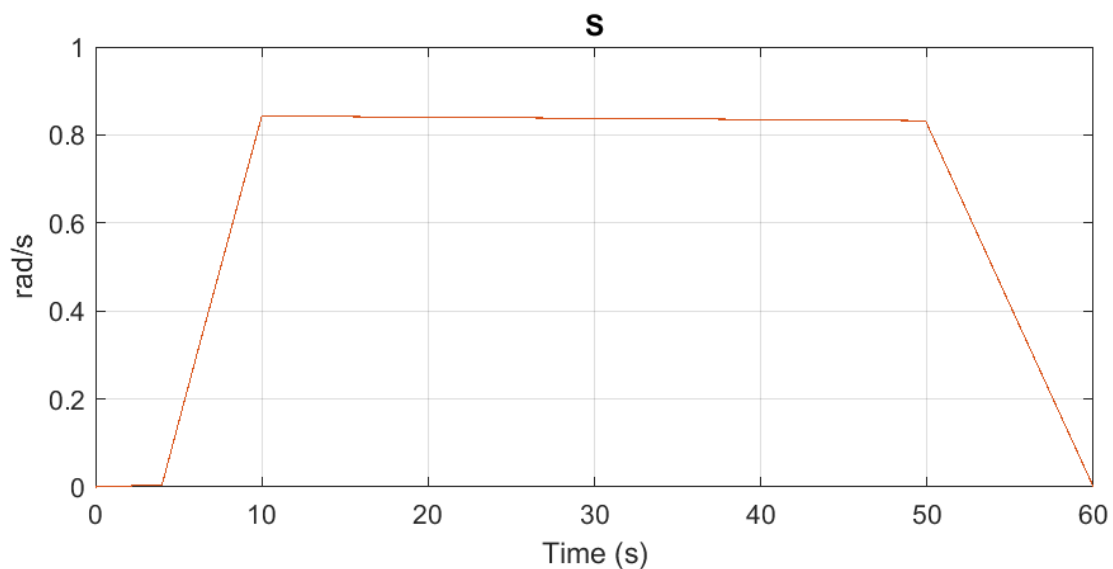


Figure 6.2.1 Y-axis shows angular velocity, and X-axis shows time

In this graph, the author estimated the angular velocity of the lead screw motor in accordance with the time. When operating the lead screw, the motor is operated as shown in figure 7.1.1. Within the first 10 seconds, the motor is gradually increased the motor speed up to 0.8 rad/s, and then it maintains the constant velocity of 0.8 rad/s seconds for the next 40 seconds. After that, the motor reduces its speed within the next 10s to stop at the unloading position. Slow speed is used to reduce the unnecessary vibration of the system and give a more smooth operation for the forklift mechanism.

Required motor torque

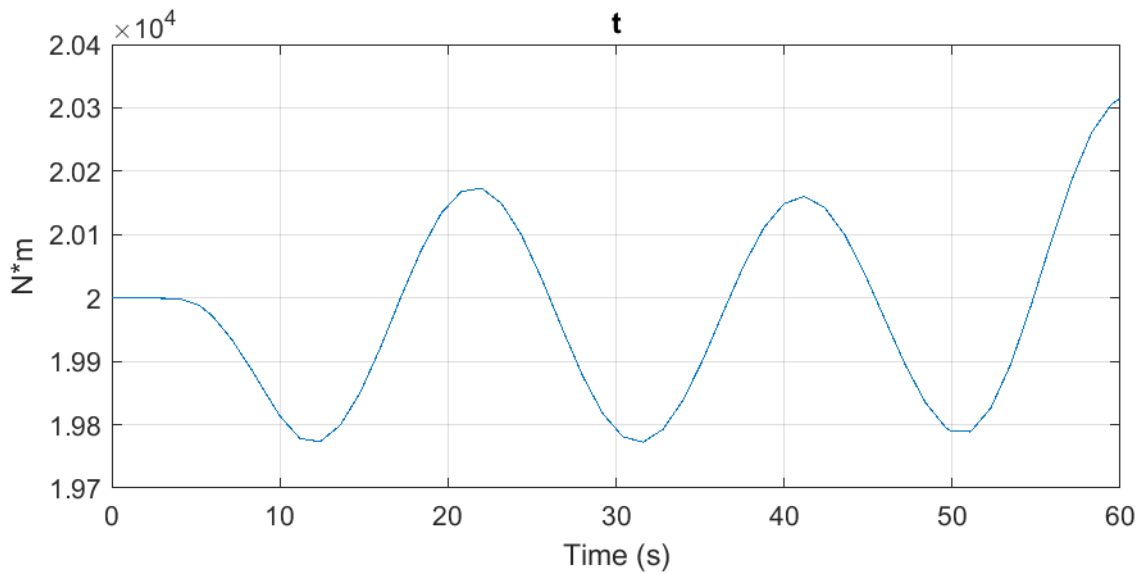


Figure 6.2.2 Y-axis shows actuator torque, and X-axis shows time

Here author looks into the actuator motor torque while pulling the load as per the time. The behavior of the motor torque is shown in the above figure. Throughout the operation, the motor is maintained about 20000 Nm torque to hold the forklift mechanism. As shown in the figure, the highest torque of the motor is generated when the forklift mechanism is at the loading position. Using the higher torque from the motor system can maintain the stability of the forklift mechanism at the loading position.

7 DYNAMIC ANALYSIS

7.1 Analysis of the lead screw with load

Lead screws are the critical components of the forklift mechanism. Lead screws are used to move the forklift mechanism along with the scissor lift platform and also hold the forklift mechanism and the external load. Therefore, designing the lead screw mechanism is the most important part of this design. When considering the overall forklift mechanism, the approximate mass of the forklift mechanism is 1000 Kg. With the external load of 1000Kg of mass, the total weight that should hold by the lead screws is 20000N. Due to the load transformation along with the scissor lift, a considerable moment is also applied to the lead screw. The maximum moment is applied to the lead screw at the loading position, which is shown in appendix 30. At that point, the maximum moment applied on the lead screw is approximately 30000 Nm which is slightly higher than the actual loading condition. Therefore, dynamic analysis of the lead screw at that point is necessary to analyze the strength of the lead screw mechanism.

Stress

In the appendix 30, the dynamic stress analysis of the lead screw at the highest bending moment point. According to the results obtain from the solidworks, it is observed that the von misses stress of the lead screw is not exceeding the yield strength of the lead screw material. Therefore it can be concluded that the lead screws are not failed during the actual operation of the machine.

Displacement

In the appendix 31, the picture shows the deformation of the lead screw at the maximum bending position. According to that, the maximum deformation of the lead screws occurs at the two corners near the bearing blocks, and the maximum deformation is approximately around 0.2 mm, which is considered the acceptable level for this mechanism. Also, the graph showing the reaction moment on the lead screw is also taken; appendix 18 shows the graph.

7.2 Stress analysis of scissor lift components

The Scissor lift cylinder is also a critical component of the mechanism. The total load of the machine is moved up and down by using the scissor lift cylinder. Therefore, analyzing the components of the scissor lift cylinder is important to validate the design.

As shown in the following figures, dynamic stress analysis of the critical components of the scissor lift mechanism from Appendix . It can be concluded that the system is stable during the operation of the machine. As shown in the dynamic analysis, it is observed that all the critical components are not failed during the operation of the system.

Cylinder mount

Here the stress analysis during the motion study was conducted on the cylinder mount of the scissor lift. The screenshot of the analysis is provided in appendix 32. The stress of the component stays below the 41500N/m^2 . The yield strength of the material is much higher than the produced stress. Hence it is proved that the component doesn't fail during the process.

Cylinder rod mount

Appendix 33 , show the image of analysis of cylinder mount. The rod mount stays within the limit much lower than the yield strength of the material during the process of lifting the load. Here from the above figure, it is shown that the maximum stress being created during the process staus below 293500 N/m^2 .

Cylinder rod

The next component the author considers is the cylinder rod. And it is very clearly indicated from the above image that the stress factor stays below 39430 N/m^2 . This quantity also stays below the yield strength of the material. Therefore it creates very less deformation and strain. As that was proved during the static analysis of the components, the author confirmed the perfect functioning of the material. Kindly refer to appendix 34.

Scissor leg guide

The guide, which is attached to the scissor leg bearing the piston, is examined. The stress factor for the component during the procedure stays within the limit of about 51610 N/m^2 , as seen in the above figure. Appendix 35 is a diagram depicting the stress analysis.

Connecting rod

The next critical component is the connecting rod which connects four different scissor legs. Even on this scissor leg, we have very less stress produced during the lifting, which in turn produces very less deformation or strain. Here the stress factor stays below 4799N/m^2 . Therefore author confirms the ready working of the system again through another successive analysis. Appendix 36 depicts the analysis of the component.

Scissor leg

The Scissor leg of the design again shows that the stress variant produced on it during the lifting process is easily acceptable for the selected material. Here from the figure, the stress factor stays below 257100N/m^2 . This quantity stays very low as we consider the yield strength from the static analysis of the same component. Appendix 37 refers to the stress analysis of the component.

8 Summary

Using SolidWorks, this thesis explains the creation of a system that combines a scissor lift with a forklift. A forklift's job is to pick up a cargo and move it to storage, but a scissor lift's job is to raise a load to its maximum height while preserving more stability. The end aim was to come up with a design that could do both tasks. i.e., picking up the cargo, loading it into a safer position, transferring and carrying it to the storage place, and then lifting and discharging it to a height considerably beyond the capacity of a regular forklift. The design was created in SolidWorks software, with each and every component based on data gathered from real-life forklift and scissor lift components. The actual lifting capability of these referred lifts was three tons, but the goal here was to raise at least one ton. Also, the recommended scissor lift had a height capability of around fifteen meters, while the goal was 10 meters.

The second goal was to ensure the design's stability and optimization when it was created. There are functions in SolidWorks that may be used to find the design's center of gravity at various phases of the lifting process, as well as the center of gravity after the weights have been loaded. The hydraulic and electrical circuits were then used to build the design's drive mechanism. Skydrol LD4 hydraulic fluid is being utilized. The leadscrew mechanism in the assembly is also controlled by an electrical circuit. The static analysis of the system was carried out after the compilation of those circuits into the design. Every significant component of the design was analyzed with nearly double the load applied to it. Stress, strain, and deformation of each component induced by such loads were examined, and it was determined that they remained within the acceptable range. Then, in Simscape, a simulation of the design was produced, with some joints eliminated and certain combinations of parts employed. Also captured are the actuator force and displacement estimate graphs for each cylinder. The force and needed torque of the lead screw mechanism are also estimated using a graph. These findings demonstrate the system's ability to function as a standard lifting machine with no faults.

1.1 Limitations

The designed design performs admirably in terms of lifting loads; however, the motion of the vehicle is not taken into account in this thesis. The author concentrated on

improving the design's lifting component. Similar to the forklift, the truck's mobility has a minor impact on the whole system, but there are several factors that create a variance in the process.

Dynamic analysis is also a time-consuming process. During the study, there were certain inaccuracies that resulted in significant changes in the design. Similarly, compiling the hydraulic and electrical circuits into the design took a long time, which resulted in the circuits being separated.

1.2 Future work

The design of this thesis was created with the intention of being operated by remote control. Because of the same reason, there is no driver cabin in the design. This also completes the design, as the lift's safety is enhanced. Human safety is also improved since when the remote control is employed, the operator may easily be removed from the process.

The system's automation will be accomplished through the use of neural networks and machine learning. The whole operation of lifting, carrying, loading, and unloading may be completed without the assistance of any human being. In a circumstance like this, this eliminates the issue of labor shortages.

KOKKUVÕTE

Käesolevas lõputöös selgitatakse SolidWorks'i abil sellise süsteemi loomist, mis ühendab käärkahveltõstukit ja kahveltõstukit. Kahveltõstuki ülesanne on laadida lasti üles ja viia see laoruumi, kuid käärkahveltõstuki ülesanne on tõsta koorem maksimaalsele kõrgusele, säilitades samal ajal suurema stabiilsuse. Lõppeesmärk oli välja töötada konstruktsioon, mis suudaks täita mõlemat ülesannet, s.t. lasti ülesvõtmine, selle turvalisemasse asendisse laadimine, selle ümberpaigutamine ja ladustamiskohale kandmine ning seejärel tõstmine ja mahalaadimine kõrgusele, mis ületab märkimisväärselt tavalise kahveltõstuki võimekuse. Konstruktsioon loodi SolidWorks tarkvaras, kusjuures iga komponent põhines tegelikest kahveltõstukite ja käärkahveltõstukite komponentidest kogutud andmetel. Nende viidatud tõstukite tegelik tõstevõime oli kolm tonni, kuid eesmärk oli siinkohal tõsta vähemalt üks tonn. Samuti oli soovitatud käärkahveltõstuki kõrgus võimekus umbes viisteist meetrit, samas kui eesmärk oli 10 meetrit.

Teine eesmärk oli tagada disaini stabiilsus ja optimeerimine selle loomisel. SolidWorksis on funktsioonid, mida saab kasutada konstruktsiooni raskuskeskme leidmiseks tõstmisprotsessi eri etappides, samuti raskuskeskme leidmiseks pärast raskuste laadimist. Seejärel kasutati hüdraulilisi ja elektrilisi vooluahelaid konstruktsiooni ajamite ehitamiseks. Kasutatakse Skydrol LD4 hüdraulilist vedelikku. Kokkupaneku juhtkruvimehhanismi juhib samuti elektriline vooluring. Süsteemi staatiline analüüs viidi läbi pärast nende vooluahelate koostamist konstruktsiooni. Konstruktsiooni iga olulist komponenti analüüsiti peaaegu kahekordse koormusega. Uuriti iga komponendi pingeid, pingeid ja deformatsioone, mida selline koormus tekitab, ning leiti, et need jäid vastuvõetavasse vahemikku. Seejärel koostati Simscape'is konstruktsiooni simulatsioon, kusjuures mõned ühendused jäeti välja ja kasutati teatavaid osade kombinatsioone. Samuti jäädvustati iga silindri jaoks toimimismehhanismi jõu ja nihke hinnangulised graafikud. Samuti on graafiku abil hinnatud juhtkruvimehhanismi jõud ja vajalik pöördemoment. Need tulemused näitavad süsteemi võimet toimida nagu tavaline tõstemasin, millel ei ole vigu.

Piirangud

Projekteeritud konstruktsioon toimib imetlusväärset tõstekoormuse suhtes, kuid käesolevas töös ei võeta arvesse sõiduki liikumist. Autor keskendus konstruktsiooni tõstekomponendi täiustamisele. Sarnaselt kahveltõstukiga on veoauto liikuvus kogu süsteemile väheoluline, kuid on mitmeid tegureid, mis tekitavad protsessis erinevusi.

Dünaamiline analüüs on samuti aeganõudev protsess. Uuringus ilmnisid teatavad ebatäpsused, mis põhjustasid olulisi muudatusi konstruktsioonis. Samuti võttis projektis hüdrauliliste ja elektriliste vooluahelate koostamine kaua aega, mille tulemuseks oli vooluahelate eraldamine.

Tulevased tööd

Käesoleva lõputöö projekt loodi kavatsusega, et seda saaks kasutada kaugjuhtimise teel. Samal põhjusel puudub konstruktsioonis juhikabiin. See täiendab ka konstruktsiooni, kuna tõstuki ohutus suureneb. Samuti paraneb inimeste ohutus, kuna kaugjuhtimise kasutamisel võib operaator hõlpsasti protsessist eemalduda.

Süsteemi automatiseerimine saavutatakse neuronivõrkude ja masinõppe abil. Kogu tõstmise, kandmise, laadimise ja mahalaadimise operatsioon võib toimuda ilma inimese abita. Sellises olukorras välistab see tööjõupuuduse probleemi.

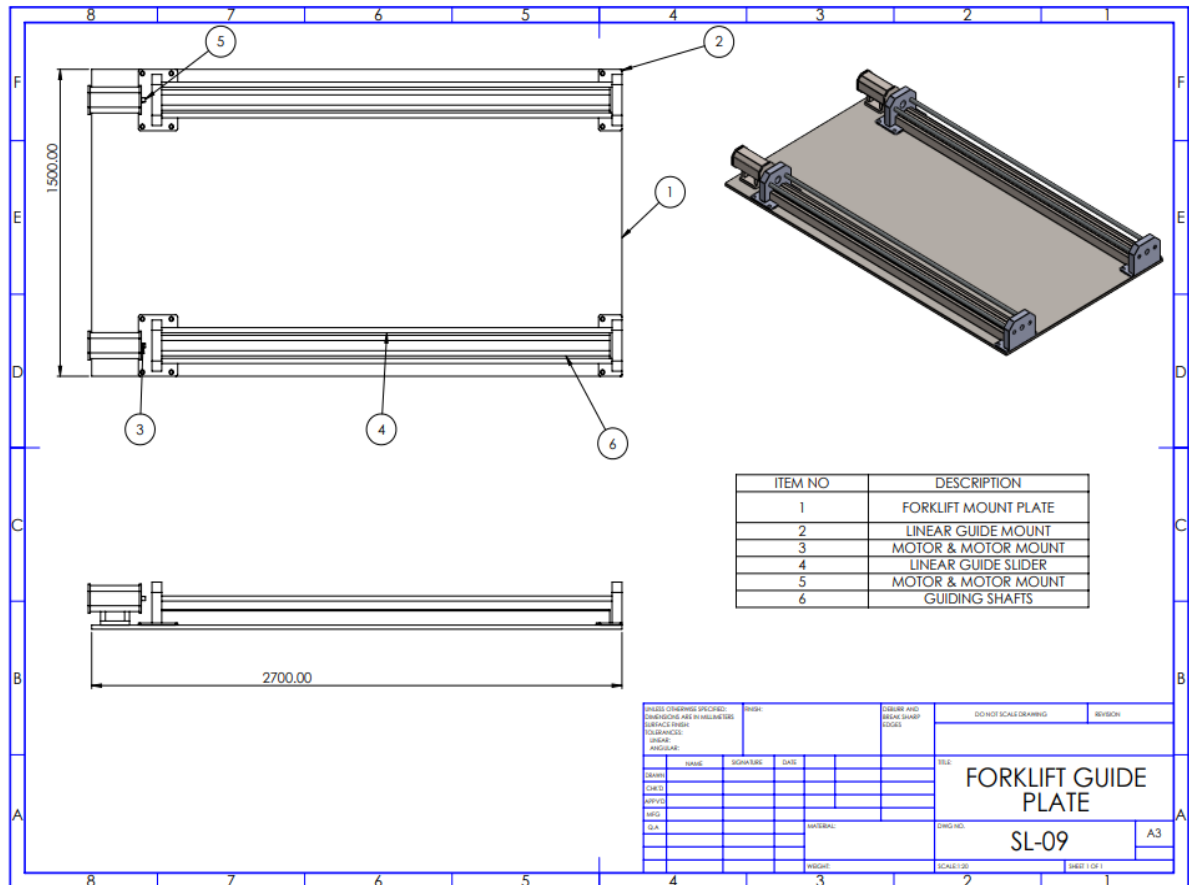
9 REFERENCES

- [1] E. Zhang, J. Zhuo, Z. Liu ja T. Guo, „Structural optimization of forklift fork based on numerical simulation and mathematical modeling of stress and fatigue,” *Revista Internacional de Métodos Numéricos para Cálculo y Diseño en Ingeniería*, p. 10, 2020.
- [2] H. Yan, W. Wang, X. Qi, H. Zhang, T. Tian ja Y. He, „Finite Element Analysis for the working device of rough terrain forklift,” *Applied Mechanics and Materials* © (2013) *Trans Tech Publications, Switzerland* , pp. 568-572, (2013) .
- [3] Ö. . Y. Bozkurt, İ. C. Dai ja Ö. Özbek, „The Finite Element Analysis and Geometry Improvements of Some Structural Parts of a Diesel Forklift Truck,” *Periodicals of Engineering and Natural Sciences*, kd. Vol.5, p. 202~209 , June 2017.
- [4] A. Sarker, S. A. Amin, S. M. Tamzidul Hafiz Tamzid ja N. Ahmed Chisty, „Design and Implementation of a Forklift with Dynamic Stability,” %1 *2017 IEEE Region 10 Humanitarian Technology Conference (R10-HTC) 21 - 23 Dec 2017,, Dhaka, Bangladesh, 2017.*
- [5] J. Felez ja A. Bermejo, „Design of a counterbalance forklift based on a predictive anti-tip-over controller,” *Integrated Computer-Aided Engineering -1 (2018) 1-16*, kd. 1, pp. 1-16, 2018.
- [6] T. Beamish , R. Zhang ja S. . J. Jilbert, „SCISSOR LIFT”. United States Patent US D859 , 773 S, 10 Sep 2019.
- [7] L. BAFILE, P. SHANKAR , E. PRASETIAWAN , J. HAO, D. LOMBARDO, D. WILLIAMS, B. KOETLINGER ja P. ACURI, „FULLY - ELECTRIC SCISSOR LIFT”. United States Patent US 2020/0317488 A1, 8 Oct 2020.
- [8] M. Murphy, E. LeBlanc ja L. J. Murphy, „SCISSOR LIFT PLATFORM”. United States Patent US 10 , 017 , 093 B1, 10 Jul . 2018.
- [9] O. Y. Ismael, M. Almagid ja A. Mahmood, „Quantitative Design Analysis of an Electric Scissor Lift,” *American Scientific Research Journal for Engineering, Technology, and Sciences (ASRJETS)*, kd. 59, nr 1, pp. 121-148, 2019.
- [10] C. G. Dengiz, M. C. Şenel, K. Yıldızlı ja E. Koç, „Design and Analysis of Scissor Lifting System by Using Finite Elements Method,” *Universal Journal of Materials Science* 6(2), kd. 6, nr 2, pp. 58-63, 2018.
- [11] T. Liu ja J. Sun, „Simulative Calculation and Optimal Design of Scissor Lifting Mechanism,” %1 *2009 Chinese Control and Decision Conference*, Weihai, 2009.

- [12] N. Takesue, Y. Komoda, H. Murayama, K. Fujiwara ja H. Fujimoto, „Scissor lift with real-time self-adjustment ability based on variable gravity compensation mechanism,” *Advanced Robotics*, kd. 30, nr 15, pp. 1014-1026, 2016.
- [13] D. Setiawan ja A. Tahir, „Design and Construction of Lifting Machine (Forklift) Equipped with Atmega 2560 Microcontroller-Based Remote Control,” %1 *The 2nd International Conference on Natural & Social Sciences*, Palopo, 2019.
- [14] T. KAMIYA ,, K. HIKA, N. KAJIYA , H. OKAMOTO ja S. GOTO, „REMOTE CONTROL SYSTEM FOR INDUSTRIAL VEHICLES , INDUSTRIAL VEHICLE , REMOTE CONTROL DEVICE , REMOTE CONTROL PROGRAM FOR INDUSTRIAL VEHICLES , AND REMOTE CONTROL METHOD FOR INDUSTRIAL VEHICLES“. United States Patent US 2020/0012274 A1, 9 JAN 2020.
- [15] W. B. Pappas, A. . D. Alford , G. Orlando ja H. S. Amin, „AUTOMATION OF SELF - LIFTING FORKLIFT“. United States Patent US 2020/0319613 A1, 8 oct 2020.
- [16] L. S. Sterling, *The Art of Agent-Oriented Modeling*, London: The MIT Press, 2009.

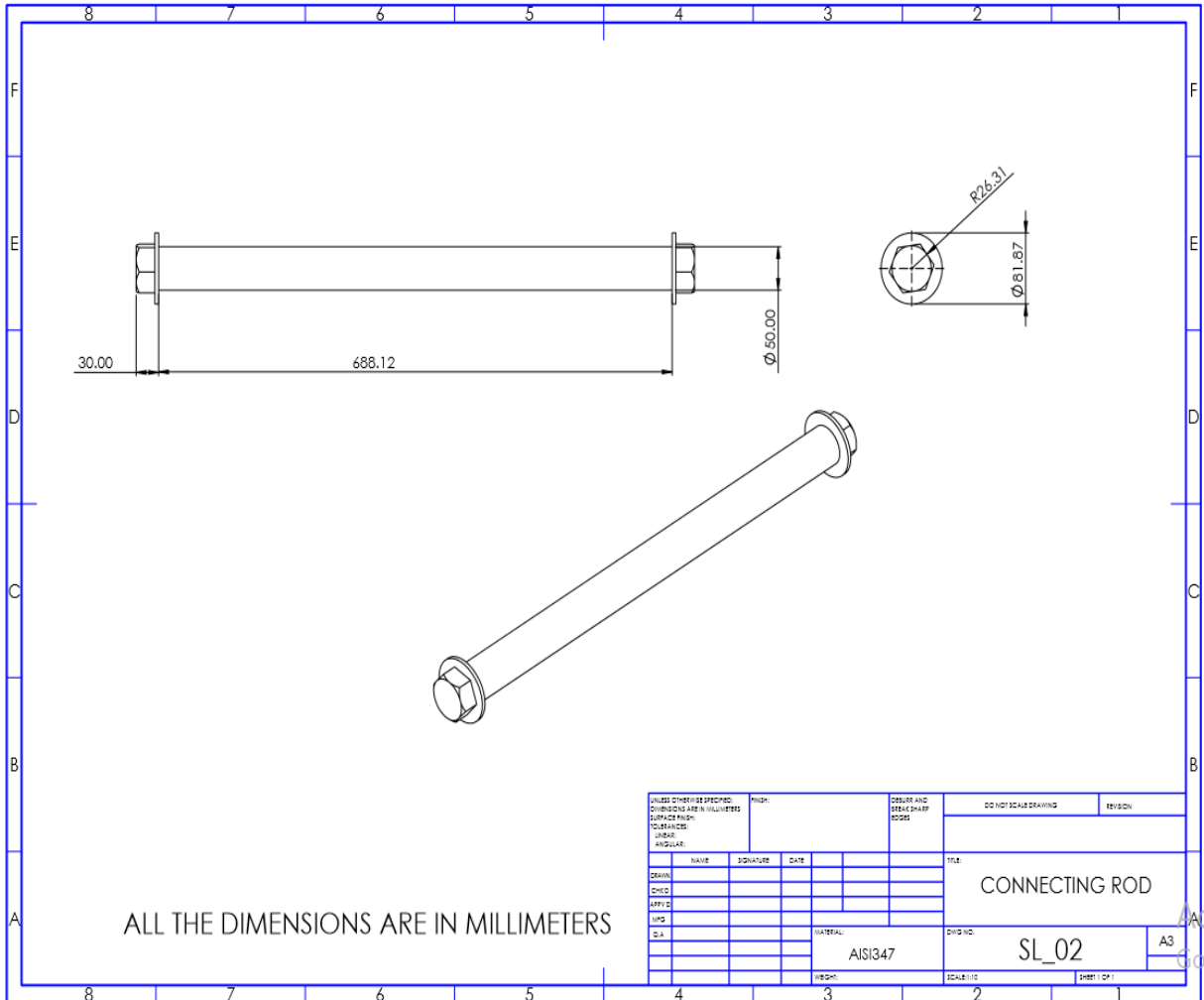
APPENDIX 1

Forklift Guide Plate



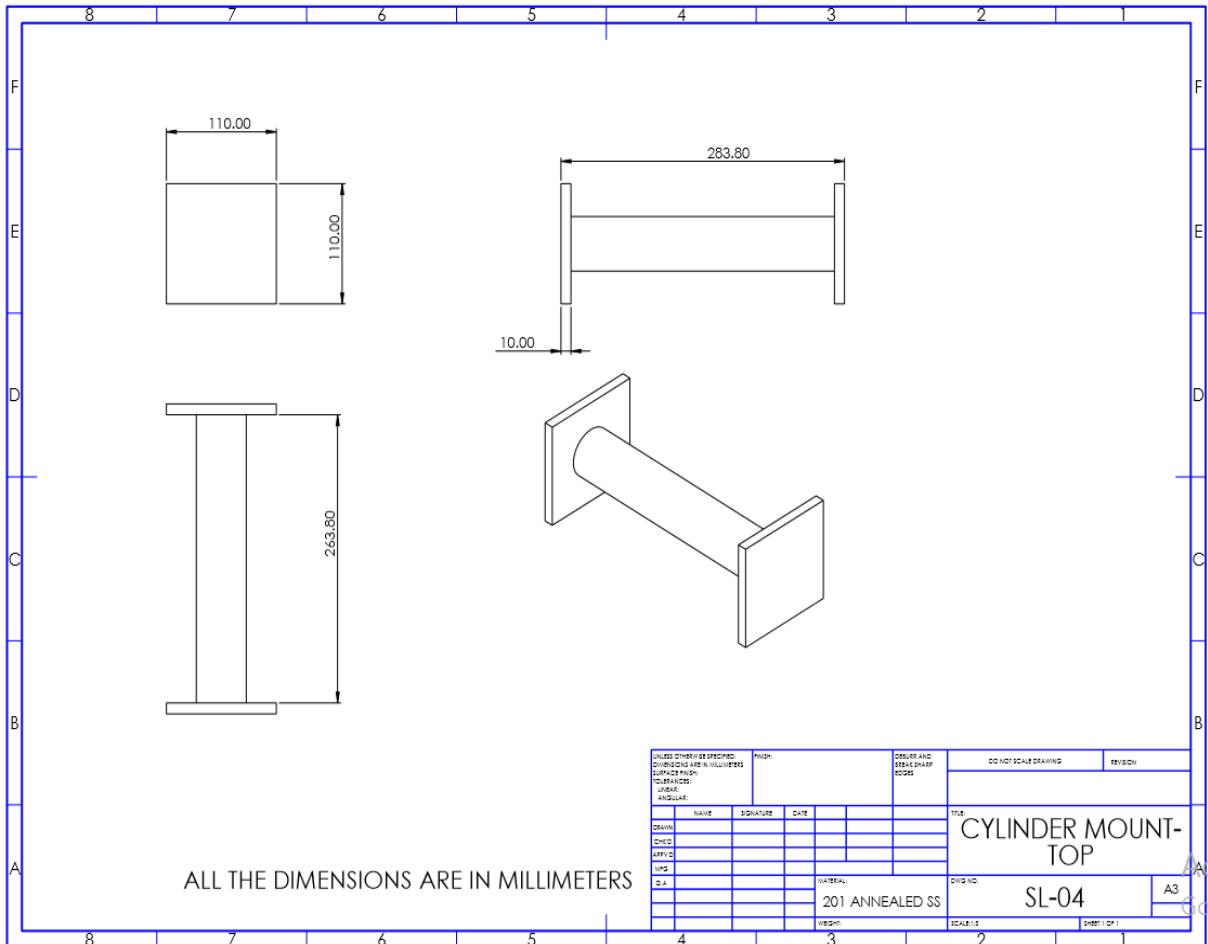
APPENDIX 2

Connecting Rod



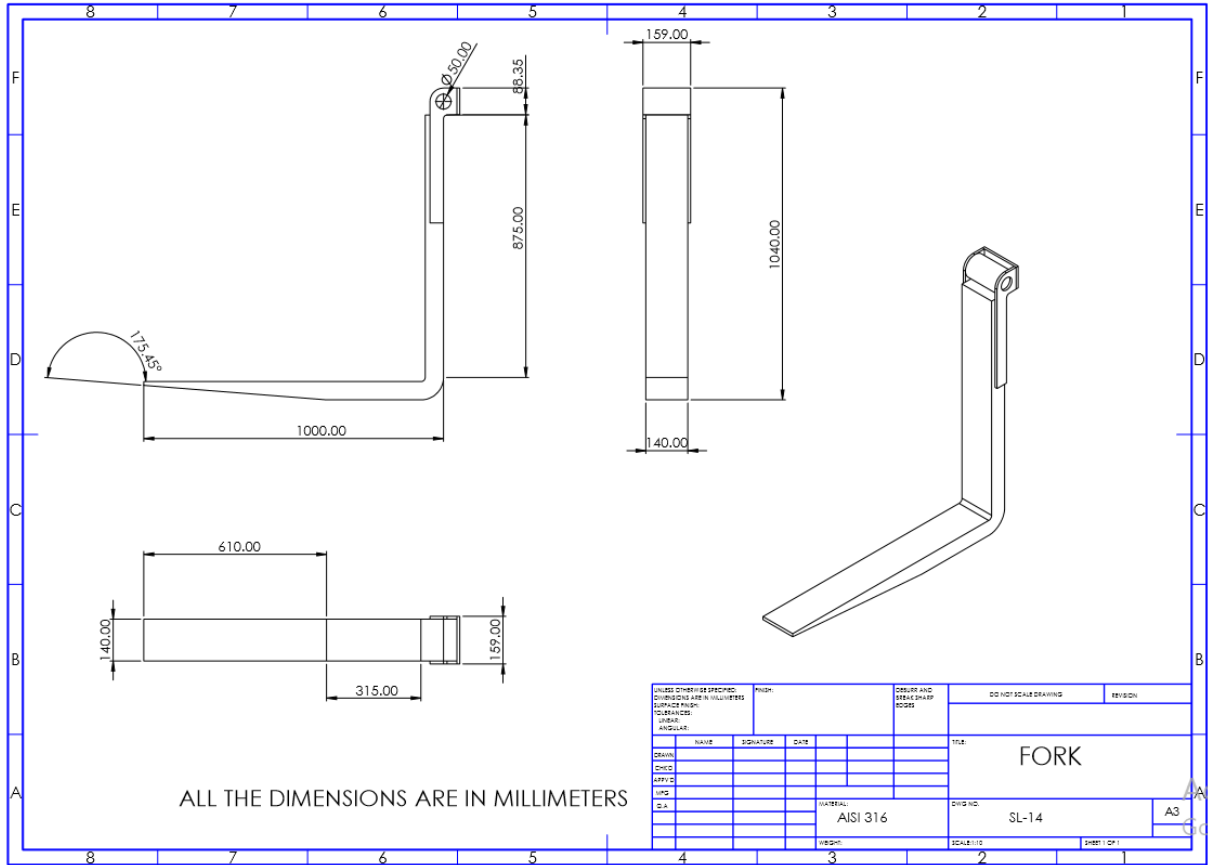
APPENDIX 3

Cylinder mount top



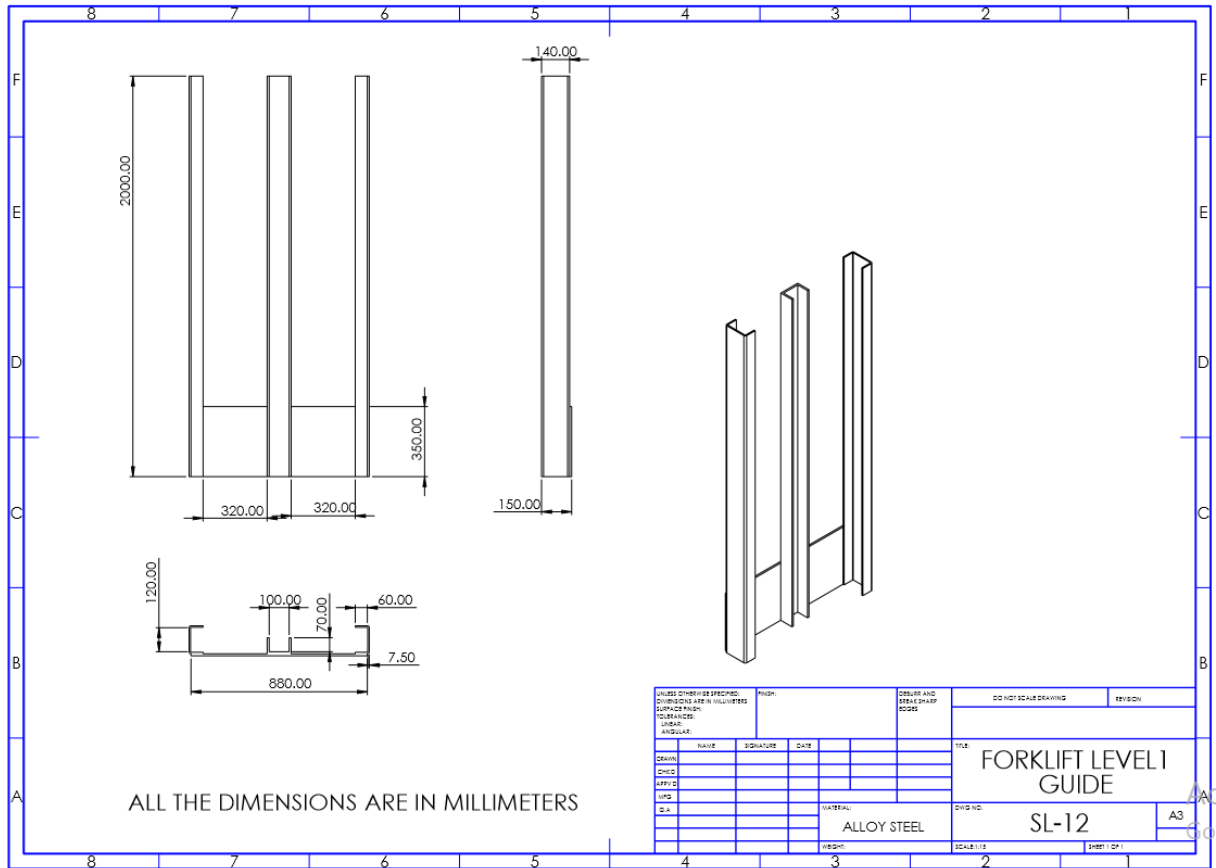
APPENDIX 4

Fork



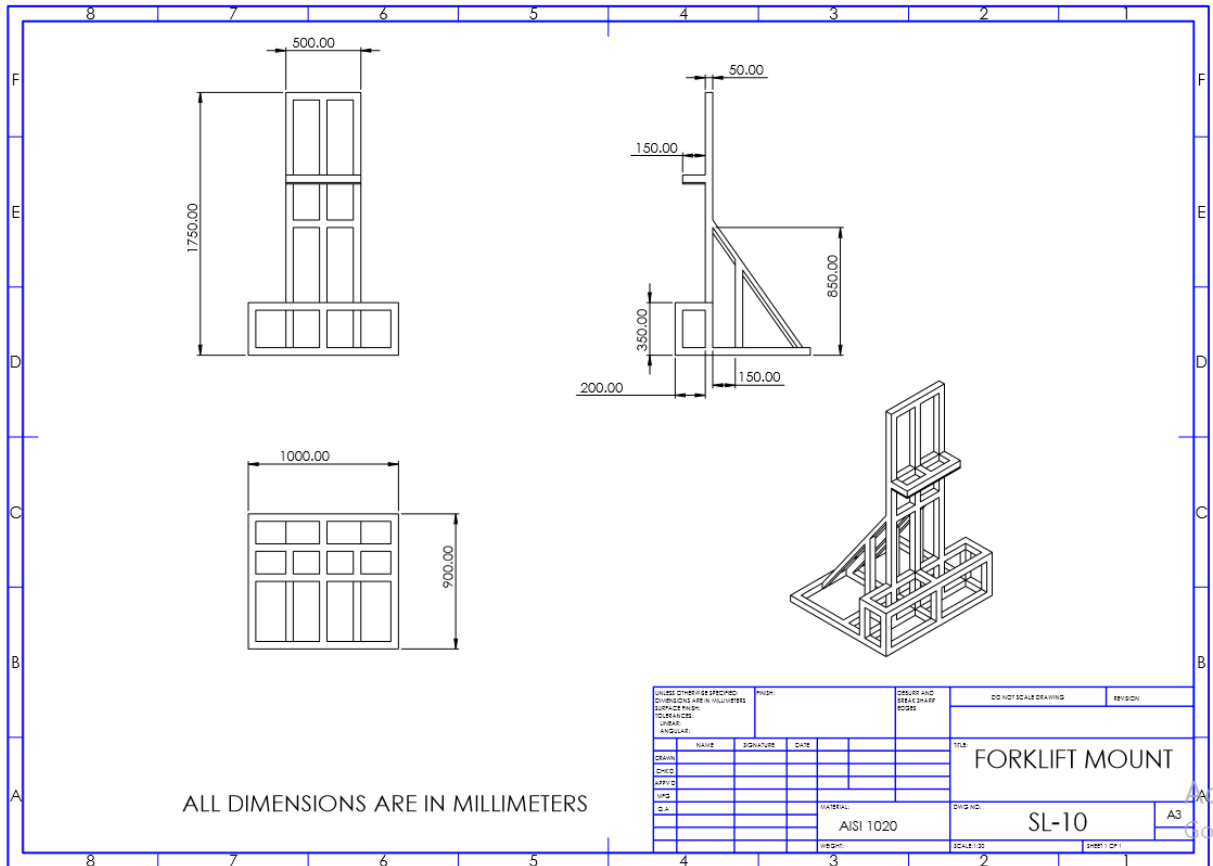
APPENDIX 5

Forklift level 1 guide



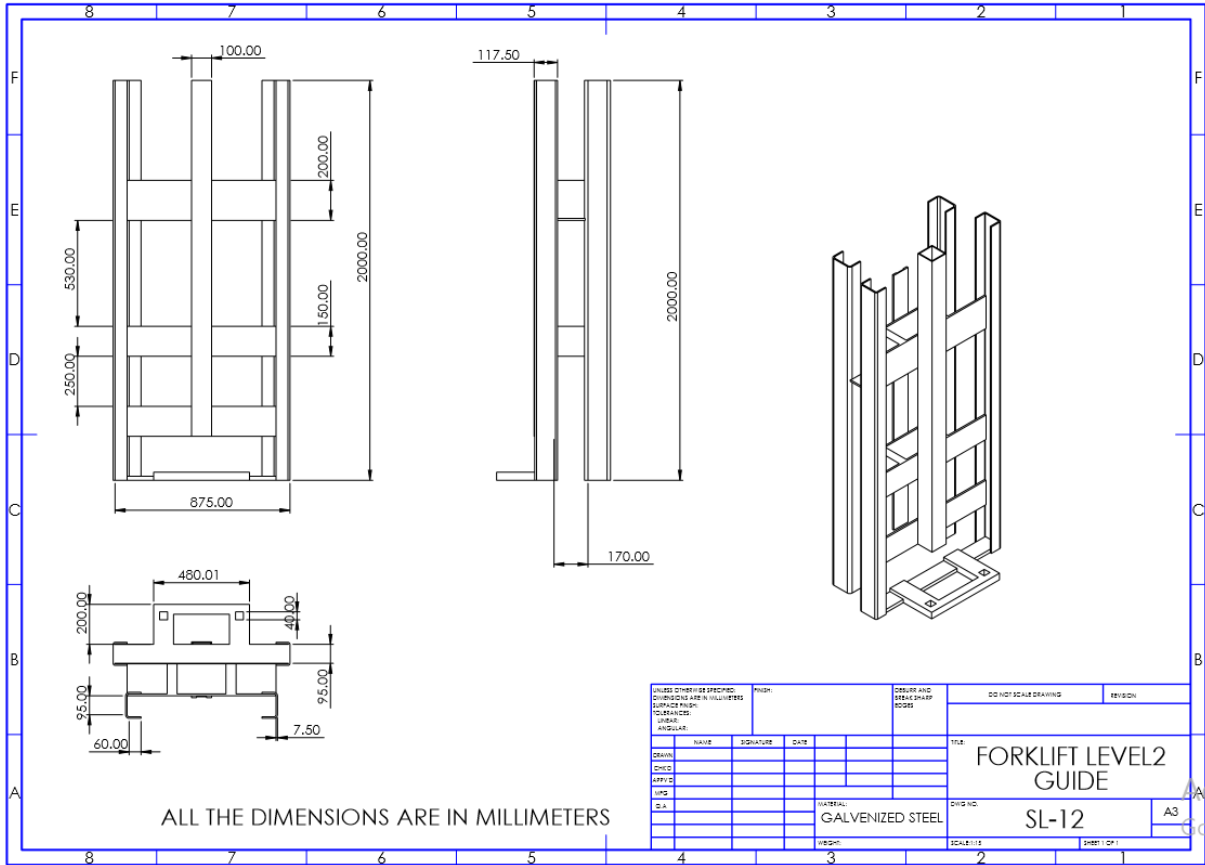
APPENDIX 6

Forklift mount



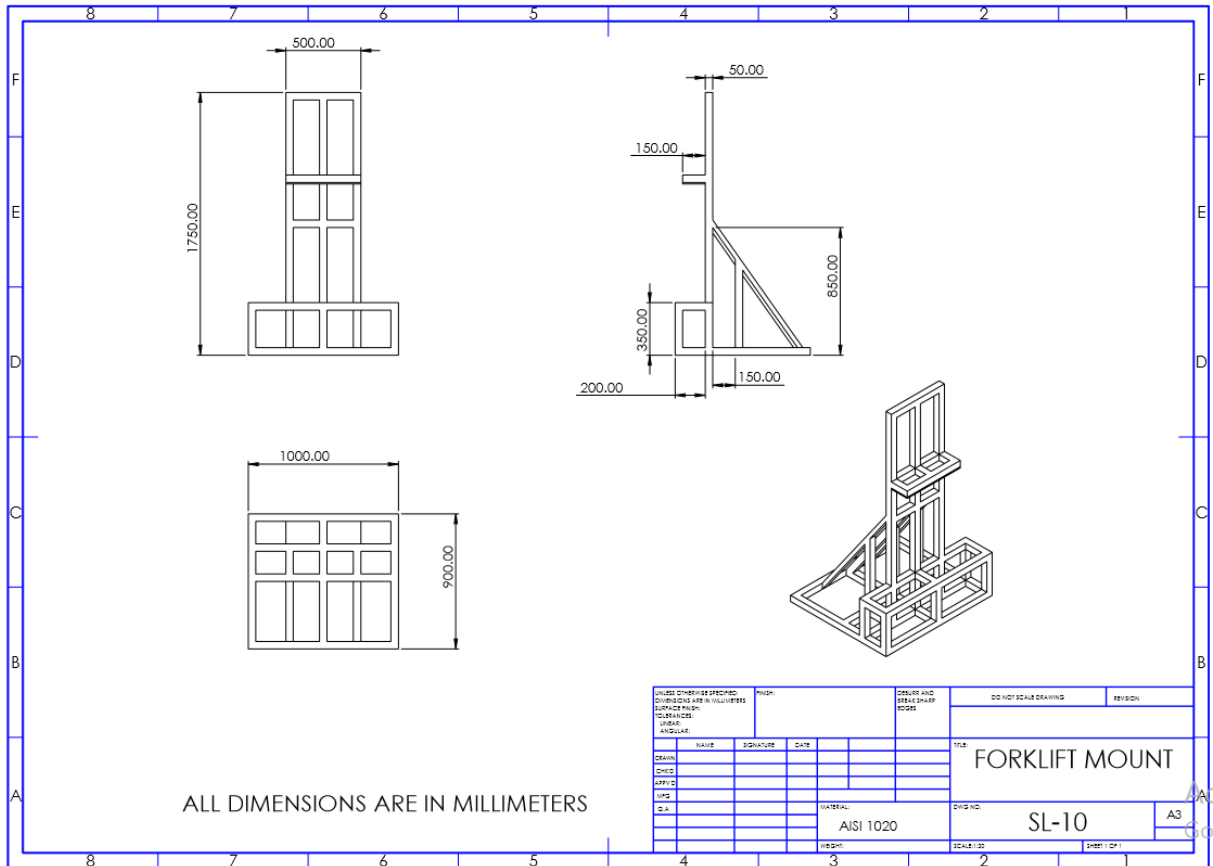
APPENDIX 7

Forklift level 2 guide



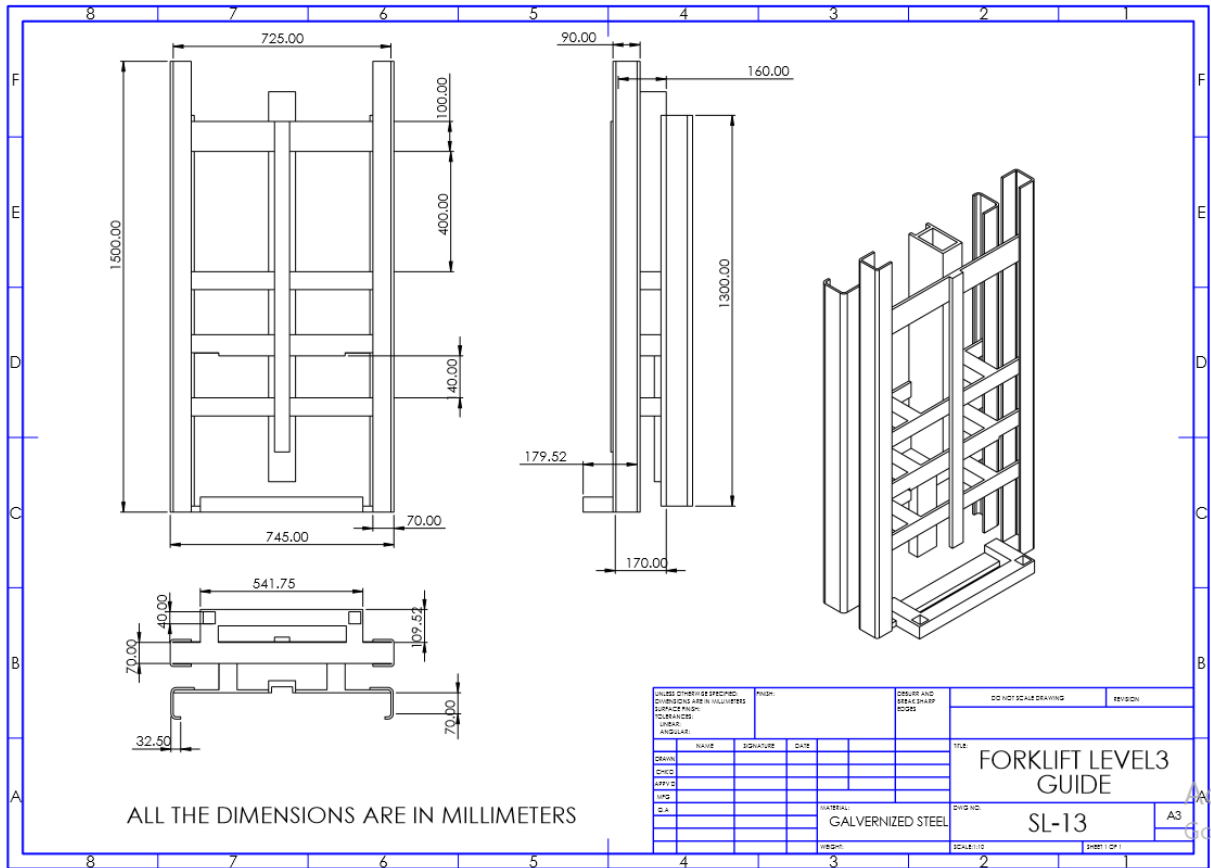
APPENDIX 8

Fork mount



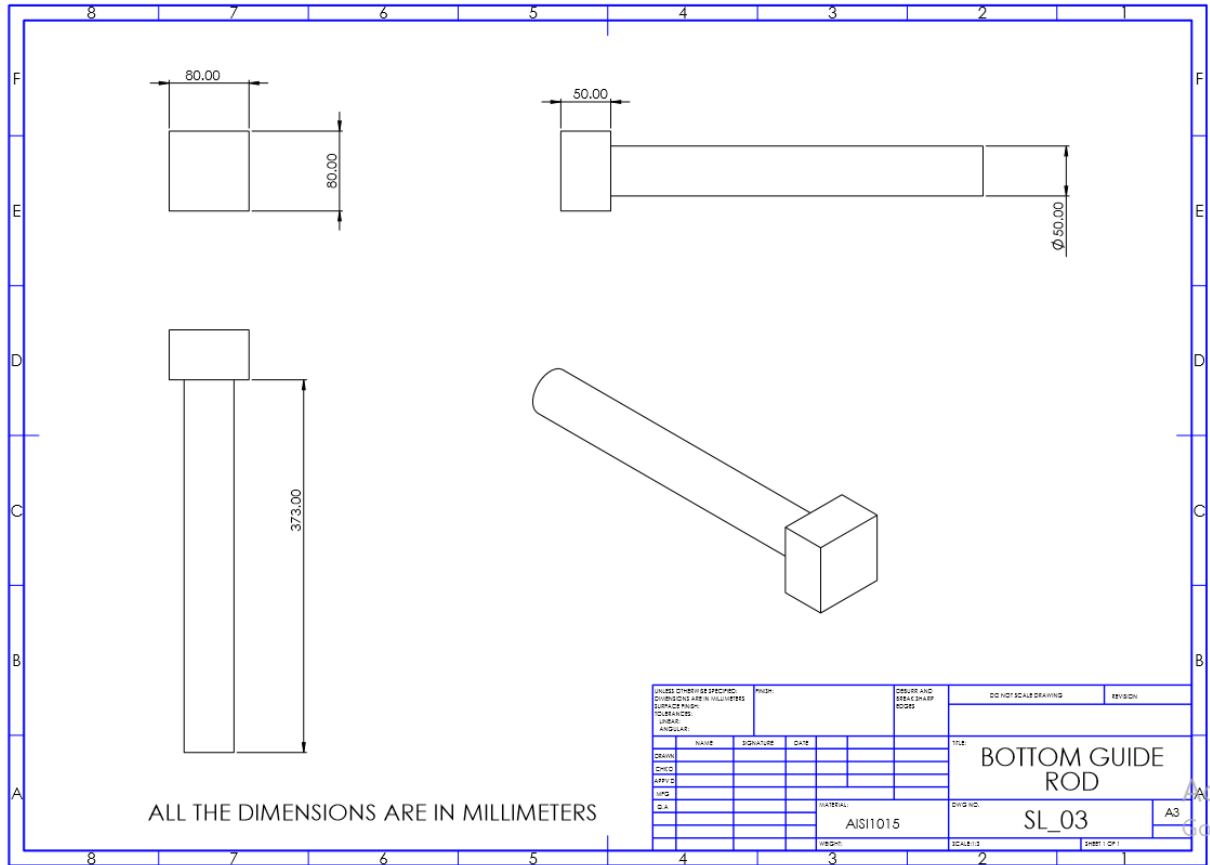
APPENDIX 9

Forklift level 3 guide



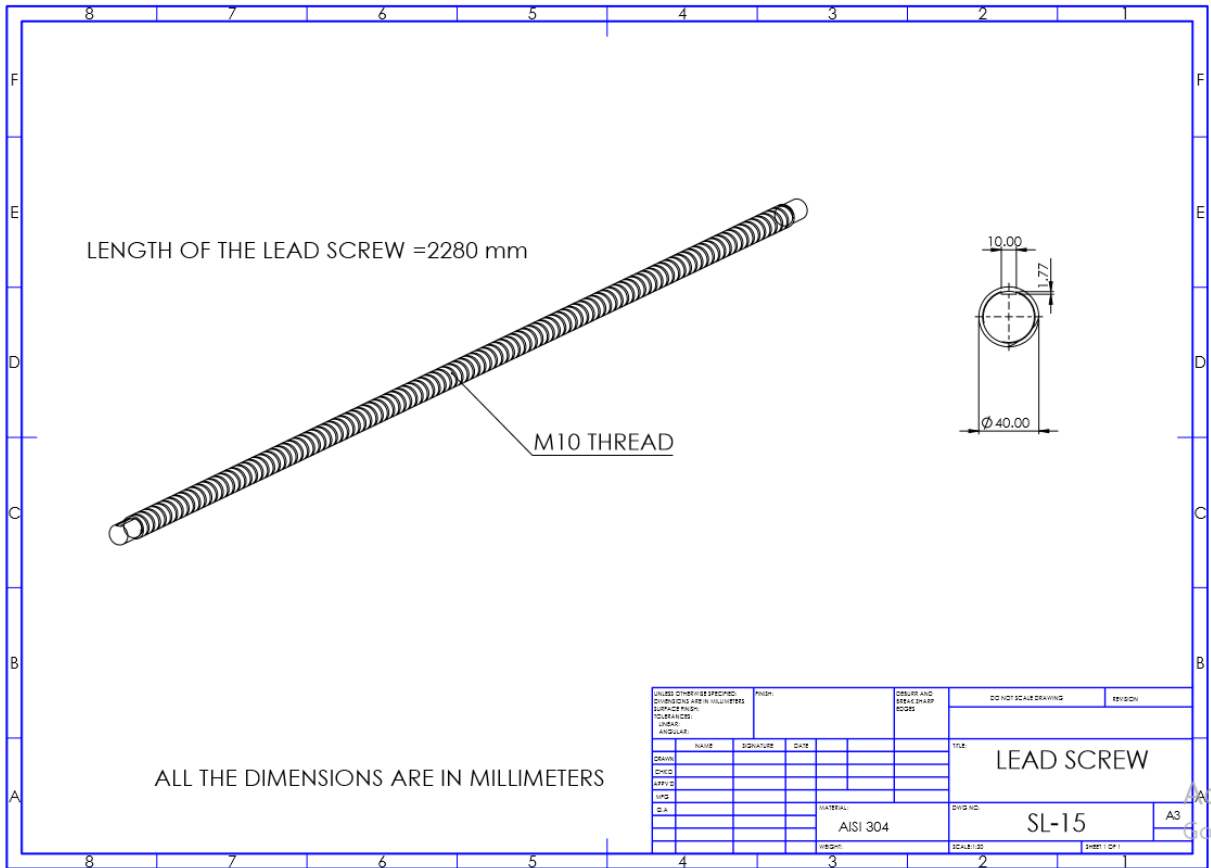
APPENDIX 10

Bottom guide rod



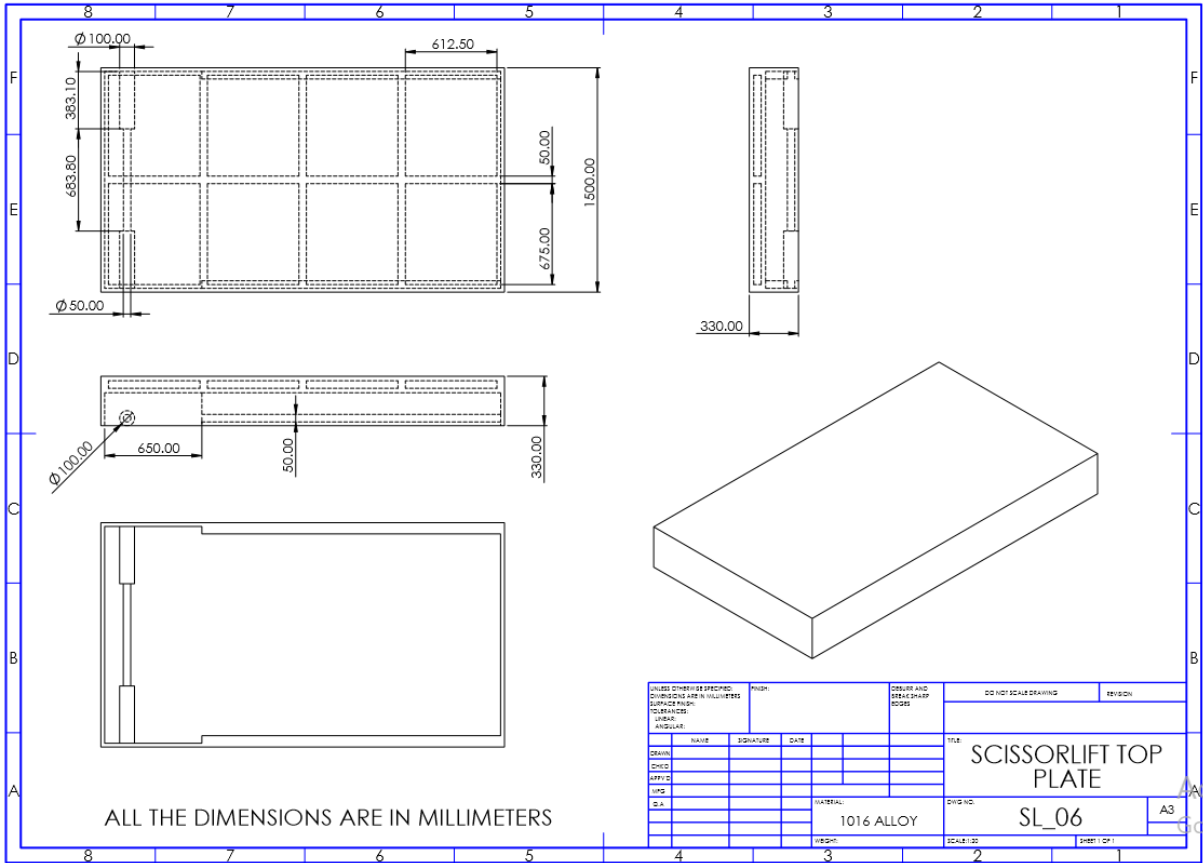
APPENDIX 11

Lead screw



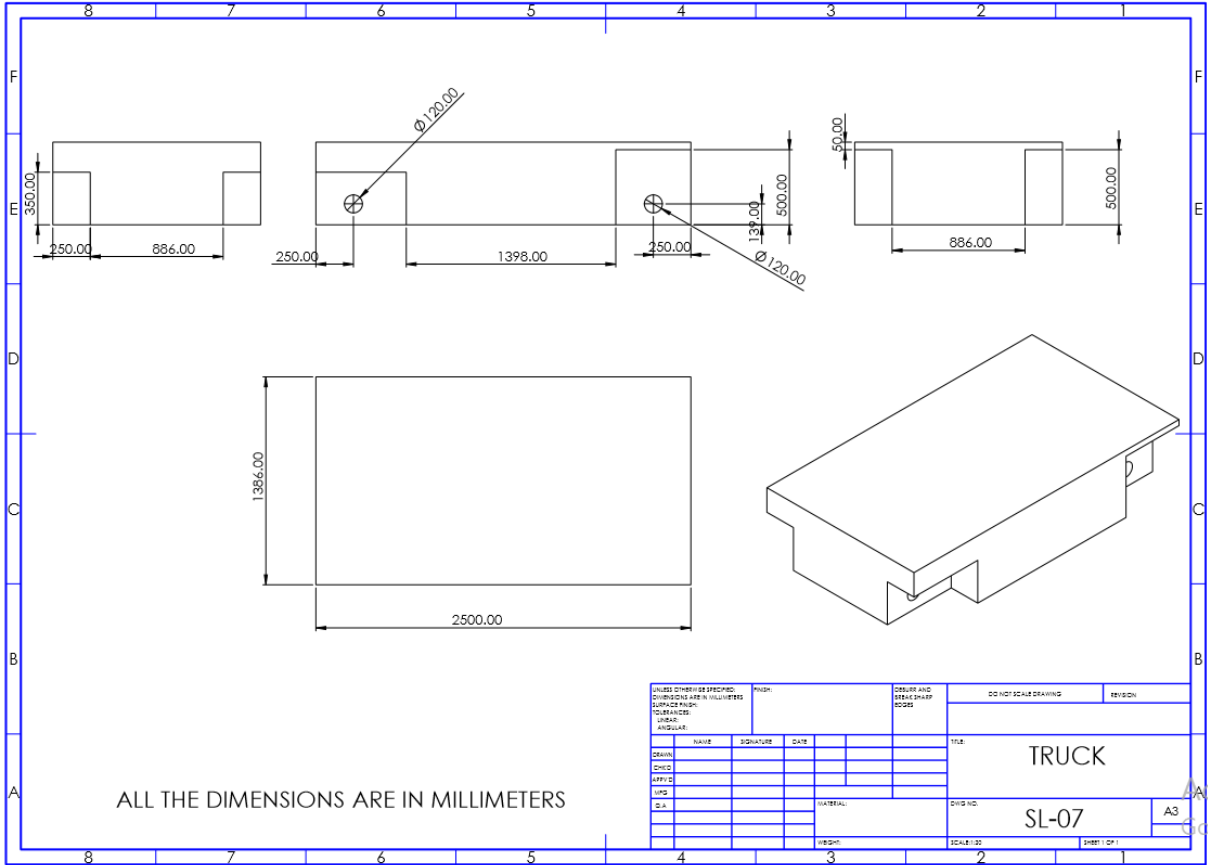
APPENDIX 13

Scissor lift top plate



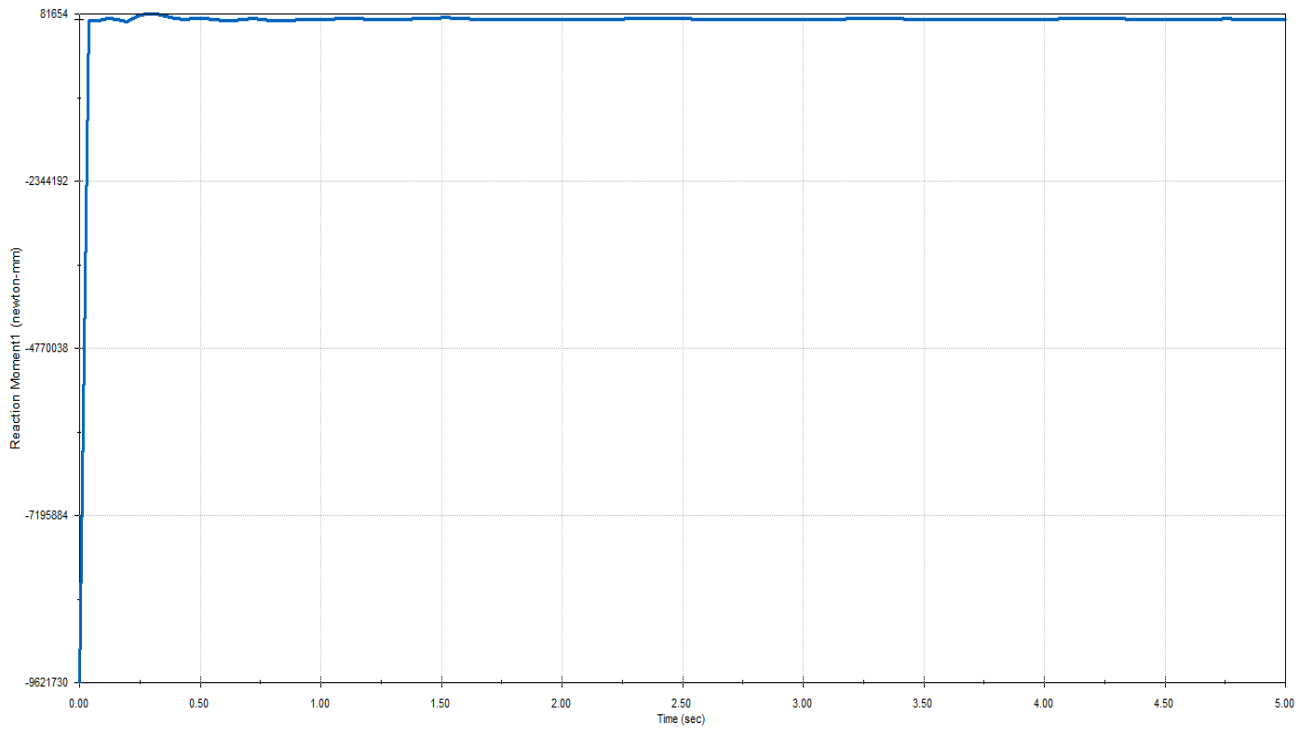
APPENDIX 16

Truck



APPENDIX 18

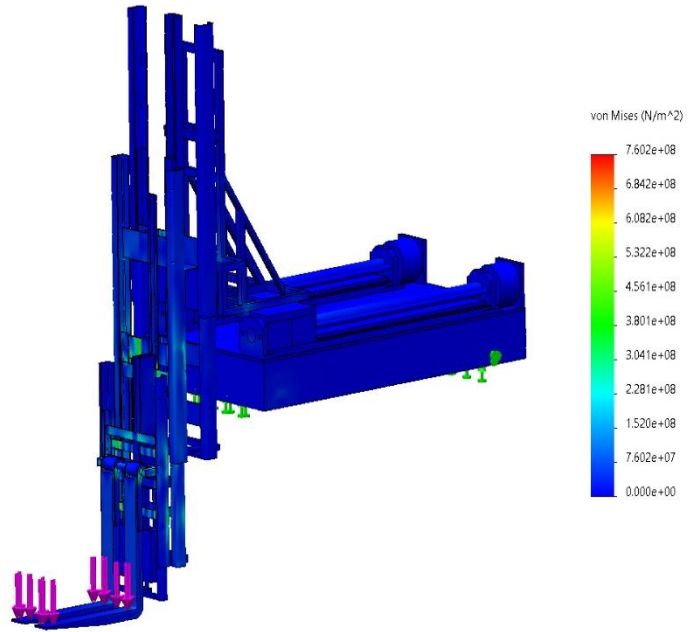
Plot1



APPENDIX 19

Stress

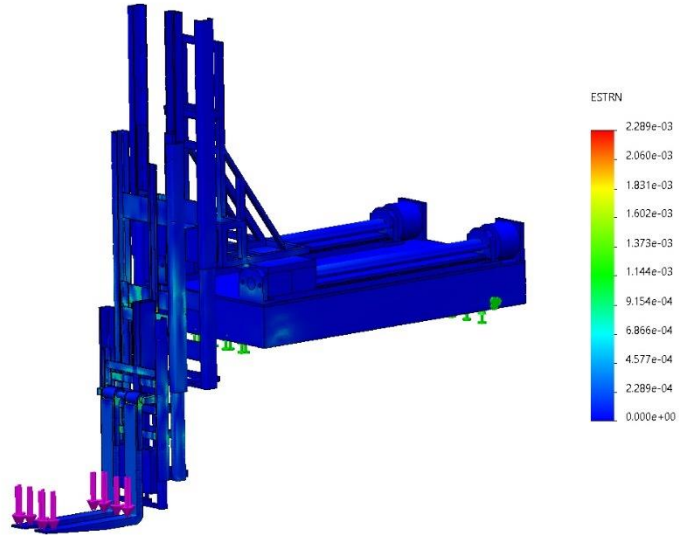
Model name: machine_assembly_final
Study name: Static 4(-Default-)
Plot type: Static nodal stress Stress1



APPENDIX 20

Strain

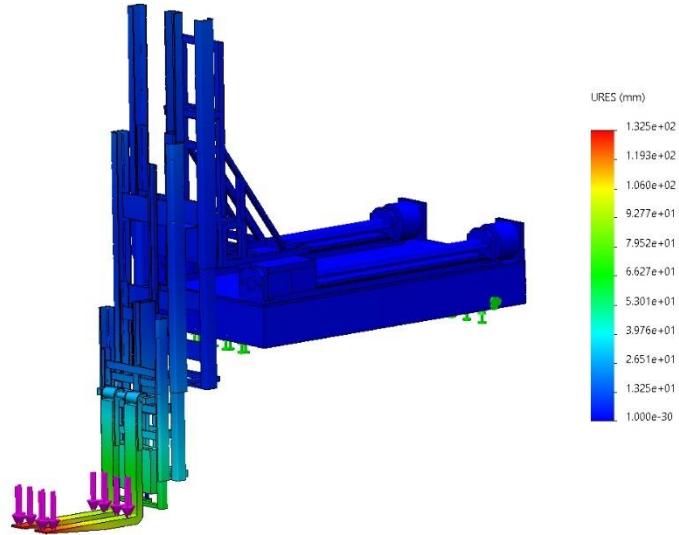
Model name: machine_assembly_final
Study name: Static 4(-Default-)
Plot type: Static strain Strain1



APPENDIX 21

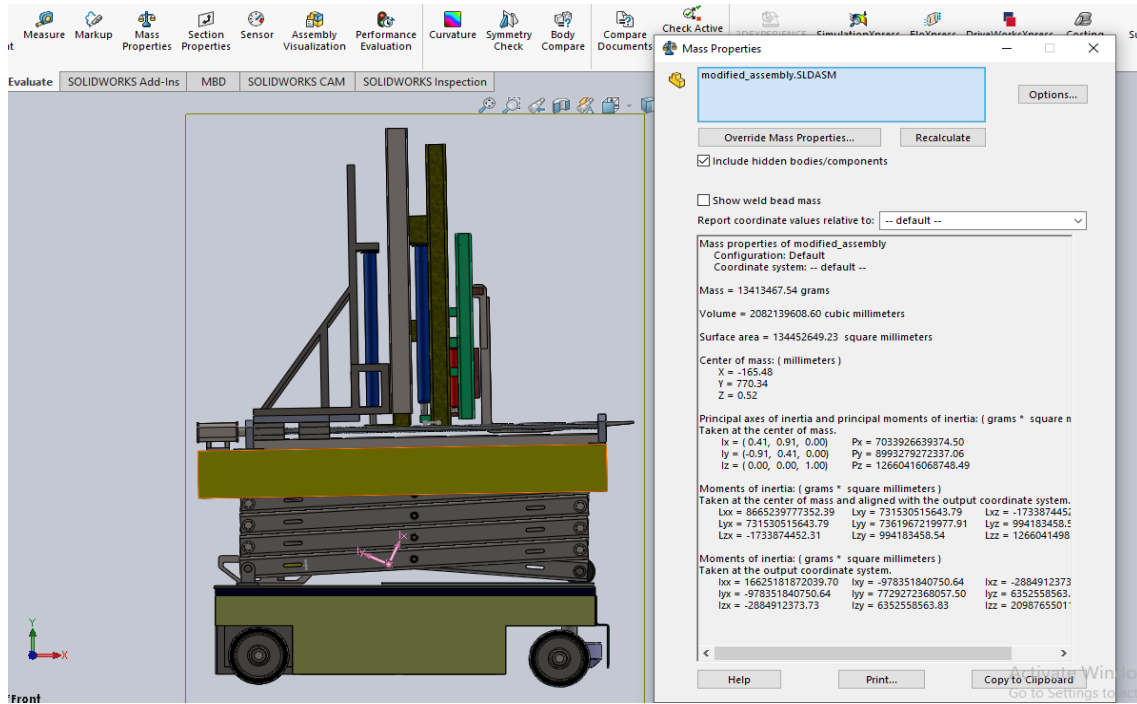
Displacement

Model name: machine_assembly_final
Study name: Static 4(-Default-)
Plot type: Static displacement/Displacement1



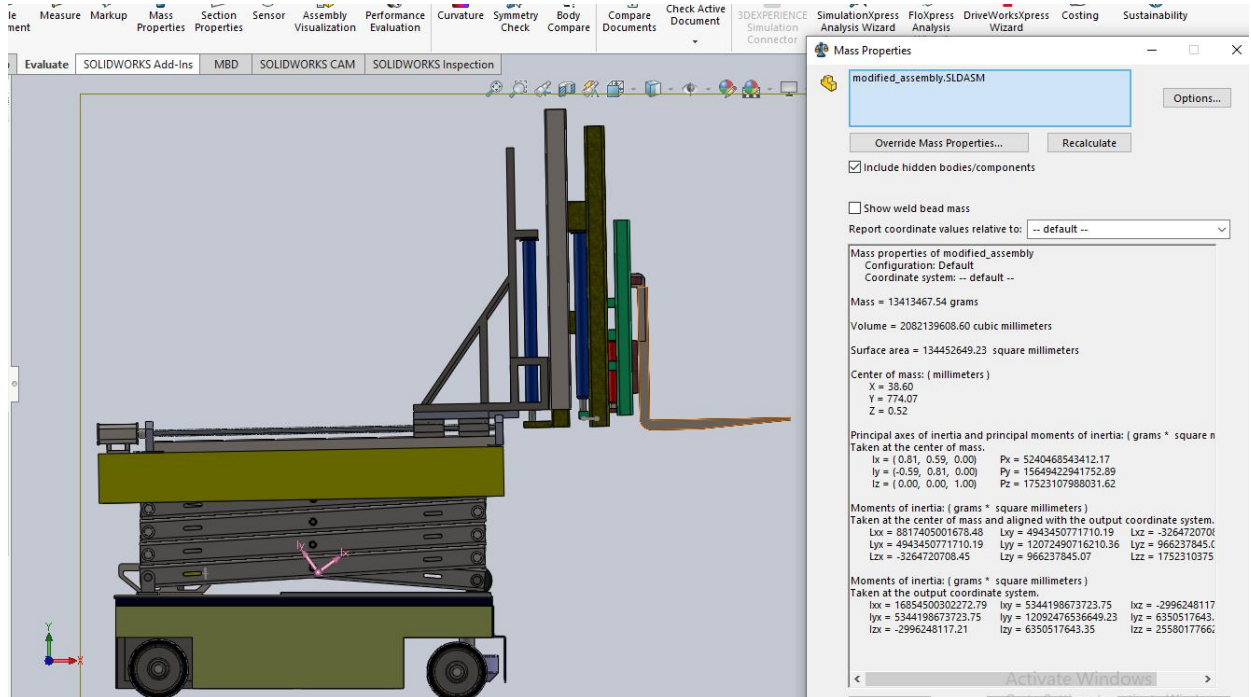
APPENDIX 22

Centre of gravity and moment of inertia details at neutral position. (without load)



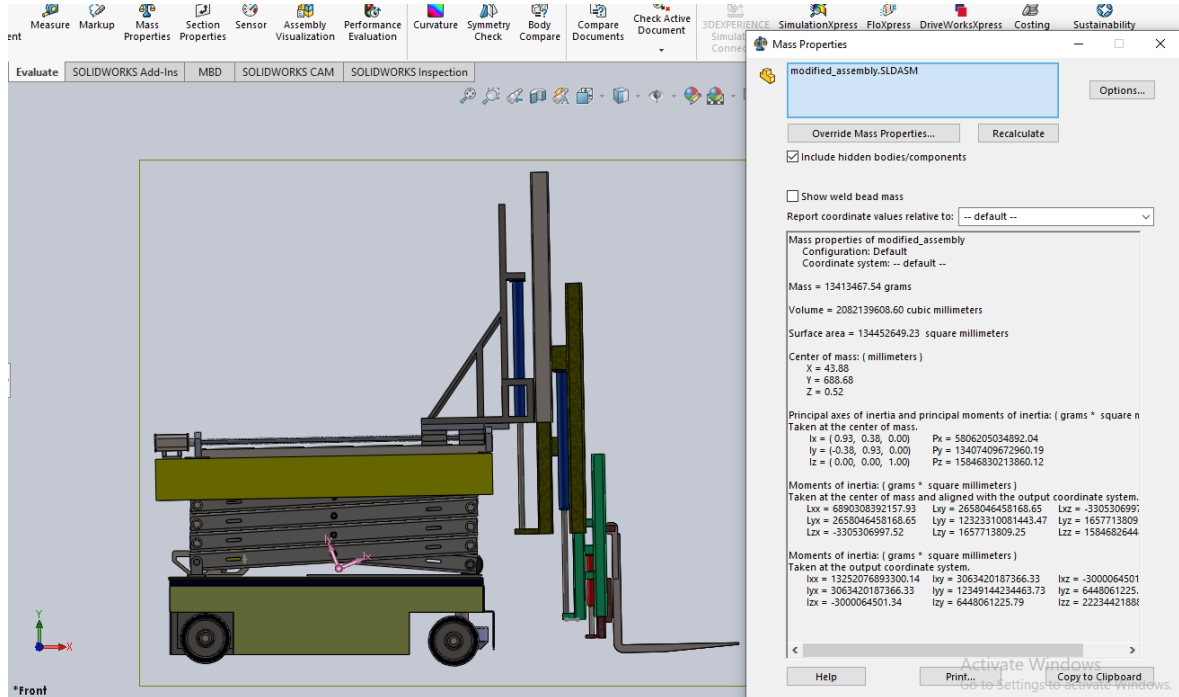
APPENDIX 23

Centre of gravity and moment of inertia details at forklift release position.
(without load)



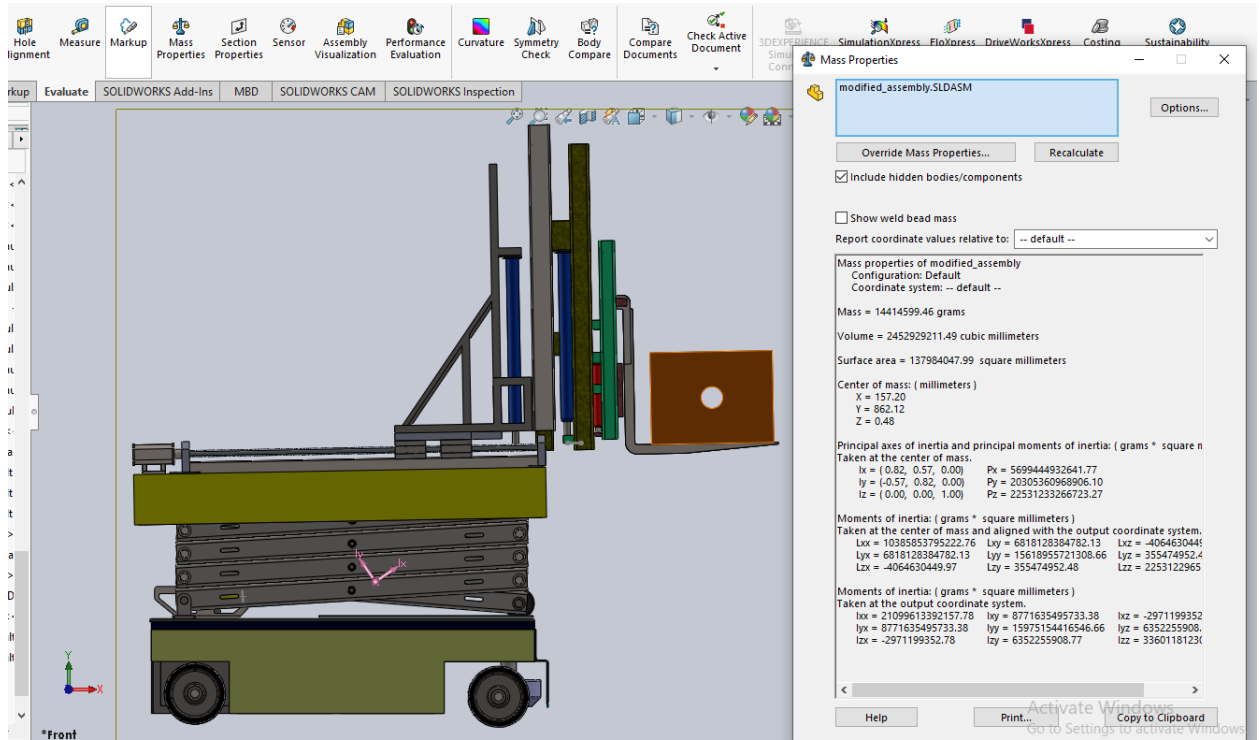
APPENDIX 24

Centre of gravity and moment of inertia details at forklift loading position.
(without load)



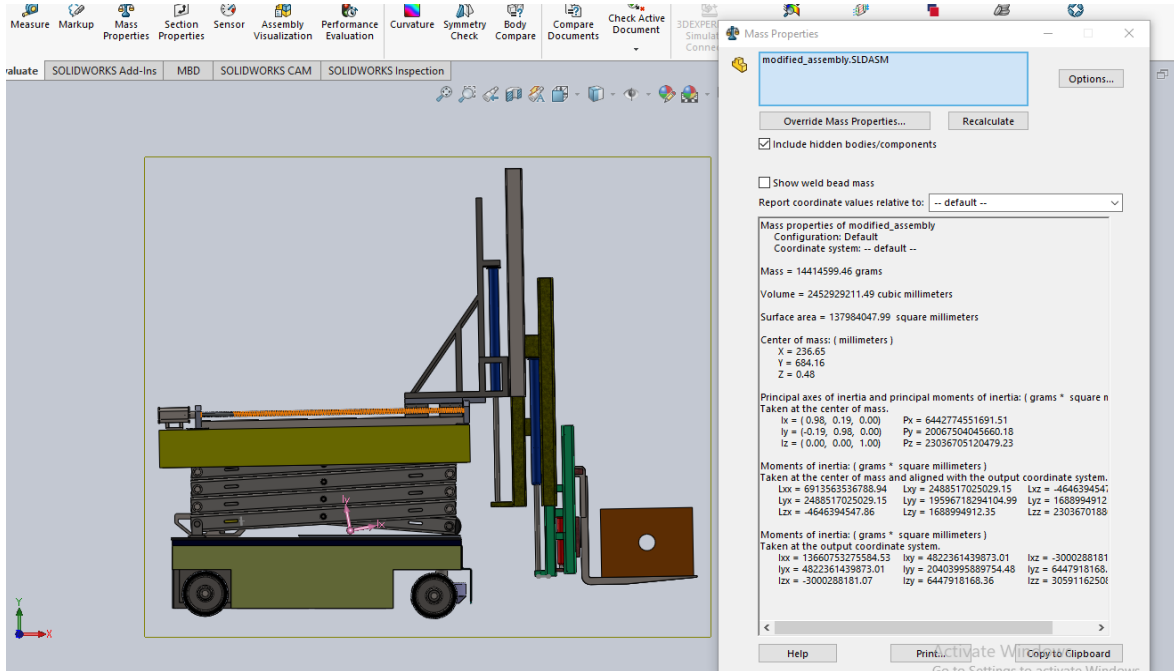
APPENDIX 25

Centre of gravity and moment of inertia details at forklift release position.
(with load)



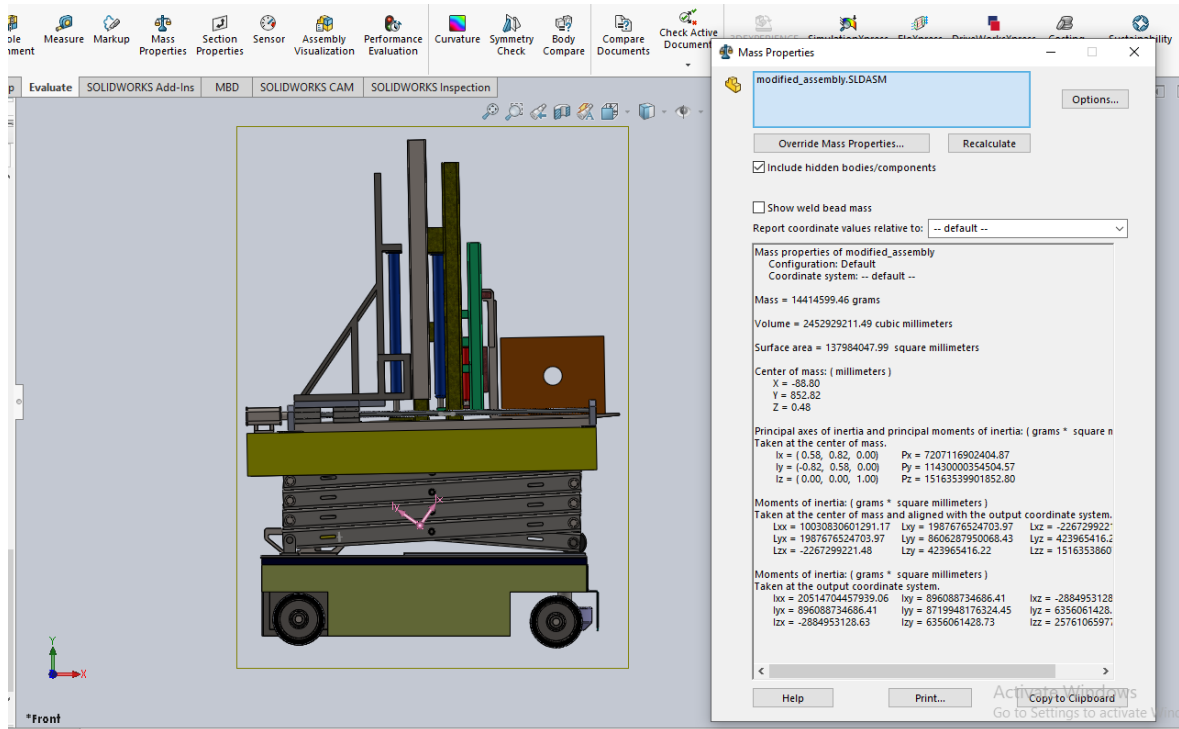
APPENDIX 26

Centre of gravity and moment of inertia details at forklift loading position. (with load)



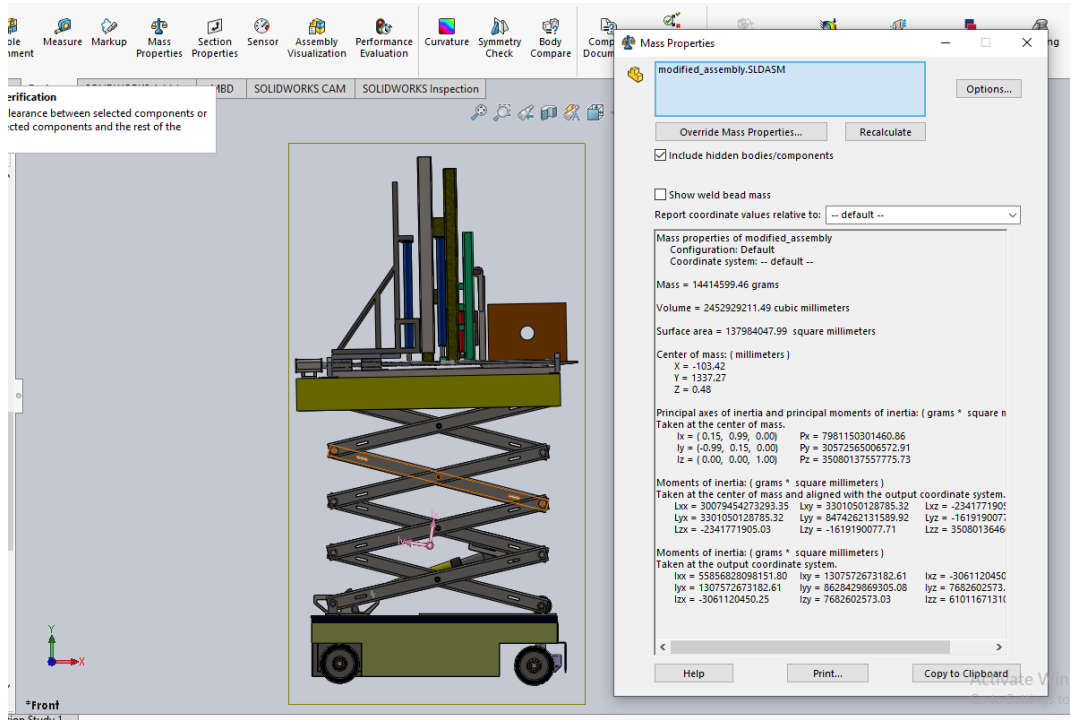
APPENDIX 27

Centre of gravity and moment of inertia details at forklift neutral position.
(with load)



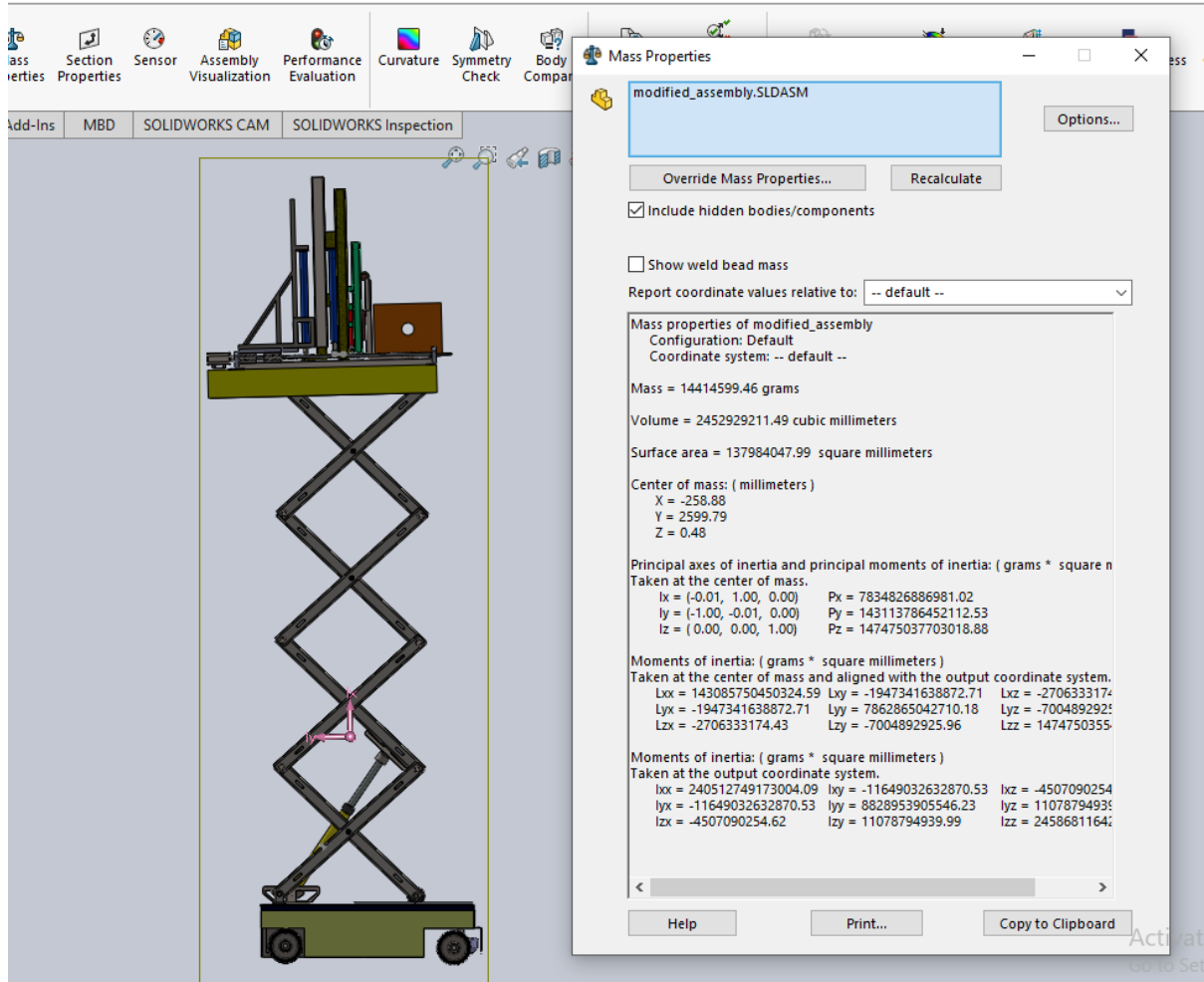
APPENDIX 28

Centre of gravity and moment of inertia details at forklift lifting at 2m. (with load)



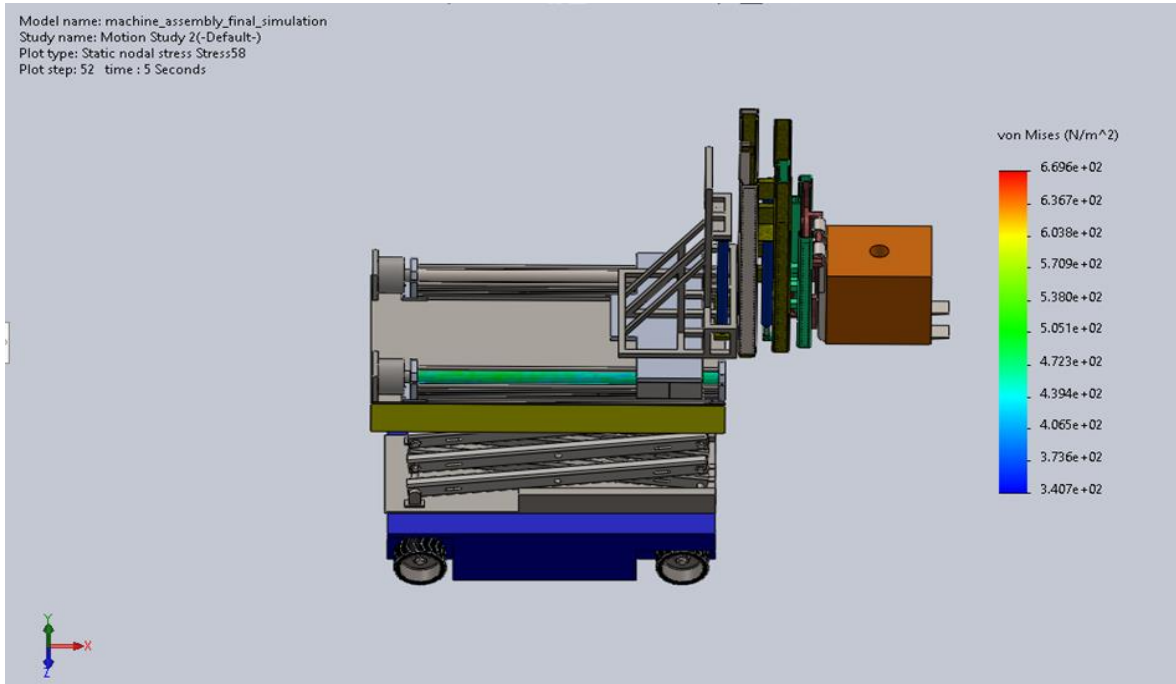
APPENDIX 29

Centre of gravity and moment of inertia details at forklift lifting at maximum height (7m). (with load)



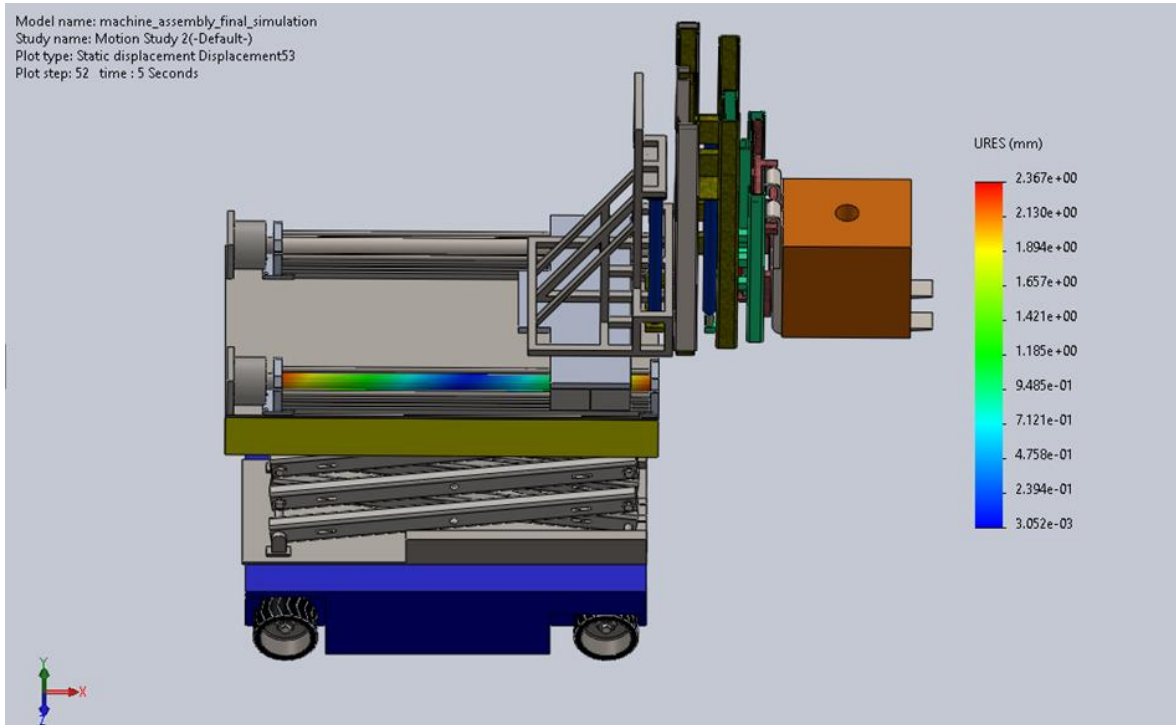
APPENDIX 30

Stress



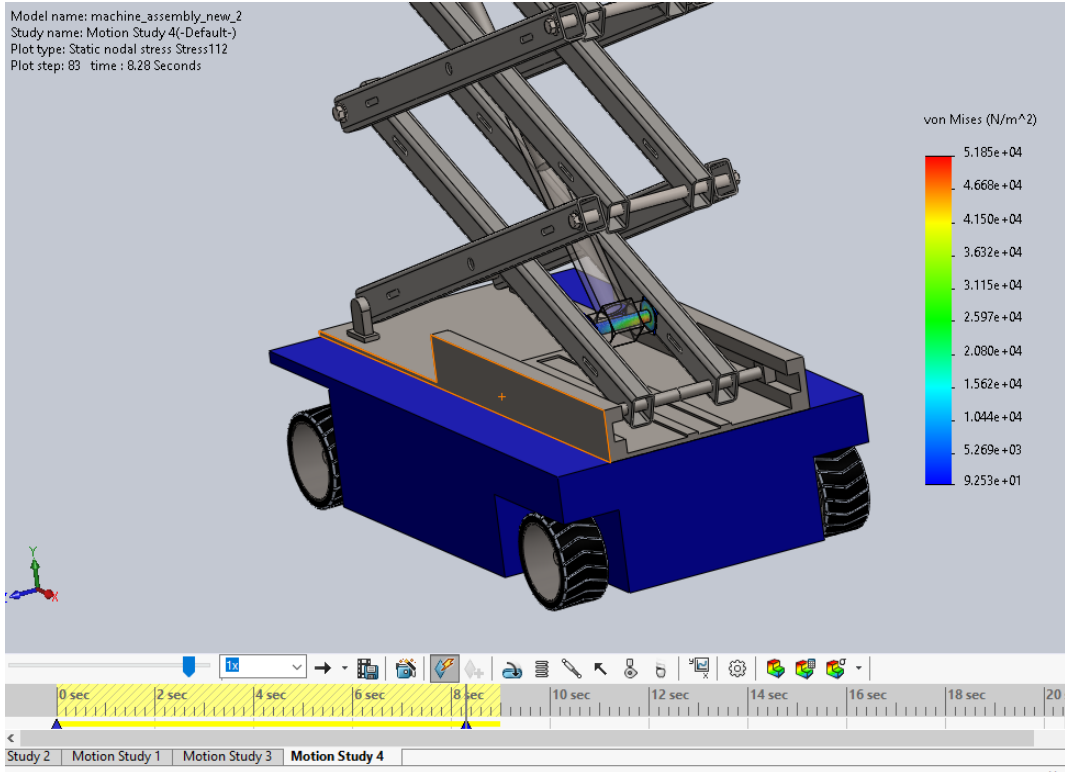
APPENDIX 31

Displacement



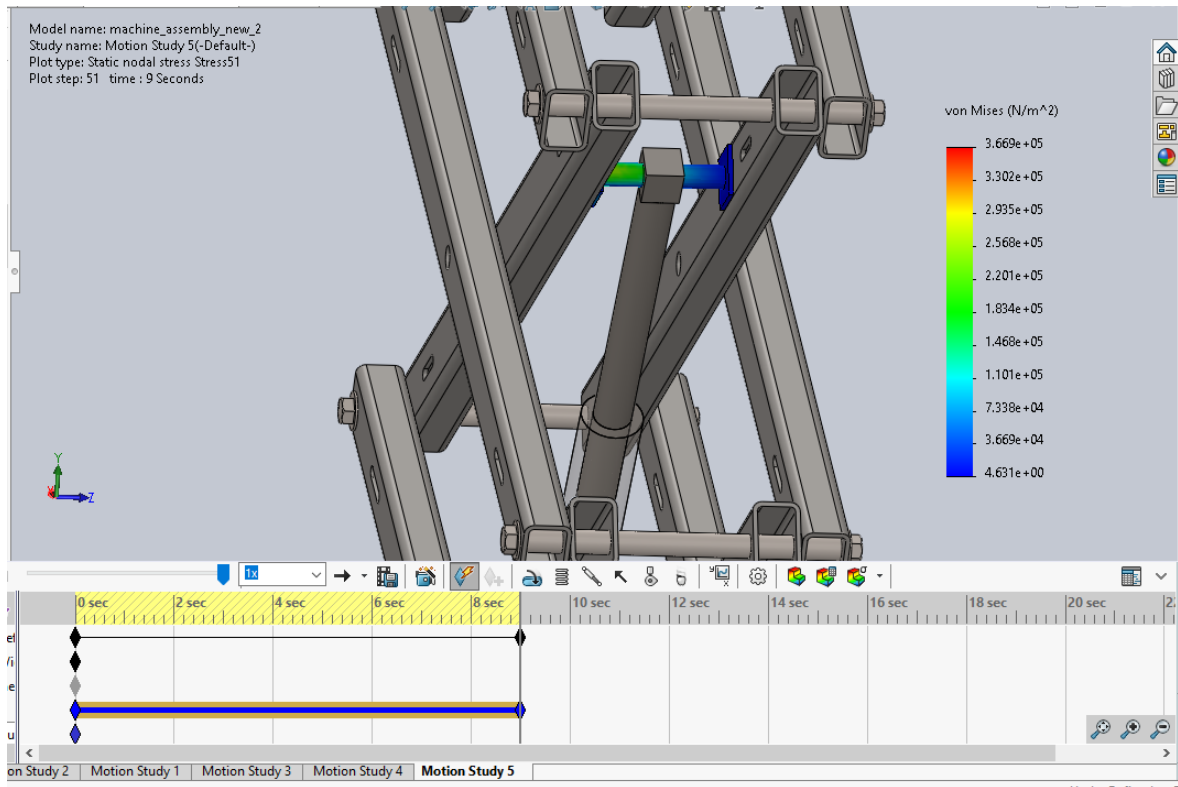
APPENDIX 32

Stress



APPENDIX 33

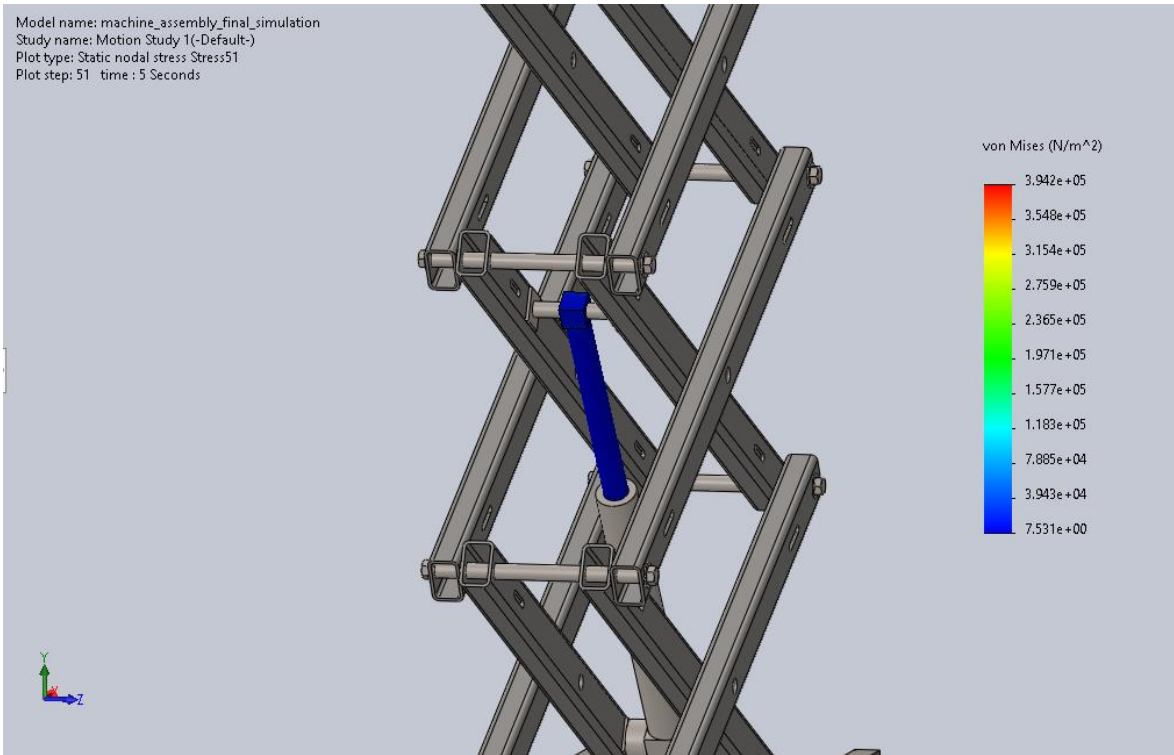
Stress



APPENDIX 34

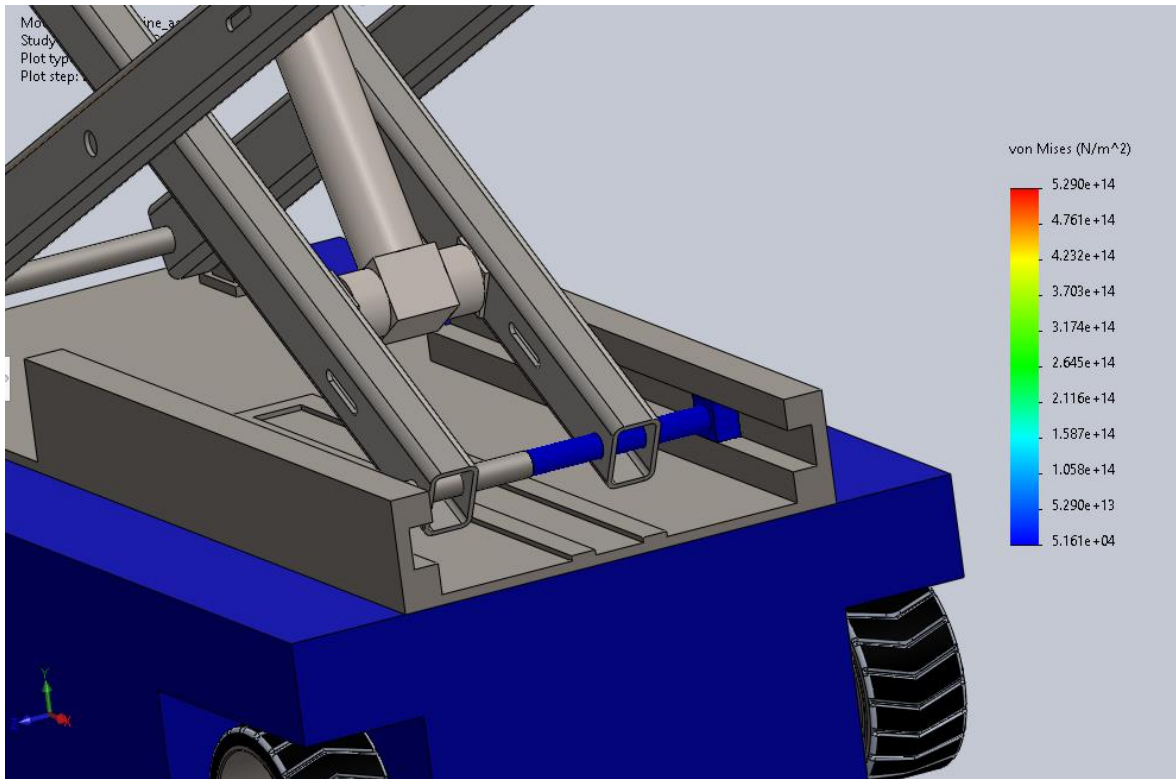
Stress

Model name: machine_assembly_final_simulation
Study name: Motion Study 1(-Default-)
Plot type: Static nodal stress Stress51
Plot step: 51 time : 5 Seconds



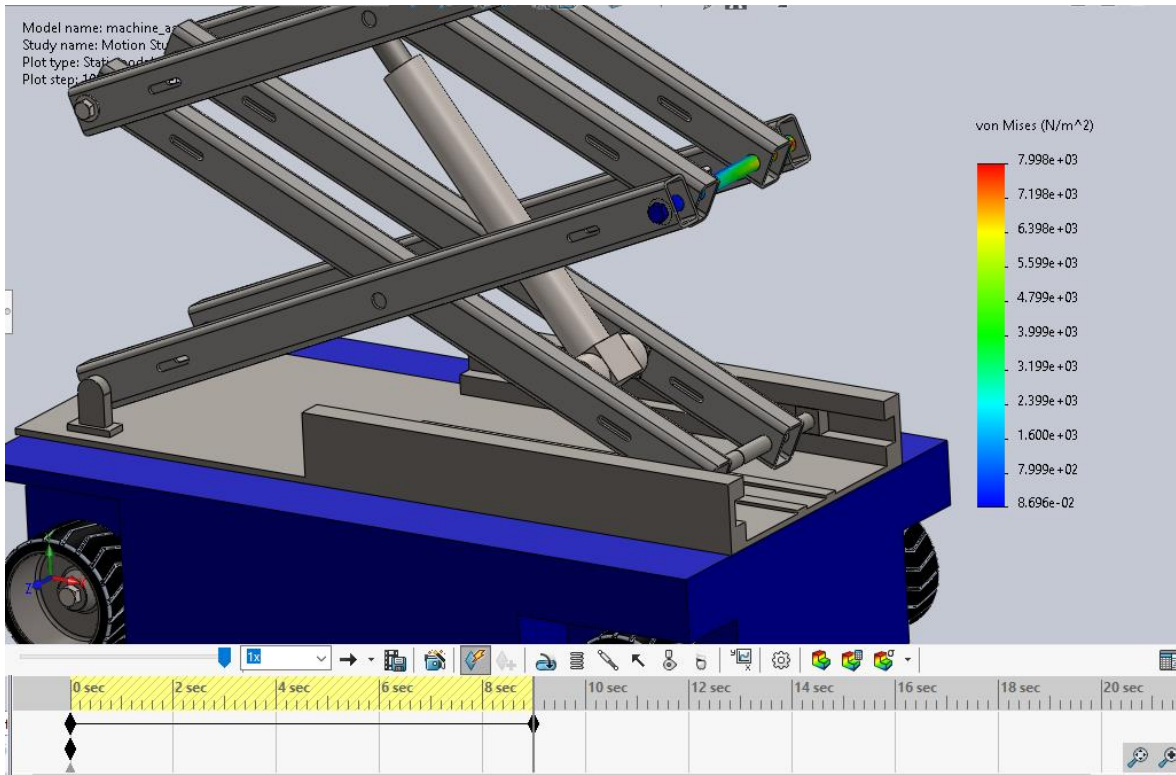
APPENDIX 35

Stress



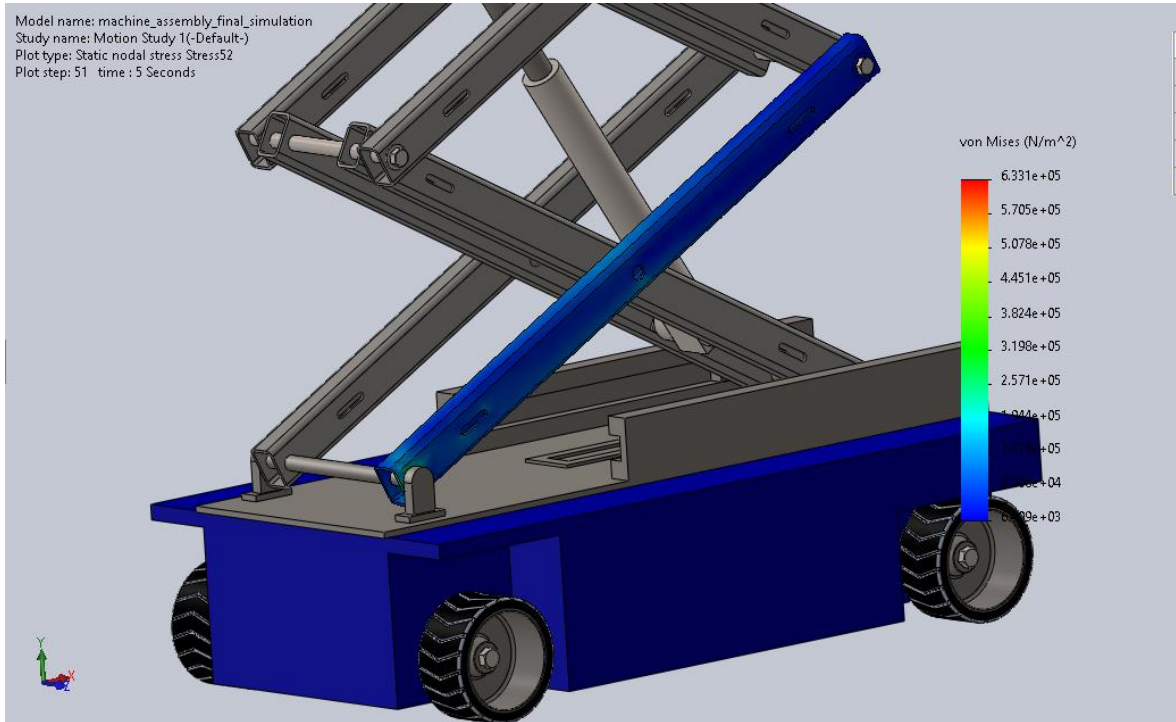
APPENDIX 36

Stress



APPENDIX 37

Stress



APPENDIX 38

Material properties of lead screw

Properties Tables & Curves Appearance CrossHatch Custom Application Data

Material properties
Materials in the default library can not be edited. You must first copy the material to a custom library to edit it.

Model Type: Linear Elastic Isotropic Save model type in library

Units: SI - N/mm² (MPa)

Category: Steel

Name: 201 Annealed Stainless Steel (SS)

Default failure criterion: Max von Mises Stress

Description:

Source:

Sustainability: Defined

| Property | Value | Units |
|-------------------------------|-----------|-------------------|
| Elastic Modulus | 207000 | N/mm ² |
| Poisson's Ratio | 0.27 | N/A |
| Shear Modulus | | N/mm ² |
| Mass Density | 7859.9999 | kg/m ³ |
| Tensile Strength | 685 | N/mm ² |
| Compressive Strength | | N/mm ² |
| Yield Strength | 292 | N/mm ² |
| Thermal Expansion Coefficient | 1.7e-05 | /K |

APPENDIX 39

Material properties of truck frame

Properties **Tables & Curves** Appearance CrossHatch Custom Application Data

Material properties
 Materials in the default library can not be edited. You must first copy the material to a custom library to edit it.

Model Type: **Linear Elastic Isotropic** Save model type in library

Units: **SI - N/m² (Pa)**

Category: **Steel**

Name: **AISI 4340 Steel, annealed**

Default failure criterion: **Max von Mises Stress**

Description:

Source:

Sustainability: **Defined**

| Property | Value | Units |
|-------------------------------|-----------|-------------------|
| Elastic Modulus | 2.05e+11 | N/m ² |
| Poisson's Ratio | 0.285 | N/A |
| Shear Modulus | 8e+10 | N/m ² |
| Mass Density | 7850 | kg/m ³ |
| Tensile Strength | 745000000 | N/m ² |
| Compressive Strength | | N/m ² |
| Yield Strength | 470000000 | N/m ² |
| Thermal Expansion Coefficient | 1.23e-05 | /K |

APPENDIX 40

Material properties of scissor link

Properties Tables & Curves Appearance CrossHatch Custom Application Data

Material properties

Materials in the default library can not be edited. You must first copy the material to a custom library to edit it.

Model Type: Linear Elastic Isotropic Save model type in library

Units: SI - N/m² (Pa)

Category: Steel

Name: AISI 304

Default failure criterion: Max von Mises Stress

Description:

Source:

Sustainability: Defined

| Property | Value | Units |
|-------------------------------|-----------|-------------------|
| Elastic Modulus | 1.9e+11 | N/m ² |
| Poisson's Ratio | 0.29 | N/A |
| Shear Modulus | 7.5e+10 | N/m ² |
| Mass Density | 8000 | kg/m ³ |
| Tensile Strength | 517017000 | N/m ² |
| Compressive Strength | | N/m ² |
| Yield Strength | 206807000 | N/m ² |
| Thermal Expansion Coefficient | 1.8e-05 | /K |

APPENDIX 41

Material properties of scissor lift top plate

Properties Tables & Curves Appearance CrossHatch Custom Application Data

Material properties
 Materials in the default library can not be edited. You must first copy the material to a custom library to edit it.

Model Type: Linear Elastic Isotropic Save model type in library

Units: SI - N/m² (Pa)

Category: Aluminium Alloys

Name: 1060 Alloy

Default failure criterion: Max von Mises Stress

Description:

Source:

Sustainability: Defined

| Property | Value | Units |
|-------------------------------|----------|-------------------|
| Elastic Modulus | 6.9e+10 | N/m ² |
| Poisson's Ratio | 0.33 | N/A |
| Shear Modulus | 2.7e+10 | N/m ² |
| Mass Density | 2700 | kg/m ³ |
| Tensile Strength | 68935600 | N/m ² |
| Compressive Strength | | N/m ² |
| Yield Strength | 27574200 | N/m ² |
| Thermal Expansion Coefficient | 2.4e-05 | /K |

APPENDIX 42

Material property of forklift linear guide

Properties Tables & Curves Appearance CrossHatch Custom Application Data

Material properties
 Materials in the default library can not be edited. You must first copy the material to a custom library to edit it.

Model Type: Linear Elastic Isotropic Save model type in library

Units: SI - N/m² (Pa)

Category: Steel

Name: AISI 1020 Steel, Cold Rolled

Default failure criterion: Max von Mises Stress

Description:

Source:

Sustainability: Defined

| Property | Value | Units |
|-------------------------------|-----------|-------------------|
| Elastic Modulus | 2.05e+11 | N/m ² |
| Poisson's Ratio | 0.29 | N/A |
| Shear Modulus | 8e+10 | N/m ² |
| Mass Density | 7870 | kg/m ³ |
| Tensile Strength | 420000000 | N/m ² |
| Compressive Strength | | N/m ² |
| Yield Strength | 350000000 | N/m ² |
| Thermal Expansion Coefficient | 1.17e-05 | /K |

APPENDIX 43

Material properties of fork mount

Properties Tables & Curves Appearance CrossHatch Custom Application Data

Material properties
 Materials in the default library can not be edited. You must first copy the material to a custom library to edit it.

Model Type: Linear Elastic Isotropic Save model type in library

Units: SI - N/m² (Pa)

Category: Steel

Name: AISI 1020 Steel, Cold Rolled

Default failure criterion: Max von Mises Stress

Description:

Source:

Sustainability: Defined

| Property | Value | Units |
|-------------------------------|-----------|-------------------|
| Elastic Modulus | 2.05e+11 | N/m ² |
| Poisson's Ratio | 0.29 | N/A |
| Shear Modulus | 8e+10 | N/m ² |
| Mass Density | 7870 | kg/m ³ |
| Tensile Strength | 420000000 | N/m ² |
| Compressive Strength | | N/m ² |
| Yield Strength | 350000000 | N/m ² |
| Thermal Expansion Coefficient | 1.17e-05 | /K |

APPENDIX 44

Material properties forklift drive guide

Properties Tables & Curves Appearance CrossHatch Custom Application Data

Material properties
Materials in the default library can not be edited. You must first copy the material to a custom library to edit it.

Model Type: Linear Elastic Isotropic Save model type in library

Units: SI - N/m² (Pa)

Category: Steel

Name: Alloy Steel

Default failure criterion: Max von Mises Stress

Description:

Source:

Sustainability: Defined

| Property | Value | Units |
|-------------------------------|-----------|-------------------|
| Elastic Modulus | 2.1e+11 | N/m ² |
| Poisson's Ratio | 0.28 | N/A |
| Shear Modulus | 7.9e+10 | N/m ² |
| Mass Density | 7700 | kg/m ³ |
| Tensile Strength | 723825600 | N/m ² |
| Compressive Strength | | N/m ² |
| Yield Strength | 620422000 | N/m ² |
| Thermal Expansion Coefficient | 1.3e-05 | /K |

APPENDIX 45

Material properties of forklift2 guide

Material properties
Materials in the default library can not be edited. You must first copy the material to a custom library to edit it.

Model Type: Save model type in library

Units:

Category:

Name:

Default failure criterion:

Description:

Source:

Sustainability:

| Property | Value | Units |
|-------------------------------|-------------|-------------------|
| Elastic Modulus | 2e+11 | N/m ² |
| Poisson's Ratio | 0.29 | N/A |
| Shear Modulus | | N/m ² |
| Mass Density | 7870 | kg/m ³ |
| Tensile Strength | 356900674.5 | N/m ² |
| Compressive Strength | | N/m ² |
| Yield Strength | 203943242.6 | N/m ² |
| Thermal Expansion Coefficient | | /K |

APPENDIX 46

Material properties of fork mount

Properties Tables & Curves Appearance CrossHatch Custom Application Def

Material properties
Materials in the default library can not be edited. You must first copy the material to a custom library to edit it.

Model Type: Linear Elastic Isotropic Save model type in library

Units: SI - N/m² (Pa)

Category: Steel

Name: Plain Carbon Steel

Default failure criterion: Max von Mises Stress

Description:

Source:

Sustainability: Defined

| Property | Value | Units |
|-------------------------------|-----------|-------------------|
| Elastic Modulus | 2.1e+11 | N/m ² |
| Poisson's Ratio | 0.28 | N/A |
| Shear Modulus | 7.9e+10 | N/m ² |
| Mass Density | 7800 | kg/m ³ |
| Tensile Strength | 399826000 | N/m ² |
| Compressive Strength | | N/m ² |
| Yield Strength | 220594000 | N/m ² |
| Thermal Expansion Coefficient | 1.3e-05 | /K |

APPENDIX 47

Material properties of fork guide

Material properties
Materials in the default library can not be edited. You must first copy the material to a custom library to edit it.

Model Type: Linear Elastic Isotropic Save model type in library
Units: SI - N/m² (Pa)
Category: Steel
Name: Galvanized Steel
Default failure criterion: Max von Mises Stress
Description:
Source:
Sustainability: Defined

| Property | Value | Units |
|-------------------------------|-------------|-------------------|
| Elastic Modulus | 2e+11 | N/m ² |
| Poisson's Ratio | 0.29 | N/A |
| Shear Modulus | | N/m ² |
| Mass Density | 7870 | kg/m ³ |
| Tensile Strength | 356900674.5 | N/m ² |
| Compressive Strength | | N/m ² |
| Yield Strength | 203943242.6 | N/m ² |
| Thermal Expansion Coefficient | | /K |

APPENDIX 48

Material properties of fork

Properties Tables & Curves Appearance CrossHatch Custom Application Data

Material properties
Materials in the default library can not be edited. You must first copy the material to a custom library to edit it.

Model Type: Linear Elastic Isotropic Save model type in library

Units: SI - N/mm² (MPa)

Category: Steel

Name: Alloy Steel

Default failure criterion: Max von Mises Stress

Description:

Source:

Sustainability: Defined

| Property | Value | Units |
|-------------------------------|----------|-------------------|
| Elastic Modulus | 210000 | N/mm ² |
| Poisson's Ratio | 0.28 | N/A |
| Shear Modulus | 79000 | N/mm ² |
| Mass Density | 7700 | kg/m ³ |
| Tensile Strength | 723.8256 | N/mm ² |
| Compressive Strength | | N/mm ² |
| Yield Strength | 620.422 | N/mm ² |
| Thermal Expansion Coefficient | 1.3e-05 | /K |